Preventing Postoperative Immunosuppression by Inhibition of PI3Kγ in Surgery-Induced Myeloid Derived Suppressor Cells

Gimantha Gayashan Tennakoon Mudiyansel, BSc.

Thesis submitted to the University of Ottawa
in partial fulfillment of the requirements
for the degree of Master of Science in Microbiology and Immunology

Microbiology and Immunology

Department of Biochemistry, Microbiology and Immunology

Faculty of Medicine

University of Ottawa

Abstract

Surgery-induced myeloid derived suppressor cells (sxMDSC)s mediate postoperative suppression of Natural Killer (NK) cells, which enables postoperative cancer recurrence and metastases. Currently, no therapeutics against sxMDSCs have been developed. Recent research has identified that the myeloid-restricted PI3K isoform (PI3Kγ) mediates MDSC activity. I targeted PI3Kγ in sxMDSCs as a therapeutic to reduce postoperative NK cell suppression and metastatic burden. Additionally, I investigated the efficacy of a sxMDSC-specific antibody-drug conjugate (ADC) with a PI3Kγ inhibitor payload. Pharmacological inhibition of PI3Kγ in sxMDSCs led to reduced AKT phosphorylation and reduced suppression of NK cytotoxicity in human and murine models. PI3Kγ inhibition also reduced postoperative metastatic burden. Despite the novelty of the sxMDSC-specific ADC, it didn't provide considerable benefits in reducing NK cell suppression compared to the unconjugated PI3Kγ inhibitor. However, this is a "first iteration" in what could be a powerful approach to targeting sxMDSCs, thereby preventing postoperative metastatic burden.

Acknowledgements

Deciding to pursue a master's degree came at a particularly difficult point in my life. Soon after I started my degree, I was diagnosed with a life-altering chronic disease. Despite having to juggle the challenges I had to face with both my health and as well the degree, I am so grateful that I have been able to persevere through this difficulty journey. Although these hurdles were overwhelming at times, I now know that I am stronger for overcoming them. However, this experience was one that I didn't complete alone, I quickly recognized the value of individuals in both by personal and professional circles to help and support me. Without their help, I honestly would not have been able to bring this project to completion.

First, I would like to thank Dr. Rebecca Auer for her support and guidance throughout the course of my project. She was patient, attentive and fostered my development as a young scientist. Thanks to her, I now see research as a symbol of hope for patients by addressing the current gaps in our medical knowledge, so that they can be truly free of the burdens of their clinical afflictions. I really appreciated that she was always understanding if I needed time to prioritize my health. I would also like to thank, Dr. Michael Kennedy, our former senior research associate, who was instrumental in guiding me through the project, helping troubleshoot issues that I faced, as well as inspiring me with his undying enthusiasm and tenacity for research. Since his departure from the lab, that torch has been passed on to two incredibly talented individuals, Dr. Rafeah Alam, and Dr. Alice Lau. They have more than filled the role that Dr. Kennedy played for my project and our lab in general. I would also like to thank Dr. Leonard Angka for the mountain of research he had done that lead to this project. It was Dr. Angka who had identified PI3K as a pathway to target postoperatively. Moreover, he was the one who taught me all the techniques necessary to conduct this project. I was inspired by his attention to detail and

technical expertise, which was the standard that I aspired for in the work that I present within this thesis. I would also like to thank Christiano Tanese de Souza, for his tremendous help to plan and complete all the animal experiments.

I really appreciate the friendships and sense of comradery that built with my lab mates, Oladunni Olanudi, Marlena Scaffidi, Henna Mistry and Sophie Branconnier, as we navigated the hurdles of our academic careers together. They are all exceptionally intelligent individuals, and I am fortunate to have worked with them. I would also like to thank my Thesis Advisory Committee (TAC) members, Dr. Ian Lorimer and Dr. Katey Rayner, for their guidance and expert opinion. They played important roles in shaping my project into the successful story it has become. I also appreciated that they were so understanding when it came to the medical challenges I faced and were willing to judge the scope of work I present within this thesis with that in mind.

Last, but certainly not least, I want to thank the individuals in my personal support system. My parents, Indu Vidyaratne and Premaratne Tennakoon, have been my stable foundation through this whole process. It is thanks to the tenacity and strength that they possessed that they we were able to uproot our lives in Sri Lanka to re-establish one here in Canada. Without their efforts, I would not be here writing this thesis today. They instilled a value system within me of strong work ethics and perseverance, which I heavily relied on while facing challenges with my degree and health. I am proud to be their son. I would also like to thank my partner, Tirani Weerapura, who has seen me go through the trials and tribulations of a master's degree as well as a debilitating health condition. She has been a huge source of support and I know I couldn't have gone through this without her there every step of the way. Finally, my

close group of lifelong friends have always been willing to lend a shoulder to lean on. I appreciated the laughs we had in times that I needed to unwind and recharge.

To each ad everyone mentioned in this thesis, from the bottom of my heart, thank you. It is because of your contributions that this thesis became reality.

Table of Contents

List of Abbreviations

ACVS	-	Animal Care and Veterinary Services
ADC	-	Antibody Drug Conjugate
ADCC	-	Antibody-Dependent
ARG1	-	Arginase-1
BM	-	Bone Marrow
CAR	-	Compensatory Anti-inflammatory Response
CCL	-	C-C Motif Ligands
CD	-	Cluster of Differentiation
ADMARE	-	Centre for Drug Research and Development
CLR	-	C-type Lectin Receptor
c-MYC	-	Cellular Myelocytomatosis Oncogene
COX-2	-	Cyclooxygenase-2
CPI	-	Checkpoint Inhibitors
CRC	-	Colorectal Cancer
CRPMI	-	Complete Roswell Park Memorial Institute
CTC	-	Circulating Tumour Cell
CXCL	-	C-X-C Motif Ligands
DAMP	-	Damage Associated Molecular Pattern
DAP	-	DNAX-activation protein
DC	-	Dendritic Cell
DFS	-	Disease-Free Survival
DNAM-1	-	DNAX Accessory Molecule-1
DTC	-	Disseminated Tumour Cell
ECM	-	Extracellular Matrix
EGF	-	Epidermal Growth Factor
EMT	-	Epithelial to Mesenchymal Transition
FasL	-	Fas Ligand
GM-CSF	-	Granulocyte-Macrophage Colony-Stimulating Factor

G-MDSC	-	Granulocytic-Myeloid Derived Suppressor Cell
GPCR	-	G-protein coupled receptor
HC	-	Haemocytometer
ICE	-	Inference of CRISPR Edits
IL	-	Interleukin
IM	-	Immunomagnetic
IMC	-	Immature myeloid cell
iNOS	-	Inducible nitric oxide synthase
ITAM	-	Immunoreceptor tyrosine-based activation motif
ITIM	-	Immunoreceptor tyrosine-based inhibitory motif
KIR	-	Killer-cell immunoglobulin-like receptor
KO	-	Knockout
LAP	-	Latency associated protein
LD	-	Low-density
LTBP	-	Latent TGF-β-binding protein
mAb	-	Monoclonal antibody
MDSC	-	Myeloid derived suppressor cell
MFI	-	Median fluorescence intensity
MHC	-	Major histocompatibility complex
M-MDSCs	-	Monocytic- Myeloid derived suppressor cell
MRD	-	Minimal Residual Disease
mTOR	-	Mammalian target of rapamycin
NCR	-	Natural Cytotoxicity receptor
Necl	-	Nectin-Like
NF-κB	-	Nuclear factor kappa B
NK	-	Natural Killer
NKG	-	Natural Killer Group
NKp	-	Natural Killer protein
NLRP3	-	NLR family pyrin domain containing 3
NLRs	-	NOD-like receptor

NO	-	Nitric oxide
NP	-	Nanoparticle
NSCLC	-	non-small cell lung cancer
OHSN	-	Ottawa Health Science Network
OS	-	Overall Survival
PAM	-	Protospacer adjacent motif
PBL	-	Peripheral blood lymphocytes
PBMC	-	Peripheral blood mononuclear cells
PDGF	-	Platelet-derived growth factor
PFS	-	Progression-Free Survival
PGE2	-	Prostaglandin E2
PH	-	pleckstrin homology
pHAB	-	Goat α FITC mIgG1-Fc-pHAb conjugate Fc-λ
PHBSP	-	Perioperative Human Blood and Tissue Collection Program
PI3K	-	Phosphoinositide 3-kinases
PIP2	-	Phosphatidylinositol 4,5-bisphosphate
PIP3	-	Phosphatidylinositol-3,4,5-trisphosphate
POD	-	Postoperative Day
PRRs	-	Pattern recognition receptor
PTEN	-	phosphatase and tensin homologue
PV	-	Poliovirus
PVR	-	Poliovirus Receptor
RBD	-	Ras binding domain
REB	-	Research Ethics Board
RNs	-	Registered Nurse
ROS	-	Reaction Oxygen Species
RT	-	Room Temperature
RTK	-	Receptor Tyrosine Kinase
SDCU	-	Surgical Daycare Unit
SEM	-	Standard error mean

sgRNA	-	Single-guide Ribonucleic acid
SMCA	-	Single Molecular Counting Assay
SREBP	-	Sterol regulatory element binding proteins
sxMDSC	-	Surgery-induced Myeloid Derived Suppressor Cell
SYK	-	spleen tyrosine kinase
TACTILE	-	T-cell activated increased late expression
TAM	-	tumor associated macrophages
Th1	-	Type 1 helper T cells
TIGIT	-	T-cell Immunoreceptor with Ig and ITIM domains
TLRs	-	toll-like receptors
TNF	-	Tumour Necrosis Factor
TRAIL	-	TNF-related apoptosis-inducing ligand
Treg	-	Regulatory T Cell
VEGF	-	Vascular endothelial growth factor
Zap70	-	Zeta-chain-associated protein kinase 70

Table of Figures

List of Tables

List of Supplemental Figures

Chapter 1

1.1 General Introduction

1.1.1 Natural Killer Cells and Cancer

1.1.1.1 Cancer

Cancer is caused by normal cells that have undergone transformations which enable their continuous unregulated proliferation and growth(1–3). However, this is far too simple of a definition to encompass the complex interactions and mechanisms that cancer utilizes to promote its survival and persistence. In reality, normal cells face many endogenous barriers that have evolved with several redundancies to prevent their transformation into malignancies(4). Moreover, any cells that do manage to become cancerous, are quickly detected and cleared by host anti-tumour immunity(5–7). Therefore, carcinogenesis, the process by which cancer develops, can be considered a Darwinian process as the transforming cells acquire specific adaptations to overcome selective pressures from endogenous anti-tumour measures(1, 2, 8–10). These adaptations can be broadly defined as the six distinct "hallmarks of cancer"(11). These hallmarks include the ability to (1) self-replicate without external stimuli, (2) resistance to growth-restricting signals, (3) evasion of apoptosis, (4) unlimited replicative capacity, (5) persistent angiogenesis, and (6) the potential for invasion and metastatic spread(11). Malignant cells acquire these hallmarks through various mutations which occur throughout one's life because of genetic susceptibilities as well as environmental and lifestyle factors. Cancers are particularly debilitating given their ability to spread to distant body organs thereby disrupting important bodily function, in a process known as metastasis(1, 3). Although cancer is the second-leading cause of death worldwide, breakthroughs in our

understanding of the disease and the use of new technologies and therapies are reducing the number of cancer-related deaths(12–14).

1.1.1.2 Metastatic disease is a primary cause of mortality

Despite the medical advances made in cancer therapeutics, approximately 90% of cancer-related deaths are caused by metastasis, making it the primary cause of mortality for cancer patients(15, 16). Once metastases arise, the 5-year survival rates for a variety of cancer types decrease(16–19). Metastases, which are defined as secondary outgrowths of tumour cells at distant anatomical sites, is most hazardous when they develop undetected. The metastatic spread was once considered to be a phenomenon observed in advanced stages of cancer as the primary malignancy reaches a sufficient size to disseminate tumour cells to distant tissues(20). However, mounting evidence has demonstrated quite the opposite – that metastasis begins even before the first signs of a primary tumour are clinically detectable(20, 21). In addition, metastases might remain quiescent in distant secondary sites for more than a decade following the removal of the initial tumour(22, 23). The formation of clinically-detectable macrometastases from these dormant tumour cells manifests as cancer recurrence in patients who may have been in remission for months or even years(22). The process by which metastases form in distant organ sites is known as the metastatic cascade.

The metastatic cascade is thought to be initiated when a subgroup of malignant cells acquire the ability to invade tissues and metastasize. These cells can integrate multiple signals from the tumour microenvironment which will cause them to undergo an epithelial to mesenchymal transition (EMT)(24). EMT is followed by is a process in which the extracellular matrix (ECM) is remodelled where cancer cells become less adherent and intravasate into the

bloodstream or lymphatic system(25). These circulating tumour cells (CTCs) experience a harsh environment in the bloodstream where they are easily recognized and eliminated by peripheral immune cells(26). These CTCs must survive until they can encounter the conditions necessary to extravasate into a distant tissue, where they are known as disseminated tumour cells (DTCs)(26). The DTCs can then persist as micrometastatic niches where they can remain quiescent for extraordinarily long periods until receiving cellular cues to form into clinically detectable secondary macrometastases(21, 23). Metastatic spread is particularly problematic given its ability to actively disseminate potential new macrometastases throughout the host system.

Fortunately, our bodies are not unprepared to combat this danger. Solid tumours shed a surprisingly large amount of CTCs, yet only a few of them successfully form macrometastases, implying the presence of many stringent barriers which impede their establishment as DTCs and micrometastatic niches(26). In fact, CTC clearance is a key determinant in the formation of metastasis(27). Studies have identified that a decrease or abolishment of CTC counts was associated with a good therapeutic response, while an increase in CTC counts signified the opposite(28, 29). Natural Killer (NK) cells are critical for immunosurveillance and elimination of CTCs, hence reducing their ability to form metastases(26). They are an essential line of defence that can rapidly react to prevent the spread of cancer.

1.1.1.3 Natural Killer Cells

NK cells are cytotoxic lymphocytes of the innate immune system that can identify and eliminate stressed, infected, or altered cells (cancerous cells)(30, 31). Despite the large number of targets that NK cells can detect, I will focus on the antitumor activity of NK cells. Between 10 and 15 percent of total peripheral blood lymphocytes are NK cells, making them the 3rd largest

population of lymphocytes after B and T cells. NK cells are not only present in the periphery, but also in the lymph nodes, spleen, thymus, peritoneal cavity, lungs, liver, and uterus during gestation(32). The absence of the T cell receptor, cluster of differentiation (CD)3, and the presence of the lineage marker CD56, are characteristic of NK cells.

NK cells perform two critical effector functions for anti-tumour immunity. Firstly, given their role as cytotoxic lymphocytes, NK cells can mediate target cell lysis through various mechanisms, including the direct release of lytic granules, such as perforin or granzyme B, or activation of death receptor-mediated apoptosis through tumor necrosis factor (TNF), Fas ligand (FasL), and TNF-related apoptosis-inducing ligand (TRAIL) production(33). NK cells can also mediate antibody-dependent cell-mediated cytotoxicity (ADCC) through the CD16 (FCγRIII) receptor that binds to the Fc portion of IgG antibodies, thereby triggering the lysis of targeted cells(34, 35). Secondly, NK cells release important immunomodulatory cytokines such as such as interferon-γ (IFN-γ), TNF-α, granulocyte-macrophage colony-stimulating factor (GM-CSF), interleukin-10 (IL-10) and interleukin-13 (IL-13), which recruit and coordinate the anti-tumour immune response(30). By far the most important cytokine derived by NK cells is IFN-γ, which has been shown to have direct anti-tumour effects and can inhibit metastasis(31). NK-cell derived IFN-γ can also promote the accumulation, activation, and NK cell-mediated cytotoxicity (NKC), generating a self-sustaining positive feedback loop(36, 37). IFN-γ can also promote T cell proliferation which is critical for activating anti-tumour adaptive immunity(38, 39).

NK cells are comparable to cytotoxic T cells, the adaptive immune cell counterpart, because their cytolytic functions overlap(40). However, as their name implies, NK cells are ready to perform effector activities immediately, without the need for priming and antigen-specific clonal selection involved with cytotoxic T cell activation. Instead, NK cells rely on a small number of

receptors encoded in the germline that, when bound to their respective ligands, can result in activating or inhibitory signals(30). NK cells have elegantly evolved to rapidly detect and eliminate tumour cells, which are typically characterized by aggressive growth and replication, to prevent them from getting out of control.

1.1.1.4 NK cell activity is determined by receptor signal integration

The choice between autoimmunity and tumour clearance is a delicate balance. Immune cells employ many strategies to discriminate between "self" (healthy tissues) and "non-self" (transformed cells, pathogens, toxins, etc.) entities in the host(41). NK cells can decide "to kill or not to kill" their targets by utilizing an array of activating and inhibitory signals from multiple, germ-line encoded receptors to determine their activity against host threats without damaging healthy cells(30). These receptors can lead to NK cell activation or inhibition.

Activating receptors on NK cells include the Natural Cytotoxicity receptors (NCRs), Natural Killer protein (NKp)30, NKp44, NKp46, and NKp80, C-type lectin-like receptors Natural Killer Group (NKG)2D and CD94-NKG2C, as well as 2B4 (CD244)(42, 43). These activating receptors recognize stress-induced ligands, which are primarily structural homologs of MHC class I molecules. As described in the "induced-self recognition model", these ligands are all expressed at low levels under normal conditions but are significantly upregulated in stressed or cancerous cells(44). Engagement of activating receptors with their respective ligand leads to the phosphorylation of immunoreceptor tyrosine-based activating motif (ITAM)(31) . ITAMs may be directly present on the receptor or through association with adaptor proteins such as DNAX-activation protein (DAP)10 or DAP12(45, 46). Once phosphorylated, ITAMs recruit and activate

tyrosine kinases leading to further downstream signaling(31). The result of these signalling events leads to the release of cytolytic granules or the transcription/translation of cytokines(47).

NK cells also require adhesion molecules to effectively interact with targets. These are known as costimulatory receptors which enable adherence to target cells but cannot initiate cytotoxic activity on their own(48, 49). Among these co-stimulatory receptors is DNAX accessory molecule (DNAM)-1 which can bind two known ligands, CD155 and CD112(50). These two molecules are normally not expressed in normal cells but upregulated in transformed and pathogen-infected cells(50). They are also expressed at the cell surface of immune cells such as monocytes, dendritic cells (DCs), and activated T cells. Therefore, DNAM-1 receptor–ligand interactions mediate the cross-talk between NK cells and other immune cells(49). Knockout or blockade of DNAM-1 on NK cells showed significant reduction of NKC, cytokine secretion and tumour clearance, highlighting its importance in NK cell activity(51, 52). Of note, blocking CD155 signalling impaired NKC of tumour cells. However, CD112 blockade failed to inhibit NKC, suggesting CD155 is the critical ligand for DNAM-1 mediated NKC(53). However, chronic stimulation by $CD155^{+}$ target cells causes a down-regulation of DNAM-1 resulting in impaired NKC(49, 54).

These activating signals are antagonized by inhibitory receptors which recognize the major histocompatibility (MHC) class I and MHC class I-like molecules(42). These receptors include the killer Ig-like receptors (KIRs) and the CD94-NKG2A heterodimer(55). These receptors have an immunoreceptor tyrosine-based inhibitory motif (ITIM), which results in downstream inhibitory signals. NK cell activity is regulated by the “missing self” hypothesis, coined by Klas Kärre(56, 57). MHC class I molecules are the main mechanism by which cells display viral or tumor antigens to cytotoxic T cells. This presents a selective pressure for tumour cells to down-

regulate MHC class I molecules, thereby masking them to T cell detection machinery, and enabling evasion of T-cell mediated immunity(58). NK cells have evolved to counter this strategy as it leads to a "missing self" state, resulting in reduced inhibitory signals, which is often coupled with increased expression of activating ligands on tumour cells(59). This results in effective anti-tumour clearance and surveillance as it also leads to both tumour cell killing and the production of cytokines that can recruit and sensitize other immune cells to the site of an otherwise "hidden" tumour.

1.1.1.5 Natural killer cells are important for cancer prognosis and reducing metastatic formation

As part of the metastatic cascade, CTCs must be able to establish themselves in a new tissue environment. As established prior, poor CTC clearance is an indicator of poor clinical outcomes(27, 28). Both circulating and tissue resident NK cells are critical components for preventing CTCs from forming metastatic niches, thereby playing a critical role in improving cancer prognosis(26). There is an inverse correlation between high amounts of circulating or tumor-infiltrating NK cells and the presence of metastases in patients with gastric(60), colorectal(61), renal(62), and prostate carcinomas(63). Along similar lines, high expression levels of NK cell activating receptors or improved NKC have been linked with good prognosis in multiple cohorts of cancer patients with or at risk of metastatic disease(64). Imai *et al.* conducted a prospective, 11-year follow-up study and showed that the risk of cancer incidence in patients was associated with the responsiveness of their peripheral blood NK cells against NK cell-sensitive K562 target erythroleukemia cells(65). Medium to high NKC against K562s was associated with

a significantly reduced risk of cancer. Taken together, this highlights that NK cells mediate clinically relevant antimetastatic activity and are critical for anti-tumour immunity.

Despite the importance of NK cells in inhibiting metastatic formation, cancer surgery, a mainstay therapy for tumour removal, has shown to cause a significant impairment of NK cell activity. In Chapter 2, I will discuss in greater detail the role of cancer surgery in NK cell immunosuppression and the resulting consequences of postoperative metastatic disease. Next, I will discuss my research to attempt to reduce post-operative immunosuppression and metastatic disease.

Chapter 2

1.2 Introduction

1.2.1 Cancer surgery directly contributes to postoperative metastatic disease

Despite the indisputable benefits of tumour resection, the outcomes of surgery may be detrimental to overall patient survival. Nearly half of all colorectal cancer (CRC) patients who have no signs of metastases before undergoing primary tumour resection will develop metastases within 5 years after surgery(66). Furthermore, Retsky *et al.* identified most relapses in breast cancer occur within 5 years of surgery and they linked this to surgery-induced metastatic initiation(67). It is well known that stress induced by surgery can aggravate postoperative metastases(68). Surgical resection causes physical disruption of the primary tumour, resulting in the inadvertent formation and release of CTCs(69). This ultimately contributes to a greater risk of metastatic establishment in the postoperative environment. In a cohort of 36 patients with pancreatic ductal carcinoma, Park

et al. demonstrated that the presence of CTCs in blood after surgery was an independent risk factor for early recurrence and for systemic recurrence (distant metastases and peritoneal dissemination)(70). There is also the possibility of leaving a small amount of occult or microscopic neoplastic cells at the surgical margin, which is also known as minimal residual disease (MRD)(71). Surgery can cause accelerated growth of MRD, ultimately leading to decreased disease-free survival (DFS) and overall survival (OS)(72, 73).

Alongside the direct contributions that surgery can have in promoting metastatic disease, surgical trauma also leads to a great deal of both physical and psychological stress and pain. This promotes the surgical stress response, a set of physiological responses important for wound healing(74). However, it ultimately leads to reduced tumour immunosurveillance which can contribute to metastatic outgrowth(75).

1.2.2 The Surgical Stress Response

To the body, surgery and the resulting excision of tumour resembles the same as any other wound that needs to be healed. Therefore, the surgical stress response should be considered an evolutionary adaptation to deal with trauma and promote wound healing(76). However, it is said that "the road to hell is paved with good intentions". In this case, the "good intentions" of the surgeon excising the tumour and the body attempting to heal the wound site are exploited by the MRD for their growth and re-establishment in the postoperative environment. It is important to consider the surgical stress response as an "ebb and flow"(77). The Ebb can be described as the immediate, "crashing wave" inflammatory response to the surgery and the Flow as the "receding" compensatory anti-inflammatory response (CAR) designed to limit excessive inflammation and return to homeostasis.

1.2.2.1 The Postoperative Ebb and Flow

The tissue trauma during surgery causes stimulation of the autonomic nervous system and the hypothalamic-pituitary-adrenal axis, which leads to the release of pro-tumour glucocorticoids and catecholamines(74). Additionally, endothelial injury triggers the release of alarmins, or damage-associated molecular patterns (DAMPs), which stimulates the release of would healing factors including epidermal growth factor (EGF), platelet-derived growth factor (PDGF) and vascular endothelial growth factor (VEGF)(78). Despite their importance for wound healing, they also enable tumour progression(79), tumour growth(80) and angiogenesis(81, 82). Indeed, several studies have found that the expression of wound healing factors is associated with poor clinical outcomes as well as metastasis in patients diagnosed with cancer(79, 83). This illustrates that the conditions required for wound healing, overlap with mechanisms necessary for the re-establishment of MRD and CTC metastatic formation(84).

Alongside the direct effects of DAMPs in promoting tumour growth, it can also upregulate factors which signal the accumulation of myeloid cells at the site of trauma which can mediate inflammation. Host cells can express surface pattern recognition receptors (PRRs), such as toll-like receptors (TLRs), C-type lectin receptors (CLRs), and NOD-like receptors (NLRs), that can detect DAMPs(85). Activation of host cells in response to DAMPs leads to the expression of IL-1β(86). Ershaid *et al.* demonstrated in a murine model of breast cancer that tissue damage in fibroblasts increased proinflammatory markers and upregulated IL-1β secretion. This facilitated tumour progression which was abrogated when IL-1β was inhibited(87). IL-1β expression causes increased secretion of C-C motif ligands (CCLs) or C-X-C motif ligands (CXCLs) that are responsible for myeloid cell accumulation at the site of surgical resection(88).

Neutrophils are the first to be recruited to the site of inflammation and the ratio of neutrophil to lymphocyte count by complete blood cell count is a measure of postoperative inflammation(89). This is followed by recruitment of monocytes, whose PRRs can also detect DAMPs and in turn trigger the NF-κB pathway(90). This monocyte activation causes a massive yet short-lived release of pro-inflammatory cytokines, including IL-1, IL-6, TNF-α, IFN-γ and GM-CSF(91). Importantly, the expansion in these pro-inflammatory cytokines is proportional to the degree of surgical stress(92, 93). Narita *et al.* compared the level of IL-6 in prostate cancer surgery patients undergoing a laparoscopic versus open surgery and reported that serum IL-6 was significantly lower in patients undergoing the less invasive, laparoscopic surgery(93).

While monocyte-derived IL-6 appears to be the major pro-inflammatory cytokine in the immediate postoperative period, it also acts as a negative feedback on TNF-α and IL-1 to halt the pro-inflammatory phase and transition into the CAR(77, 91). Therefore, following the acute pro-inflammatory phase, the prevailing anti-inflammatory properties of IL-6 set the stage for the next phase of surgical inflammation. Moreover, the magnitude of the CAR is directly proportional to the degree of the preceding pro-inflammatory phase(94). This IL-6 mediated switch triggers a sustained anti-inflammatory phase, which can last up to several weeks(95) – an adaptive response to limit excessive inflammatory damage(96). The immunosuppressive phase involves the release of anti-inflammatory cytokines (TGF-β, IL-4, IL-5, IL-10, IL-13) and prostaglandin E2 (PGE2),(97, 98). Many of these factors are known to cause impaired anti-tumour immunity by direct suppression of NK cells(77, 99–102) which I will discuss in further detail in the next section.

The Ebb and Flow relationship between the pro- and anti-inflammatory phases exists to maintain a balanced response to surgery to protect against the damaging effects of excessive

inflammation. It is argued that the CAR of the surgery stress response works to suppress immune effector cells to quickly achieve homeostasis(75). However, in the context of tumour resection, the CAR creates a significant pro-metastatic and suppressive host environment, which enables tumour cells to evade the immune response(73). Moreover, the degree of induced stress and the invasive nature of the procedure is correlated with the magnitude of postoperative immune suppression(93). A major target of this postoperative immunosuppression is NK cells(77, 100, 103).

1.2.3 Natural Killer Cells are Dysfunctional after Surgery

The physiological toll and consequences of surgery have direct effects on NKC, IFN-γ secretion, and activating receptor expression, including DNAM-1 and NKG2D(99, 104–107). Tai *et al.* first confirmed this in murine models of surgical stress, where suppression of NK cells from surgical stress was correlated with significantly greater postoperative metastatic burden(103). In clinical trials, our group(99, 103–105, 108, 109) and others(110, 111) have reported that surgery results in a pronounced suppression of NKC and IFN-γ secretion which persists for up to 1 month post-operation, with the suppressed phenotype being the most profound within 24 hours after surgery(99, 104). This highlights the rapid physiological signalling cascades that are activated in the surgical stress response and their potent, cumulative effect on NK cell immunosuppression. Taken together, the role of the surgery stress response in the formation and persistence of CTCs, coupled with suppression of NK-mediated CTC immunosurveillance, provides an ideal window of opportunity for CTCs to establish metastatic niches in the postoperative period.

The events that lead to NK cell suppression after surgery are numerous. As described in section 1.2.2, surgery results in an anti-inflammatory cytokine milieu which systemically affects the immune system. The postoperative cytokine milieu is dominated by elevated IL-6 which has

been shown to downregulate NK activity(112). In a phase 1 clinical trial with a cohort of 20 patients with advanced colon and pancreatic cancer, those given recombinant (r)IL-6 suffered a significant reduction in NKC(113). Recent studies have demonstrated that IL-6 inhibits NKC by decreasing perforin and granzyme production(114–116). IL-6 can also lead to the production of PGE2 which has been reported to have direct suppressive effects on NK cells(117).

Alongside PGE-2 and IL6, TGF-β is also highly abundant in the postoperative environment, given its key role in wound healing. However, it is known to suppress NK cell function and responsiveness to activating cytokines(118–120) .Slattery *et al.* demonstrated that in addition to reduced IFN-γ production and NKC, TGF-β caused clear metabolic deficits including reduced glycolysis and oxidative phosphorylation in patients with metastatic breast cancer(118). Moreover, TGF-β mediated inhibition is dominant over IL-2 activation and causes a reduction in surface expression of NKG2D and DNAM-1(121). TGF-β causes a direct reduction in the transcription of DNAM-1 mRNA, leading to reduced protein expression(122). Additionally, TGF-β suppresses the transcription of DAP10, the critical adaptor of NKG2D, leading to the down-regulation of NKG2D in human NK cells(123). Since IL-6 drives TGF-β production from various cell types and TGF-β itself may enhance IL-6 release, the resulting feedback loop may perpetuate post-surgical immune suppression(124–126). Taken together, the prolonged elevated presence of IL-6, PGE2, and TGF-β in the postoperative period could cumulatively lead to reduced NK cell effector functions, anti-tumour immunity and CTC clearance, thereby providing a window of opportunity for CTCs and MRD to promote metastatic disease as a consequence of surgery.

1.2.4 Myeloid Derived Suppressor Cells are potent immunosuppressive cells

Alongside suppression of NK cells, the surgical stress response also leads to the expansion of "myeloid derived suppressor cells (MDSCs)" which, themselves, exhibit a potent capacity to inhibit NK cell effector functions(127). Their expansion is mediated by emergency myelopoiesis, which can be triggered by several physiological stressors, including the inflammatory phase induced by surgical stress. In the context of surgery, this process aims to meet the demands for myeloid cells from the bone marrow which migrate toward the site of injury(128, 129). Although it contributes to an overall increase in the myeloid population which can aid in healing, it also in part leads to the generation of immature myeloid cells (IMCs)(130) which are defined as MDSCs. These postoperative MDSCs demonstrate significantly decreased expression of HLA-DR, a marker of immune competence, antigen presentation, and maturation state(91, 131, 132). In this section, I will describe MDSCs, their ability to inhibit NK cell effector function and their role in postoperative immunosuppression.

MDSCs are characterized as a heterogenous population of myeloid lineage immunoregulatory cells. MDSCs can be subdivided into granulocytic-MDSCs (G-MDSCs) and monocytic-MDSCs (M-MDSCs) and they phenotypically resemble neutrophils and monocytes, respectively. Key studies have helped develop a common phenotyping strategy based on their surface markers. For murine MDSC populations, M-MDSCs were identified as $CD11b^{+}/Ly6G^{-}/Ly6C^{+}$ while G-MDSCs were $CD11b^{+}/Ly6G^{+}/Ly6C^{Lo}$ (133, 134). For human MDSCs, Bronte *et al.* recommended the following guidelines: the absence of T, B and NK cell lineage markers (CD3, CD19 and CD56, respectively) and the presence of the myeloid lineage marker, CD33. M-MDSCs can be separated by the presence of monocyte marker CD14 and the absence of CD15 ($Lin^{-}/CD33^{+}/CD14^{+}/CD15^{lo}$), while the opposite is true for G-MDSCs ($Lin^{-}/CD33^{+}/CD14^{-}$

/CD15^{+})(133). MDSCs have increased reactive oxygen species (ROS) formation, high expression of ARG1, inducible nitric oxide synthase (iNOS), cyclooxygenase-2 (COX-2), and anti-inflammatory cytokines TGF-β and IL-10(135) than conventional monocytes or neutrophils.

MDSCs play a critical role in mediating tumorigenesis and immune evasion. MDSCs can directly promote tumor progression by affecting TME remodelling and angiogenesis via soluble factors like VEGF and can inhibit tumor cell senescence by antagonizing IL-1α. MDSCs contribute to the development of the tumour microenvironment by producing factors that interfere with effector immune cell function or promoting the generation of FOXP3^{+} regulatory T (Treg) cells(136). Clinically, peripheral MDSCs are an independent indicator of poor prognosis and clinical outcomes in both solid and hematological malignancies and can help predict response to cancer therapies(137). Veglia *et al.* summarized pre-clinical and clinical studies investigating the role of MDSCs in cancer. A positive correlation between circulating MDSCs and cancer stage/tumor burden has been reported in colorectal carcinomas, non-small cell lung cancer (NSCLC), breast, bladder, and thyroid cancers(138). Wang *et al.* performed a systematic review of 40 studies assessing the relationship between MDSCs and the prognosis of patients with solid tumors and reported elevated circulating MDSCs were an independent indicator of poor patient outcomes including OS, progression-free survival (PFS) and disease-free survival (DFS)(139). M-MDSC numbers correlated with reduced survival in patients with lymphoma (Hodgkin's, non-Hodgkin's, and diffuse late B cell)(140). Ahn *et al.* highlighted that high M-MDSC counts, and not G-MDSCs counts, was associated with tumour progression and poor prognosis(141).Moreover, Weber *et al.* demonstrated that the frequency and immunosuppressive function of MDSC in cancer patients can be used as a predictive marker for patient resistance to checkpoint inhibitors

(CPIs)(142). Thus, the presence of MDSCs is detrimental to cancer patients and provides a potential target for cancer immunotherapies.

1.2.4.1 MDSCs are suppressors of NK cell tumour surveillance

Various groups have reported on different mechanisms of NK cell suppression likely owing to the context-dependent, heterogeneous nature of MDSCs. Several studies have demonstrated that *ex vivo* co-culture of MDSCs with NK cells leads to a significant reduction in NKC, IFN-γ secretion, and NKG2D expression(143). Sceneay *et al.* demonstrated that NKC in a murine breast cancer model is significantly decreased in the presence of MDSCs, resulting in increased metastatic potential(144). It is now known that MDSCs boast a vast array of suppressive machinery that can negatively regulate NK cell activity through cell-to cell contact, and secretion of soluble molecules or extracellular vesicles in the extracellular milieu.

Sarhan *et al.* demonstrated that separating the MDSCs and NK cells via transwell inserts, which allowed for exchange of soluble factors but prohibited direct cell-to-cell contact, attenuated suppression and therefore suggests the critical role of cell-to-cell contact(145). To determine which receptor enables this contact, Hoechst *et al.* co-cultured MDSCs and NK cells in the presence of anti-NKG2D, anti-CD94, anti-NKp44, anti-major histocompatibility complex I (MHC I), anti-MHC-II, or anti-NKp30 antibodies. They identified that blockade of NKp30 reversed the suppression of NKC and IFN-γ secretion, while the addition of all other tested blocking antibodies had no effect(146). This suggested that NKp30 is the critical receptor for mediating MDSC:NK cell-to-cell contact. In a separate study, the CD155/TIGIT (T-cell Immunoreceptor with Ig and ITIM domains) axis was also found to be critical for contact-dependent MDSC-mediated

suppression of NK cells, which was confirmed by TIGIT blockade(147). Membrane bound TGF-β expressed on the surface of MDSCs was also shown to cause NK cell suppression, which was reversed by antibody blockade(148).

Numerous groups have also described the ability of MDSCs to inhibit NK cells through secreted factors or by depletion of essential nutrients. MDSCs express high levels of arginase 1 (ARG1) which catalyze arginine into metabolites and soluble factors, leading to arginine depletion(149). Arginine is critical for NK cell function and its depletion significantly impacts NKC and reduces IFN-γ secretion(150, 151). MDSC function is mediated by autocrine reactive oxygen species (ROS) production and studies have shown that MDSC-derived ROS can significantly hinder NK cell function(152). MDSCs also demonstrate significant expression of iNOS, leading to the production of nitric oxide (NO) which is a potent immunosuppressive factor. Stiff *et al.* showed that MDSCs can impair the Fc-receptor mediated ADCC and the production of cytokines in NK cells through NO production(153). MDSCs can also release immunosuppressive cytokines, such as TGF-β, which can significantly reduce NK cell activity(148). Recently, Tumino *et al.* demonstrated the role of MDSC-derived exosomes in NK cell suppression(154). Taken together, MDSCs are a subset of immunoregulatory cells that are implicated in postoperative NK cell suppression through both contact dependent and independent mechanisms.

1.2.4.2 MDSCs are mediators of postoperative NK immunosuppression and metastatic burden

Our group, as well as others, have observed a specific expansion of M-MDSCs in colorectal cancer(155), lung cancer(156) and hepatocellular carcinoma(127) patients undergoing curative

resection compared to preoperative conditions. In a cohort of 183 hepatocellular carcinoma patients, Gao *et al.* identified a significant positive correlation between high systemic inflammation after surgery and the expansion of M-MDSCs(127). Moreover, a large expansion of M-MDSCs, due to postoperative inflammation, was correlated with a significantly shorter time to recurrence and OS. Alongside MDSC expansion, the surgery stress response also leads to the accumulation of MDSCs, primarily at the site of resection(157, 158). Li *et al.* found that in a colon cancer mouse model, abdominal surgical trauma induced the release of large amounts of HMGB1 DAMPs into the abdominal cavity, contributing to the recruitment of MDSCs and promoting the formation of peritoneal metastases(159). DAMPs lead to the upregulation of CXCL8 on affected tissue(160), an important ligand and migration signal for CXCR1/2, which are expressed on MDSCs(161). Taken together, the surgery stress response activates an array of pathways that leads to the expansion and accumulation of "surgery-induced" MDSCs (sxMDSC)s.

Following expansion and accumulation, our group and others have established that sxMDSCs are responsible for both NK cell suppression and cancer metastases in a murine model of surgical stress(103, 105, 108). SxMDSCs are shown to be significantly more immunosuppressive than their preoperative counterparters(162). sxMDSCs demonstrate significantly greater expression of Arg1, IL-10, and ROS than preoperative counterparts(108). This suggests that surgical stress may promote sxMDSC activity. To corroborate this, several studies have demonstrated that DAMPs commonly released following surgery, such as HMGB1(163), as well as IL-6 and PGE-2(158, 164, 165), not only contribute to MDSC expansion, but also increase their suppressive activity. Activation of TLR4 or RAGE by HMGB1 leads to significantly greater production of IL-10 and ROS in MDSCs and improved suppression of tumour NKC in an *ex vivo* co-culture model(163, 166). Taken together, not only does the surgery stress response led to the

expansion of sxMDSCs, but it also heightens their suppressive activity. These surgery-induced immunoregulatory cells then act as drivers of immunotolerance in the aftermath of surgery to quickly re-establish homeostasis.

However, despite the important role MDSCs play in regulating excessive inflammation in the context of tumour resection, they inadvertently enable the inhibition of tumour immunosurveillance mediated by NK cells. We have confirmed that these cells are highly suppressive of NKC in an *ex vivo* co-culture assay compared to preoperative controls(162). When these sxMDSCs were adoptively transferred to tumour challenged control mice that did not receive surgery, the effects of postoperative stress, including impaired NKC and increased metastatic burden, were recapitulated(108).

Taken together, MDSCs represent a potent subset of immunoregulatory cells that are involved in tumour growth and metastasis by inhibiting anti-tumour immunity. Surgical stress "supercharges" the immunosuppressive capacity of this population by inducing their expansion, accumulation, and activation postoperatively. The synergistic effects of surgery-induced expansion, activation of sxMDSCs and their ability to suppress NK cell activity, may greatly contribute to CTC survival and reduced clearance. This in turn would exacerbate the potential for the formation of distant metastases postoperatively. To re-emphasize, low CTC clearance postoperatively is a prognostic marker of poor survival outcomes(167–169). This necessitates the need for therapeutics that target sxMDSCs in the perioperative period to reduce the risk of recurrence and metastatic disease.

1.2.5 Identifying PI3K as a therapeutic target for sxMDSC Inhibition

As far back as 2003, Coffey *et al.* highlighted the perioperative period as a critical window of opportunity for immunotherapies(72). However, it has been largely ignored in the development of new immunotherapies. Currently, less than 1% of registered cancer trials are investigating the perioperative period(170). To identify therapeutic targets that attenuate suppression in sxMDSCs, Dr. Angka, a former PhD student in our lab, conducted a high-throughput screen of small molecules (Supplemental Figure 1) in collaboration with the Centre for Drug Research and Development (ADMARE). The screen used a miniaturized *ex vivo* suppression assay (explained in section 4.1.6) where MDSCs, isolated on postoperative day 1 (POD1) from cancer surgery patients, are co-cultured with NK92 (effector) and K562 (target) cells. This screen identified the pan-PI3K inhibitor, LY294002, as a top MDSC antagonist (Supplemental Figure 1). The PI3K/AKT pathway has been shown to control the suppressive phenotype of "M2" macrophages in addition to controlling myeloid cell accumulation and trafficking(171). However, PI3K is important for many cell functions(172), therefore clinical administration of a pan-PI3K inhibitor would have many toxic effects. In contrast, PI3Kγ is a myeloid-cell specific isoform(171), which would be a better tolerated target for inhibiting sxMDSC activity. Studies using PI3Kγ$^{-/-}$ mice or PI3Kγ specific inhibitors have shown that disabling PI3Kγ signalling leads to reduced tumour progression via a mechanism that prevents the recruitment and activation of MDSCs(171).

1.2.5.1 PI3K and its function

PI3Ks are a family of lipid kinases which play critical roles in many cellular processes, such as cell survival, proliferation, differentiation, and motility(172). PI3Ks catalyze the phosphorylation of the 3-hydroxyl position on inositol phospholipids, resulting in phosphorylation

of phosphatidylinositol$_{(4,5)}$P3 (PIP2) into the secondary messenger phosphatidylinositol$_{(3,4,5)}$P3 (PIP3)(173). PI3Ks are mainly grouped into three classes (Class I, II, and III) according to their structure and lipid substrate specificity. Class I PI3Ks are the most well-studied to date due to their frequent dysregulation in various cancers(172). Class I PI3Ks are heterodimeric enzymes, consisting of a regulatory subunit and catalytic subunit, p110. These can be further subdivided based on the associated p110 isoforms, of which there are 4 (α, β, γ, and δ). For p110α, p110β, and p110δ, the most common regulatory subunit is p85, while p110γ associates with the p101 or the p87 (also known as p84) regulatory subunit(173). In fact, p110γ has a complete loss of the binding domain necessary for interaction with p85(174). While class 1A isoforms, α, β and γ, are activated and transduce signals via receptor-tyrosine kinases (RTK)s. PI3Kγ is the only Class 1B isoform, given its unique association and signal transduction from G-protein coupled receptors (GPCR)s(173). However, PI3Kγ can indirectly be activated from RTKs through Ras. Indeed, Ras can be activated by both RTKs and GPCRs and it can engage all class I PI3Ks through their Ras-binding domain (RBD). Unlike the ubiquitously expressed PI3Kα and PI3Kβ, PI3Kγ is preferentially expressed in myeloid cells(175). The restricted expression pattern of PI3Kγ can alleviate the risk of undesirable side effects when targeting PI3K, which has motivated the development of PI3Kγ-specific inhibitors(176).

1.2.5.2 PI3Kγ signaling

Ligand binding and activation of the GPCR causes the allosteric activation of heteromeric G proteins, which consist of three subunits, called alpha, beta, and gamma subunits, or Gα, Gβ, and Gγ. Activation causes Gα to dissociate from Gβγ, allowing both to act as downstream signalling effectors. P101 is the crucial adaptor for Gβγ stimulation of PI3Kγ, thereby enabling

direct signal transduction following GPCR activation(177). The binding affinity of p101–p110γ for Gβγ was five-fold greater than for p110γ alone, suggesting that p101 sensitizes PI3Kγ for Gβγ-mediated activation. Interestingly, the p87 regulatory subunit shows little binding towards Gβγ and instead seems to sensitize PI3Kγ for Ras-mediated activation(177). In fact, Ras seems to be the most important for p87-mediated, rather than p101-mediated, membrane recruitment and activation of p110γ(178). Following activation, PI3Kγ follows a similar downstream signalling pathway to other class 1 PI3K isoforms.

As mentioned prior, PI3K phosphorylates PIP2 to PIP3 which is an important secondary messenger for downstream signalling. This activity is antagonized by phosphatase and tensin homologue deleted on chromosome 10 (PTEN), which is a PIP3 phosphatase(173). The signalling pathways coordinated by PIP3 is a highly complex network and would require an extensive review of its own. Instead, I will focus on an abbreviated view of the PI3K/AKT/mTORC axis. PIP3 serves as a "platform" that recruits and coordinates downstream effector proteins in close proximity for signal transduction. The pleckstrin homology (PH) domain, which is present on the constitutively active kinase, PDK1, and AKT are necessary for binding to PIP3. This enables the phosphorylation of AKT by PDK1(179). Therefore, monitoring the phosphorylation of AKT can be an indicator of PI3K activity. AKT has several sites of phosphorylation, the significance of which is yet to be understood(179). However, its activity depends on the phosphorylation of residues T308 (in the activation loop) by PDK1, and S473 (in the hydrophobic loop) by mTORC2 complex(180). Alessi *et al.* identified that T308 and S473 phosphorylation does not depend on one another(181). Therefore, if we are to determine PI3K activity via AKT activity, it is important to determine which residue is most consistent with AKT signalling. Currently, in most studies of AKT in cancer, the measurement of phosphorylation on Ser473 has been used as an indicator of

AKT activity. However, using Ser473 as a measure of AKT activity often leads to contradictory conclusions regarding whether AKT activity is prognostic for various cancers. For example, contradictory observations of AKT on has been correlated with poor prognosis in breast and ovarian cancer(182, 183), whereas other studies find this not to be the case(184).

A more reliable biomarker of AKT activity may be the phosphorylation of T308(180), arguably the more important regulator of AKT activity(185). Although much more rarely investigated than S473 phosphorylation, there are reports that the phosphorylation of T308 correlates with poor survival in NSCLC(186) and acute myeloid leukaemia(187), while no such correlation was seen with AKT S473 phosphorylation, in both reports. In samples of early-stage human NSCLC, Vincent *et al.* compared the phosphorylation status of T308 and S473 with that of three separate AKT substrates – PRAS40, TSC2, and TBC1D4(180). They demonstrated that AKT T308 phosphorylation correlated with the phosphorylation of each AKT substrate tested, whereas AKT S473 phosphorylation did not correlate with the phosphorylation of any of the substrates examined. AKT phosphorylates PRAS40 and TSC2 which suppresses their capacity to inhibit mTORC1 activity(188, 189). The phosphorylation of the T308 residue form is essential, and S473 is not needed, for AKT activity, in the context of activation of mTORC1, S6K, and protein synthesis(190, 191). Moreover, PI3K directly leads to the activation of PDK1 which phosphorylates T308(180). In comparison, S473 phosphorylation requires the recruitment of mTORC2 which can be under the control of other regulatory pathways, independent of PI3K activity(192). Taken together, if one were to investigate AKT signalling as a surrogate marker of PI3K activity, investigating phosphorylation of T308 would be more accurate than phosphorylation of the S473 residue.

1.2.5.3 PI3Kγ transduces signals from the surgery stress response

Interestingly, a body of work that was conducted outside of perioperative research demonstrated that factors that are abundantly present in the postoperative period such as IL-1B, IL-6, PGE-2, and DAMPs can transduce signals through PI3Kγ expressed on sxMDSCs, leading to their expansion, accumulation, and potentiation of suppressive activity. Schmid *et al.* identified that IL-1β and IL-6 stimulated Rap-GTP loading in $CD11b^+$ cells, in a PI3Kγ-dependent manner(193). This potentiated their suppressive activity. Very recently, Yang *et al.* demonstrated that IL-6 signalled through PI3Kγ, leading to the proliferation and activation of MDSCs, as well as inducing the suppression of cytotoxic $CD8^+$ T lymphocytes. Blockade of PI3Kγ reversed the observed expansion and potentiation of suppressive activity(194). PI3Kγ signalling was also found to be critical in mediating myeloid cell proliferation and viability in response to DAMPs(195). PGE-2 induces chemotaxis via activation of the downstream PI3K target, mTOR. PGE-2 was found to induce activation of mTORC1 as indicated by increased p70S6K and 4E-BP1 phosphorylation, and activation of mTORC2, as indicated by increased phosphorylation of AKT. Inhibition of mTORC1 or mTORC2 lead to a significant reduction in chemotaxis(196). Taken together, PI3Kγ may be involved in transducing signals from factors that are present during the surgery stress response to mediate the expansion and activation of sxMDSCs.

1.2.5.4 Targeting PI3Kγ as an inhibitor of MDSC activity

To further corroborate the role of PI3Kγ in prompting MDSC activity, Kaneda *et al.* demonstratedthat this signalling pathway controls an immunosuppressive transcriptional program in myeloid cells. In studies using $p110\gamma^{-/-}$ mice and PI3Kγ small molecule inhibitors (IPI-549),

they demonstrated that genes associated with immune suppression were downregulated in the myeloid cells, as compared to controls(171). The mechanism was sustained p65RelA phosphorylation with simultaneous inhibition of C/EBPβ and AKT phosphorylation. This is coupled with increased phosphorylation and activation of the NF-κB pathway which promotes an immunostimulatory transcriptional program that restores anti-tumour immunity and cytotoxicity. The investigators demonstrated significant upregulation of IL-12β and IFN-γ transcripts and effector molecules, coupled with downregulation of IL-10 and ARG1(171, 197). Moreover, T cells from these animals expressed more IFN-γ and Granzyme B with less IL-10 and TGF-β. These mice had a significant reduction in tumour growth, which was found to be dependent on myeloid cells and $CD8^+$ T cells by using depletion and myeloid-cell specific PI3Kγ knockout. Moreover, PI3Kγ was abundantly expressed in the myeloid cells and absent in the cancer models tested(171), suggesting that the reduction in tumour growth was due to a reprogramming of the myeloid cell compartment. The concept of PI3Kγ as a master regulator of myeloid cell polarization was further solidified by Li *et al.* They demonstrated that dual blockade of PI3Kγ and CSF-1R induced immunosuppressive tumor associated macrophages (TAM) remodeling effects by reducing M2 TAM levels and elevating M1 TAM levels, and also suppressed tumor infiltration of MDSCs(198). Consequently, this remodelling of TAM subsets was associated with activated antitumor immune responses and enhanced anti-pancreatic tumor effects via PI3Kγ blockade and downregulation of CSF-1R. More recently, it has been demonstrated that p110γ mediates GPCR-dependent ROS generation by binding and phosphorylating protein kinase C (PKCα)(199).

Davis *et al.* identified that targeting MDSCs in the tumour microenvironment with IPI-549 for PI3Kγ inhibition, led to enhanced responses to PD-L1 blockade(200). They identified that these improvements were due to reduced suppressive activity in tumour-infiltrating MDSCs, which

induced $CD8^+$ T lymphocyte-dependent primary tumor growth delay and prolonged survival. Zhang *et al.* investigated the efficacy of encapsulated IPI-549 in targeted polymeric nanoparticles (NP) for inhibiting PI3Kγ in tumour-infiltrated myeloid cells in both murine pancreatic cancer and melanoma models(201). They identified that IPI-549 NP significantly decreased tumor growth and prolonged host survival in both models. Importantly, IPI-549 NP treatment reduced the suppressive tumor microenvironment by decreasing suppressive myeloid cells in the tumour. A phase I first in-human clinical trial of IPI-549, in combination with the PD-1 inhibitor, nivolumab, is currently ongoing with early clinical and immune activity(202). Given the therapeutic potential of PI3Kγ targeting in the myeloid compartment, this is an attractive candidate small molecule target for perioperative attenuation of sxMDSCs.

1.3 Objective, Rationale, and Hypothesis

1.3.1 The Primary Objective

The main goal of my thesis was to identify the PI3Kγ signalling pathway as a therapeutic target for reducing postoperative NK cell dysfunction and metastatic burden. This goal encompassed investigating the role of PI3Kγ in the highly immunosuppressive phenotype observed in postoperative MDSCs.

1.3.2 Rationale

Surgical stress leads to significant metastatic burden in several animal models. This observation is coupled with the rise of highly active and immunosuppressive sxMDSCs in the postoperative environment. The cascade of physiological signals released in response to surgical stress is a strong promoter of these "supercharged" sxMDSCs. Gao *et al.* demonstrated that high

systemic inflammation following surgery was correlated with a greater expansion of sxMDSCs. As well, the degree of expansion of sxMDSCs was correlated with a lower time to recurrence and OS(127). Moreover, the surgery itself causes the formation, release, growth, and persistence of CTCs, which are typically targeted and eliminated by NK cells(27, 28). However, given the role of sxMDSCs in NK cell dysfunction, it provides a window of opportunity for these CTCs to re-establish distant metastases(69, 72, 77, 203). Studies have identified that poor CTC clearance following tumour resection is a strong indicator of early cancer recurrence(27–29, 70).

Altogether, this narrative identifies sxMDSCs as a "bad actor" in postoperative tumour surveillance, sabotaging the efforts of host defenses and surgery teams alike, by preventing clearance of residual tumour cells and enabling cancer recurrence. This highlights the importance of therapeutic targets capable of inhibiting sxMDSC activity. One such target is PI3Kγ, which Dr. Angka identified as a key player in the suppressive activity of sxMDSCs. Moreover, genetic knockout or pharmacological inhibition of PI3Kγ leads to a significant reduction of tumour volume and improved anti-tumour immune response(171). Several PI3Kγ inhibitors are now being investigated for clinical applications in various phase 1 clinical trials(204, 205). However, despite the attention this pathway has received with respect to conventional cancer therapeutics, to date, PI3Kγ has never been reported as a target for the prevention of metastatic recurrence and NK cell dysfunction in the perioperative setting. Targeting this pathway for the blockade is favourable since this isoform is primarily expressed in myeloid cells which, from a clinical perspective, reduces the potential for toxic side effects compared to pan-PI3K inhibition(201). However, as a contingency, in case there are any side effects with systemic PI3Kγ inhibitor administration, I also investigated the efficacy of an MDSC-specific antibody drug conjugate (ADC) based PI3Kγ

inhibitor therapeutic. Taken together, PI3Kγ is a very appealing and novel perioperative therapeutic for reducing postoperative NK cell dysfunction and reducing metastatic burden.

1.3.3 Hypothesis

I hypothesize that PI3Kγ mediates the immunosuppressive mechanisms of sxMDSCs which contributes to NK cell suppression and post-operative metastatic disease.

1.3.3.1 Aims

1 Investigate the postoperative alterations in PI3Kγ signalling in postoperative MDSCs.

2 Determine the role of PI3Kγ in the immunosuppressive activity of MDSCs.

3 Investigate the effects of PI3Kγ inhibition as a therapeutic to reduce postoperative metastatic burden.

4 Investigate the efficacy of a clinically actionable PI3Kγ ADC in inhibiting the suppressive capacity of MDSCs.

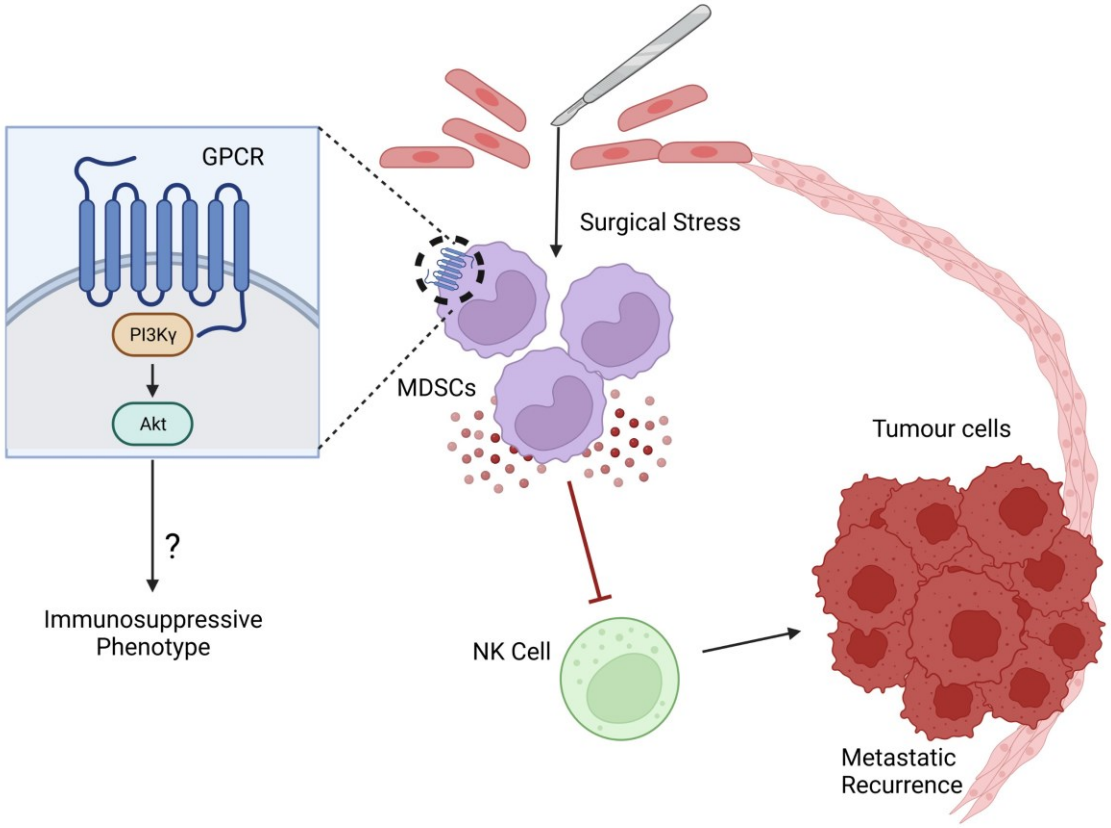

Figure 1: Hypothesized Model of Surgical Stress. Surgical stress unleashes a cascade of signals resulting in the expansion, persistence, and activation of postoperative sxMDSCs. sxMDSCs can directly inhibit NK cell anti-tumour immunity, thereby preventing tumour cell clearance and enabling metastatic recurrence. My project investigated the role of PI3Kγ signalling in the immunosuppressive activity of sxMDSCs, NK cell dysfunction, and postoperative metastatic disease.

4.1 Methods

4.1.1 Cell Lines

K562 (human leukemia, ATCC CCL-243™) and YAC-1 (murine lymphoma, ATCC TIB-160™) cells were obtained from the American Type Culture Collection (ATCC; Manassas, VA) and maintained in HyClone™ Roswell Park Memorial Institute (RPMI) 1640 medium (GE Healthcare; Mississauga, ON) supplemented with 10% Fetal Bovine Serum (FBS; Sigma-Aldrich, St. Louis, MO), labelled as Complete RPMI (CRPMI). NK92 MI (human NK cell, ATCC CRL-2408™) was also obtained from ATCC and maintained in HyClone™ RPMI 1640 (GE Healthcare; Chicago, IL) supplemented with 10% FBS (Sigma-Aldrich; St-Louis, MO), 50,000 Units (U) of Penicillin-Streptomycin (Pen-Strep; Thermo Fisher Scientific, Waltham, MA), 10mM HEPES (Sigma-Aldrich) and 55μM β-mercaptoethanol (Sigma-Aldrich). B16F10-LacZ (murine melanoma expressing LacZ) were previously transfected by Christiano T. de Souza and maintained in HyClone™ Minimum Essential Medium α (MEM α; GE Healthcare) supplemented with 10% FBS (Sigma-Aldrich). All above cell lines were cultured in a 37°C incubator with 5% CO_2.

4.1.2 Reconstitution and dosing regimen of pan-PI3K/PI3Kγ inhibitors

All inhibitors were purchased from Selleckchem Technologies, Houston, TX. For *ex vivo* studies, lyophilized pan-PI3K inhibitor, LY294002, and PI3Kγ specific inhibitors, TG100-115 and IPI-549, were reconstituted in DMSO to a stock concentration of 10mM. Inhibitors of PDK1 (GSK2334470), AKT (MK-2206), and S6K (LY2584702) were also reconstituted in DMSO to a stock concentration of 10mM. Reconstituted drugs were stored at -80°C for a maximum of 6 months. For *in vivo* studies, desiccated TG100-115 and IPI-549 were reconstituted in DMSO to 15mg/mL and 75mg/mL, respectively. *In vivo,* formulations for TG100-115 was prepared at

3mg/kg of body weight or 6mg/kg of body weight in PBS with 30% (v/v) PEG-300 (Sigma-Aldrich). IPI-549 was prepared at 15mg/kg of body weight or 30mg/kg of body weight in PBS with 40% (v/v) PEG-400 (Sigma-Aldrich). These formulations were prepared fresh every morning prior to administration. All drug treatments for mice began 1 day before surgery (Day -1) and were administrated daily up to POD1 (3 days in total). IPI-549 was administered by oral gavage twice daily while TG100-115 was administered once daily intraperitoneally. 200µL of either formulation was administered. Compound 17, which was only used for *ex vivo* studies, shares a similar chemical structure to TG100-115 and was generated by our collaborators at ADMARE using the protocol described by Palanki *et al.*(206).

4.1.3 Animals

All C57Bl/6 mice were purchased from Charles River Laboratories (Wilmington, VA) and housed under strict pathogen-free conditions at the University of Ottawa Animal Care and Veterinary Services (ACVS) facility (Ottawa, ON). Murine protocols complied with the Canadian Council on Animal Care guidelines and were approved by the University of Ottawa Animal Research Ethics Board prior to initiating experiments.

4.1.4 Perioperative Human Blood and Tissue Collection Program

Cancer patients were consented through the *Perioperative Human Blood and Tissue Collection Program* (PHBSP), which was approved by the Ottawa Health Science Network (OHSN) Research Ethics Board (REB) under protocol number 2011884. For recruitment, any patient over 18 years of age with diagnosis of resectable primary malignancy was included. The following exclusion criteria were used: haemoglobin levels below 90, immunosuppressive conditions such as Lupus, Rheumatoid Arthritis, or steroid use, as well as recent neoadjuvant

chemotherapy and/or radiation therapy within the last 4 weeks. Blood was drawn by registered nurses in the surgical day care unit (SDCU) at baseline before surgery and on the surgical wards on POD1. A total of 40mL of blood was collected into BD Vacutainer™ sodium heparin collection tubes (Thermo Fisher Scientific) for each timepoint and processed within 2 hours. Blood was gently overlaid on Ficoll-Paque PLUS (Thomas Scientific; Swedesboro, NJ) and centrifuged with the parameters indicated in the manufacturer's protocol(207). Peripheral blood mononuclear cells (PBMCs) were isolated from the buffy coat, washed with HyClone™ Phosphate-Buffered Saline (PBS; GE Healthcare), and counted on the Vi-Cell XR™ (Beckman Coulter; Brea, CA) for further experimentation.

4.1.5 MDSC Immunophenotyping

The panel of MDSC markers were chosen with slight modifications based on published guidelines to harmonize human MDSC reporting led by the Association for Cancer Immunotherapy, Cancer Immunoguiding Program(208). Freshly isolated PBMCs were resuspended in PBS and first labelled with a fixable viability stain BV510 (BD Biosciences; San Jose; CA) in PBS at room temperature for 10 minutes. Next, an extracellular MDSC antibody mastermix was added for an additional 20 minutes at 4°C in the dark. The antibodies in the MDSC mastermix were used at individually titrated dilutions and included: CD33 Pe-Cy7 Clone P67.6 (Biolegend, San Diego, CA), CD14 Clone MφP9 APC-Cy7 (BD Biosciences), CD15 Clone MMA efluor450 (Thermo Scientific), and lineage markers CD3 Cline HIT3a FITC (Thermo Scientific), CD56 Clone NAM16.2 FITC (BD Biosciences) and CD19 Clone HIB19 FITC (Biolegend). For murine MDSCs, the following antibody panel was used: Ly6G Clone 1A8 BV605 (BD Biosciences), Ly6C Click HK1.4 AF700 (Biolegend), and CD11b Clone M1/70 FITC (Biolegend). All antibody master mixes were prepared in Flow Buffer, comprised of PBS (GE Healthcare),

0.2% (v/v) UltraPure™ 0.5M EDTA (Thermo Fisher Scientific), and 0.5% (w/v) Bovine Serum Albumin (BSA; Bioshop Canada; Burlington, ON).

4.1.5.1 Phospho-signalling functionality assay

For *in vitro* phospho-AKT staining, PBMCs (humans) or splenocytes (mouse) were incubated for 3 hours with or without PI3Kγ inhibitor treatment in CRPMI at 37ºC in a 5% CO_2 chamber. During the last 15 minutes of incubation, MDSCs were stained with the fluorophore-conjugated antibody master mix as described in section 4.1.5. Prior experiments confirmed the stability of these antibodies and their conjugated fluorophores to the harsh fixation and permeabilization process involved with phosphoprotein flow staining. Splenocytes underwent a simultaneous Lyse/Fix step using Lyse/Fix buffer (BD Biosciences) while PBMCs were fixed with fixation buffer (BD Biosciences), and both were incubated for 10 minutes at 37ºC. Samples were then permeabilized according to the BD Phosflow protocol III using Perm buffer III (BD Biosciences)(209). Cells were washed twice with flow buffer and then stained with AKT pT308 Clone D25E6 PE (Cell Signalling Technology; Danvers, MA) and AKT pS473 Clone M89-61 AF647 (BD Biosciences) for 1 hour on ice in the dark. A final wash was performed with flow buffer and the phosphorylation status of AKT was determined by flow cytometric analysis on the BD Fortessa (BD Biosciences).

4.1.6 MDSC:NK92 Suppression Assay

Bulk sxMDSCs (M-MDSCs and G-MDSCs) were sorted from freshly isolated PBMCs on POD1 by automatic magnetic bead separation using the Automacs Cell sorter (Miltenyi; North Rhine-Westphalia, Germany) with positive selection using CD33 immunomagnetic (IM)

microbeads (Miltenyi) according to the manufacturer's protocol(210). MDSCs were washed with pre-warmed CRPMI, counted by hemocytometer (HC), and resuspended to 8 x 10^5 cells/mL. They were then plated in triplicates on a tissue-culture treated, V-bottom 96 well plate (Corning). The IL-2 independent NK cell line, NK92-MI, was also washed with CRPMI, counted on HC, resuspended to 2x10^5 cells/mL, and plated in a co-culture with the MDSCs. MDSCs and NK cells were plated at a ratio of 8:1 (1.6x10^5 MDSCs : 2x10^4 NK cells per well), 4:1 (8x10^4 MDSCs : 2x10^4 NK cells per well), 2:1 (4x10^4 MDSCs : 2x10^4 NK cells per well), and 1:1 (2x10^4 MDSCs : 2x10^4 NK cells per well). However, the 4:1 ratio is considered the most biologically relevant. As a control, NKC in the absence of MDSCs was examined by plating NK cells in triplicates at the following diluted concentrations for effector-to-target (E:T) ratios 8:1 (4x10^4 NK cells : 5x10^3 targets per well), 4:1 (2x10^4 NK cells : 5x10^3 targets per well) and 2:1 (1x10^4 NK cells : 5x10^3 targets per well). For these control wells, plated NK cells underwent the same 20-hour incubation and K562 target cells were added following this period. Pan-PI3K inhibitor, LY294002, or PI3Kγ specific inhibitors, IPI-549 or TG100-115, was added at the concentrations indicated in the respective figure legends (in most experiments it was 1μM) at the start of this incubation period.

Following the 20-hour incubation, K562 target cells were washed in PBS, resuspended to 1 x10^6 cells/mL, and labelled with Cell Proliferation Dye eFluor™ 450 (CP450; eBioscience; San Diego, CA, USA) for 15 minutes at 37ºC. Labelling was stopped by washing with CRPMI. K562 target cells were counted by HC and resuspended to a concentration of 1 x10^4 cells/mL. 5x10^4 CP450-K562 cells were then added to all wells in the MDSC:NK co-culture in triplicates and incubated for 4 hours at 37ºC. NKC was then measured by adding viability dye Ethidium homodimer (EtHD, Thermo Scientific) to each well just before acquiring the samples by flow cytometry. Samples were analyzed using the high-throughput sampler on the BD Celesta™ (BD

Biosciences) at the University of Ottawa Flow Cytometry Core Facility (Ontario, ON). NKC was measured as the percentage of dead CP450-labelled K562 target cells gated on $CP450^{+}/EtHD^{+}$. To calculate %MDSC suppression, I used Equation 1.

$$\left(1 - \frac{(\%\text{dead K562}_{\text{MDSC: NK}})}{(\%\text{dead K562}_{\text{NK alone}})}\right) \times 100\% = \%\ \text{MDSC suppression}$$

Equation 1: Calculation of % Suppression.

4.1.7 Isolation of M-MDSC and G-MDSC Sub-populations

POD1 PBMCs were split into two workflows: one-third of the PBMC pool was used for M-MDSC isolation, while the rest were used for G-MDSC isolation. PBMCs that were used for M-MDSC isolation underwent CD33 IM positive selection as described in section 4.1.6. Next, the positive fraction was counted on HC and stained with the MDSC panel described in section 4.1.5, however the following substitutions were made, 1) LIN markers were not included, 2) CD15 PE (BD Biosciences) replaced CD15 efluor450, 3) L/D APC (Thermo Scientific) replaced L/D BV510. Following counting on HC, positive fraction was resuspended at $2x10^6$ cells/mL concentration. A small aliquot ($1x10^6$ cells) of the stained positive fraction (Bulk sxMDSCs) was left aside at 4ºC for the final suppression assay plating. The remaining stained $CD33^{+}$ cells underwent fluorescence activated cell sorting (FACS) to isolate live $CD33^{+}CD14^{+}CD15^{-}$ cells using the MA900 Multi-Application Cell Sorter (Sony; San Jose, CA).

A similar procedure was used to isolated G-MDSCs. The PBMC fraction underwent a positive selection using CD15 IM microbeads (Miltenyi). The positive fraction was counted,

stained, and resuspended as described above. The stained positive fraction underwent FACS to isolation $CD33^{+}CD14^{-}CD15^{+}$ fraction which was labelled as G-MDSCs. Sorted M-MDSCs, G-MDSCs and bulk sxMDSCs were washed twice in CRPMI, counted on HC, and plated according to the *ex vivo* suppression assay described in 4.1.6.

4.1.8 Measurement of TGF-β in MDSC Supernatant by ELISA

PBMCs were first isolated on POD1 from cancer surgery patients as outlined in section 4.1.4. SxMDSCs were then sorted according to section 4.1.6. SxMDSCs were plated at a $1x10^6$ cells/mL concentration and incubated for 24 hours at 37°C in the presence or absence of 1μm IPI-549, or 10ng/mL IL-4, or both. Following incubation, sxMDSCs were pelleted at 500g for 5 minutes and the supernatant was collected.

The R&D Quantikine® Enzyme Linked Immunoassay (ELISA) Human TGF-β Immunoassay was used to quantify TGF-β in MDSC supernatant. Measurement of total TGF-β required acid activation of latent TGF-β, while measurement of active TGF-β did not. This assay was performed using the R&D Quantikine® ELISA protocol(211).

4.1.9 MDSC Supernatant Suppression Assay

Isolated POD1 sxMDSCs were cultured for 24 hours with or without 1μM IPI-549. Following this treatment period, cells were spun down at 500g for 5 minutes. The supernatant was then collected, while ensuring that the cell pellet was not disturbed. This MDSC-conditioned media was mixed with fresh media at a 1:1 ratio (50% supernatant, 50% fresh media) and plated with NK cells co-cultured with target K562 cells in a killing assay. Control killing assay with fresh media and 100ng/mL rTGF-β was included to compare the effects of MDSC-conditioned media.

4.1.10 Bioactive TGF-β Cell-based Quantification Assay

HEK-Blue™ TGF-β (Invivogen; San Jose, CA) cells were used as a cell-based assay to detect bioactive TGF-β. These cells were engineered from the human embryonic kidney (HEK) 293 cell line with the stable overexpression of a Smad-inducible secreted embryonic alkaline phosphatase (SEAP) reporter. The binding of TGF-β to its receptor on the surface of HEK-Blue™ TGF-β cells trigger a signaling cascade that induces the transcription, expression, and secretion of SEAP. HEK-Blue™ TGF-β cells were maintained, passaged and used to quantify bioactive TGF-β according to the manufacturer's protocol(212). Briefly, $2.77x10^5$ cells/mL of HEK-Blue™ TGF-β cells were plated on a 96-well plate, along with the supernatant samples collected (including media alone and 100pg/mL rTGF-β controls) in section 4.1.9, and incubated for 24 hours. During this incubation, bioactive TGF- β would cause signalling in the HEK-Blue™ cells, leading to measurable accumulation of SEAP. Therefore, SEAP expression is proportional to the quantity of TGF- β in the supernatant sample. SEAP was measured using the QUANTI-Blue™ assay (Invivogen) according to the manufacturer's protocol(213). This a colorimetric alkaline phosphatase assay and samples were incubated for 1 hour, followed by measurement of absorbance at 650nm using a spectrophotometer.

4.1.11 Reveserse transcriptase (RT) quantitative PCR (qPCR)

MDSCs were isolated and counted as outlined in section 4.1.6. MDSCs were diluted to a concentration of 1x106 cells/mL in the presence or absence of 1μM IPI-549 for 24 hours at 37oC. 2x106 MDSCs were used for RNA extraction using the RNaeasy Kit (Qiagen), according to the manufacturer's protocol. Extracted RNA was quantified on the NanoDrop One Spectrophotometer (ThermoScientific) instrument. cDNA was prepared using 1μg RNA with the

Applied Biosystems™ High-Capacity cDNA Reverse Transcription Kit with RNase Inhibitor (Fisher Scientific), according to the manufacturer's protocol. PCR primers were titrated and optimal melting temperature was determined by preliminary melt curve experiment. Sybr green-based qPCR was performed using human primers to Arg1, Il10, Tgfb, Il1b, Il12b, Tbp and Tnfa, using the SsoAdvanced™ Universal SYBR® Green Supermix (Bio-Rad). mRNA levels were normalized to Tbp (ΔCt = Ct gene of interest – CtTbp). mRNA expression was normalized to baseline samples (ddCt = 2^-(ΔCtsample – ΔCt baseline)).

4.1.12 Murine Model of Surgical Stress

Within a few days, surgical stress can impact NKC and ultimately, lead to greater metastatic burden. We examined the systemic effects of surgery on NKC and postoperative metastatic burden, using the methodology described in sections 4.1.12.2 and 4.1.12.3 respectively. Drug administrations were performed as outlined in section 4.1.2.

4.1.12.1 Inducing surgical stress in a murine model

Surgical stress was induced by performing an invasive left nephrectomy. This is followed by abdominal closure using 5-0 Polysorb suture (Covidien; New Haven, CT) and skin staples. On POD1 or POD3, the mice were sacrificed by lethal buprenorphine IP injection at 0.1 mg/kg body weight, followed by cervical dislocation. Spleens were harvested via the left upper quadrant abdominal incision and splenocytes were dissociated through sterile 70 µm Cell Strainers (Thermo Fisher Scientific). Splenocytes were washed once in CRPMI, counted, and used for subsequent experiments.

4.1.12.2 Ex-vivo Murine MDSC:NK Suppression assay

On POD1 endpoints, processed splenocytes were pooled for each treatment group (minimum 4 mice per group). Treatment groups included mice that received surgery, drug administration, and a combination of both or none as controls. MDSCs were isolated from pooled splenocytes using the mouse MDSC isolation kit (Miltenyi) by immunomagnetic positive selection on the AutoMacs^{TM} Cell Sorter, according to the manufacturer's protocol(214). NK cells were isolated from pooled splenocytes processed from healthy mice that did not receive surgery or drug administration using the EasySep^{TM} Mouse NK Cell Isolation Kit (Stemcell; Vancouver, CA) as per the manufacturer's protocol for immunomagnetic negative selection. NK cells and MDSCs were washed, counted and plated as described in section 4.1.6. Yac-1, a murine lymphoma cell line, were used as targets (instead of K562s) and underwent the same labelling, plating, and viability staining as described in section 4.1.6 to assess murine NKC.

4.1.12.3 Assessing the postoperative metastatic burden

This animal model of surgical stress has been previously published(103, 108). B16F10-LacZ melanoma cells ($3x10^5$ cells, minimum 90% viability) were injected via intravenous (IV) tail vein into C57Bl/6 mice. 3 days following the tumour challenge, our standardized LacZ staining protocol was used for lung metastases(103). On the first day, lungs were washed twice in Wash Buffer (1M magnesium chloride, 1% deoxycholate, 2% nonidet-P40, 0.1M sodium phosphate buffer pH 7.3), and then stained overnight at 37^{o}C with X-Gal^{TM} solution, 25 mg/mL in Dimethylsulfoxide (X-Gal in DMSO; Bioshop Canada). The next day, lungs were washed twice with Wash Buffer and incubated for 24 hours at 4^{0}C. On the third day, lungs were transferred into

10% buffered formalin for permanent fixation. Lungs were imaged using the Axiovision software v4.8 (Zeiss; Oberkochen, Germany) on the Zeiss SteREO^{TM} Discovery Modular Microscope (Zeiss). From these electronic images, lung metastases were quantified using Fiji ImageJ.

4.1.12.4 Adoptive Transfer

To assess the effects of MDSC-specific inhibition of PI3Kγ, I utilized an MDSC adoptive transfer method(103). Here, donor mice received TG100-115, IPI-549, or no treatment following the dosing regimen outlined in section 4.1.2 (n = 8 per group). One day after drug administration began, surgery was conducted as described in section 3.8.1. As a control, a group of donor mice that did not receive surgery was included. On POD1, MDSCs were isolated as described in section 4.1.12.2 and resuspended to $1x10^7$ cells/mL concentration. Next, $5x10^6$ isolated MDSCs were adoptively transferred to each recipient mice from their respective donor experimental group, except for the no transfer control group. One hour after the adoptive MDSC transfer, donor mice were tumour challenged with B16F10-LacZ, and lung metastases were counted on day 3 as outlined in section 4.1.12.3.

4.1.13 Statistical Analysis

Statistical tests were performed using GraphPad Prism 9. Unless stated otherwise in the figure legend, unpaired, non-parametric Mann-Whitney tests were performed when comparing between two groups *(i.e.,* Baseline vs POD1). When comparing more than 2 groups *(i.e.,* Baseline, POD1, and healthy), an unpaired, non-parametric Kruskal-Wallis test was used with Dunnett's multiplate comparisons test. Significance was denoted as *p≤0.05; **p≤0.01; ***p≤0.001; ****p≤0.0001.

4.2 Results

4.2.1 Demographic Data

The demographic data for 42 cancer patients who participated in this study is summarized in Table 1. Patients were diagnosed with various forms of cancer, in order of decreasing frequency: colorectal (30%), prostate (21%), lung and pancreatic (11%), renal (9%) ovarian, and neuroendocrine (7%), with an even spread in the cancer staging.

Table 1: Study participant demographics

Category	Sub-Category	Result
Total (n)	N/A	42
Gender (n)	Male	24
	Female	18
Age (mean yrs; *95% CI*)		64; *60 - 67*
Duration of surgery (mean hrs; *95% CI*)		3.40; *2.76 – 4.04*
Type of cancer (n)	Prostate	9
	Colorectal	13
	Lung	5
	Ovarian	3
	Renal	4
	Neuroendocrine	3
	Pancreatic	5
Staging (n)	I	7
	II	9
	III	11
	IV	9
	Unknown	6

4.2.2 Myeloid Derived Suppressor Cells Expand Following Surgery in Cancer patients

The expansion and persistence of sxMDSC in the postoperative period has been reported previously. I profiled a cohort of cancer surgery patients (n=10) from various cancer histologies, surgical procedures, sex, and ages for changes immediately following surgery (POD1) using a harmonized multicolour flow cytometry panel for human MDSCs (Figure 2)(208). I specifically focused our analysis on the expansion and characterization of myeloid cells ($CD33^{+}Lin^{-}$), which was observed to be elevated before surgery in cancer patients compared to healthy volunteers. On POD1, there was a significant increase in the proportion of $CD33^{+}Lin^{-}$ myeloid cells (Figure 2C, $p<0.0001$). G-MDSCs did not undergo any expansion post-operatively (Figure 2D). In contrast, the majority of sxMDSCs on POD1 were M-MDSCs and they underwent significant expansion (Figure 2E). In Moreover, it was previously shown in our lab by Dr. Angka that HLA-DR MFI is significantly lower in sxMDSCs than on baseline (Supplemental Figure 2).

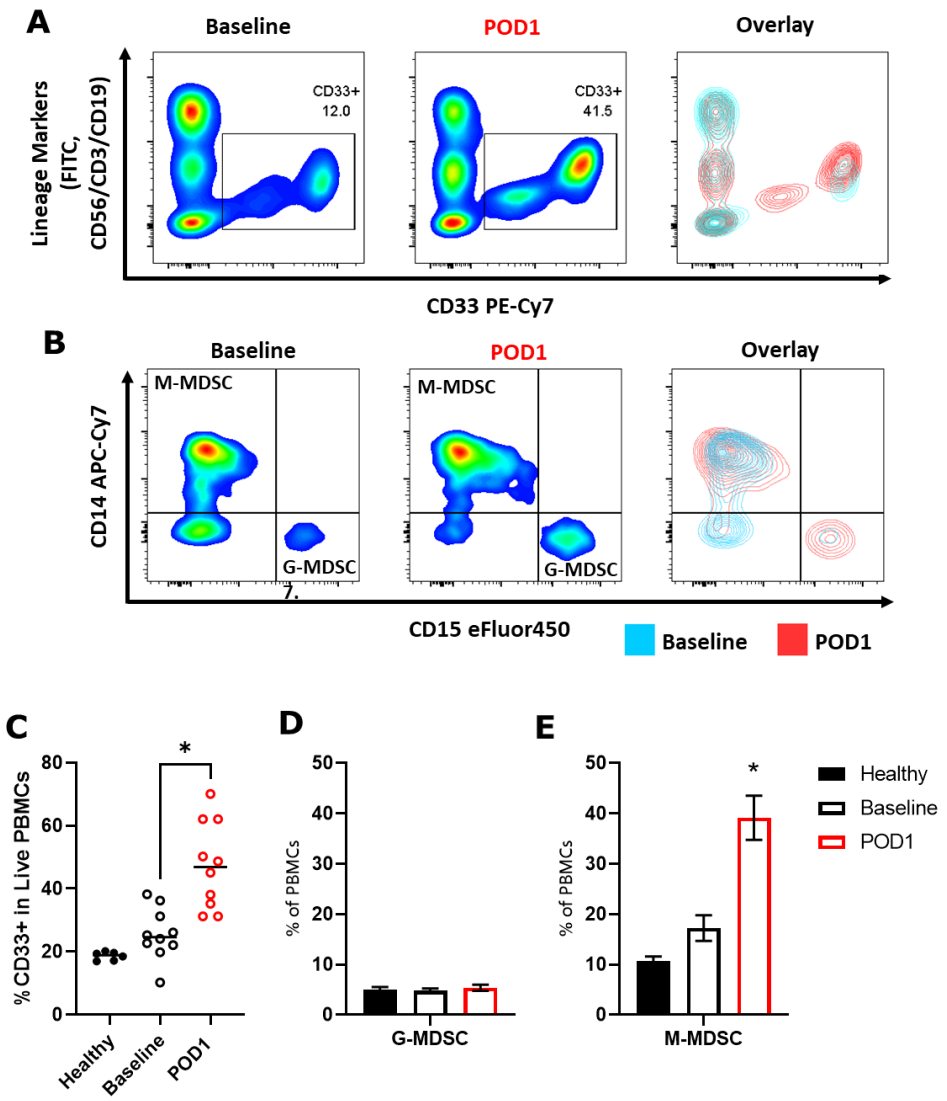

Figure 2: Significant expansion of primarily M-MDSCs following surgery (POD1). Blood was collected from patients before surgery (baseline) and on postoperative day 1 (POD1). PBMCs were isolated by Ficoll-paque density centrifugation and stained with a harmonized multicolour flow panel for human MDSCs. **A)** Representative flow plots showing CD33 versus Lineage Markers (CD3/CD56/CD19) for Baseline (blue) and POD1 (red) PBMCs. **B)** Representative flow plots gated on $CD33^{+}Lin^{-}$ MDSCs showing CD15 versus CD14 expression. **C)** Mean ± standard error mean (SEM) of healthy controls (n=6), baseline and POD1 patients

(n=10) proportion of bulk $CD33^{+}Lin^{+}$ MDSCs, **D)** M-MDSC ($CD14^{+}CD15^{-}$) and **E)** G-MDSC ($CD14^{-}CD15^{+}$) subsets (mean ± SEM shown).

4.2.3 Surgical stress potentiates the suppressive activity of sxMDSCs

To measure the suppressive capacity of MDSCs, I co-cultured NK cells with MDSCs isolated from POD1 PBMCs before determining the NKC of target tumour cells in a suppression assay (Figure 3A). Isolated MDSCs were determined to be more than 90% pure, with little contamination from other cell types (Figure 3B). Moreover, suppression of NK cells was not due to MDSCs being targeted by NK92s because the viability of $CD33^{+}$ cells was not affected following 6 or 24hr co-cultures with NK92 cells (Supplemental Figure 3). Fluorescently labelled K562 target tumour cells ($V450^{+}$) were gated and killing was determined using a viability dye (PI^{+}) (Figure 3C). Postoperative sxMDSCs demonstrated significantly greater suppressive capacity than baseline counterparts (Figure 3D).

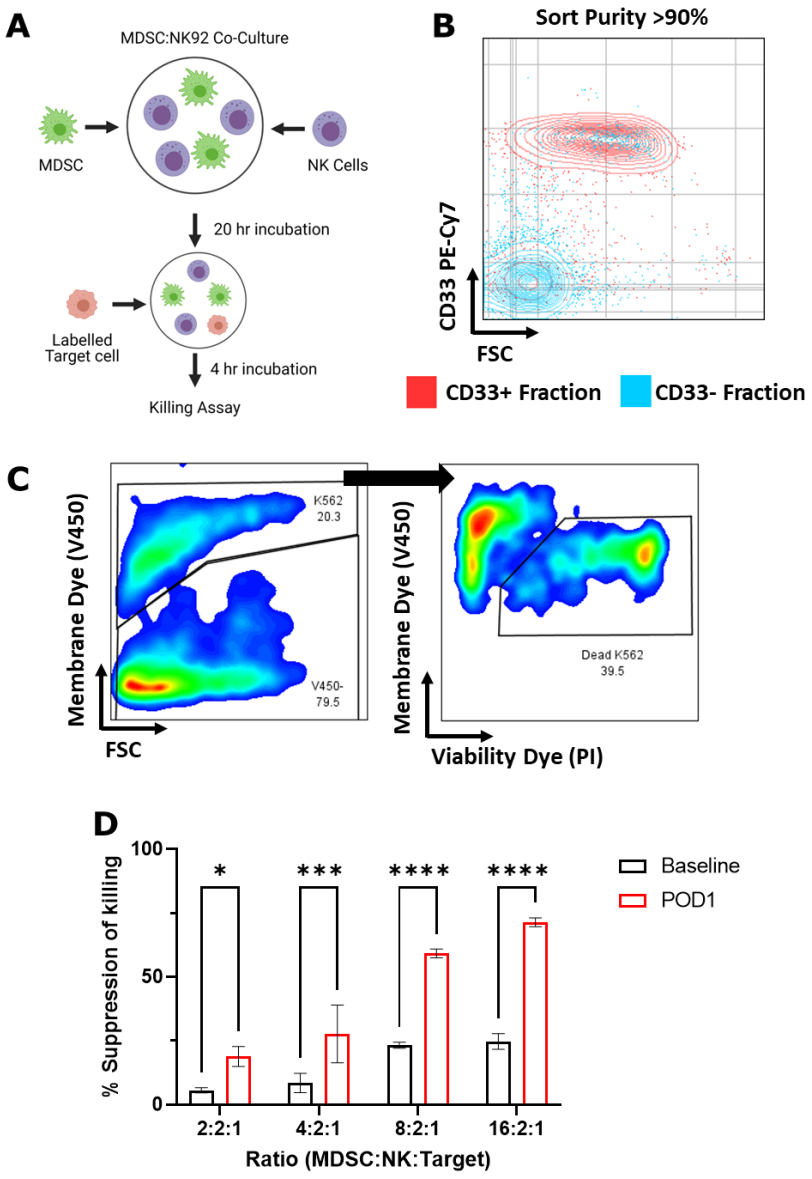

Figure 3: sxMDSCs mediate suppression of NK cell cytotoxicity. A) Schematic of suppression assay workflow. $CD33^{+}$ myeloid cells (MDSC)s were isolated from PBMCs, either on baseline or POD1, using a CD33 IM positive selection. MDSCs were co-cultured with NK92-MI cells for 24 hours. In the final 4 hours, fluorescently labelled NK-sensitive K562 target cells were added to the co-culture and killing was quantified by flow-based assay. **B)** $CD33^{+}$ (red) and CD33- (blue) fraction following CD33 positive selection. **C)** Gating strategy for identifying

K562 cells labelled with fluorescent membrane dye ($V450^+$) and killing (Viability Dye, PI^+) **D)** Mean ± SEM of suppression assay with increasing relative concentration of MDSCs isolated from baseline or POD1 PBMCs (n=3). %Suppression of killing is shown which was determined by comparing NKC in wells containing MDSC:NK to control wells where MDSCs weren't present (0:2:1, MDSC:NK:K562 ratio). Equation 1 was used to calculated % suppression of killing. Statistics were performed by two-way ANOVA with Šídák's multiple comparisons test, with a single pooled variance.

4.2.4 Surgery-induced M-MDSCs specifically mediate suppression of NKC

I isolated surgery induced (sx)M-MDSC and sxG-MDSCS using FACS to determine the suppressive capacity of each subpopulation. Given the slow rate of FACS, both sxM- and sxG-MDSCs had to be pre-sorted prior to isolation of each specific sub-population. As mentioned in section 4.1.6, CD33 IM positive selection was used to isolate sxMDSCs. The positive fraction, which is used for suppression assay plating, contains both sxM- and sxG-MDSCS. However, as noted in Supplemental Figure 4B, the negative fraction has a large population of leftover sxG-MDSCs. Therefore, a separate CD15 IM positive selection must be employed to acquire an appropriate sxG-MDSC pre-sort for FACS. As a result, POD1 PBMCs were split and either underwent a CD15 or CD33 IM pre-sort, stained and underwent FACS to isolate the sxM- and sxG-MDSC sub-populations (Figure 4A). Through this methodology, I was able to isolate >98% pure sxM-MDSCs ($CD33^+CD14^+CD15^-$) and sxG-MDSCs ($CD33^+CD14^-CD15^+$) (Figure 4B). Bulk-sxMDSCS (CD33 IM positive selection pre-sort), as well as FACS isolated sxM- and sxG-MDSCs were plated in an *ex vivo* suppression assay. Here, I determined that only sxM-MDSCs mediate suppression of NKC (Figure 4C, n = 3).

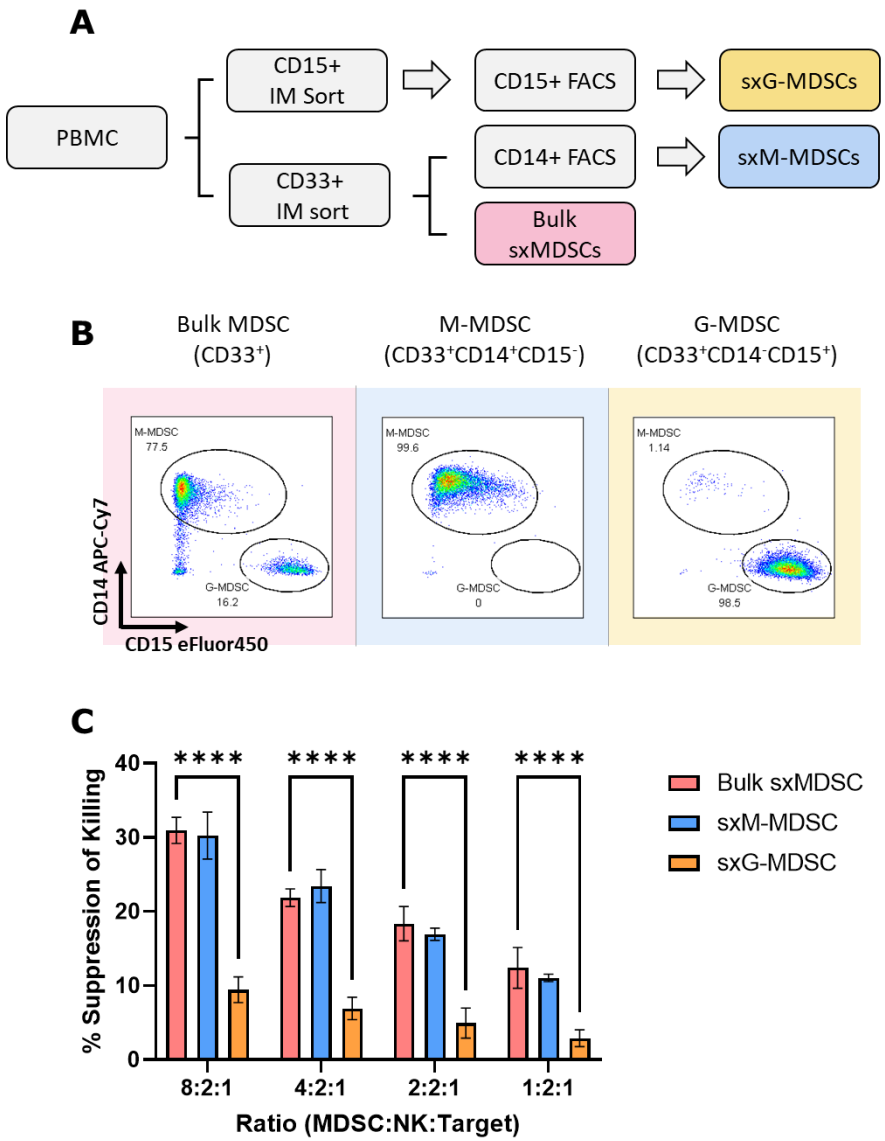

Figure 4: Surgery-induced M-MDSCs mediate suppression of NK cytotoxicity, not G-MDSCs. A) Experimental workflow for the isolation of bulk, sxM- and sxG-MDSCs. POD1 PBMCs were split for pre-sorting with immunomagnetic (IM) positive selection using CD15 (G-MDSC isolation) or CD33 (M-MDSC isolation) microbeads. CD15 and CD33 positive fractions were stained with fluorescent markers for CD33, CD15 and CD14. A portion of the $CD33^+$ fraction was left aside for plating bulk sxMDSCS. The remaining $CD33^+$ fraction and $CD15^+$ fraction was used for FACS of sxG- ($CD33^+CD14\text{-}CD15^+$) and sxM-MDSCS

(CD33^{+}CD14^{+}CD15-). Isolated bulk, sxM- and sxG-MDSCs were plated in an *ex vivo* suppression assay. B) Flow plot CD14 vs CD15 of bulk, sxG- and sxM-MDSCs following gating out cell debris, doublets, dead and CD33- cells. C) Mean ± SEM bulk, sxG- and sxM-MDSCs mediated suppression of NKC following 24 hour co-culture in *ex vivo* assay (n=3). Plated Ratio of MDSCs, NK cells and Targets (K562s) are shown.

4.2.5 PI3Kγ signalling is upregulated in sxMDSCs

It was previously observed that PI3Kγ is important for the suppressive activity of MDSCs(171). Genetic knockout or pharmacological inhibition led to a reduction in the suppressive phenotype of these cells, improved anti-tumour immunity and tumour clearance(171). Given the increased suppressive capacity of sxMDSCs, as well as the specific expansion and activation of sxM-MDSCs, I wanted to investigate if PI3Kγ signalling could contribute to this phenotype (Figure 5A). First, I determined if there were alterations in sxMDSC PI3K signalling. Since PI3K signalling leads to AKT phosphorylation, specifically at residue T308, I concluded that monitoring the phosphorylation status of this important "master regulator" could be a reporter of PI3K activity (Figure 5B)(180, 187). Phosphorylation of AKT at T308 residue was significantly greater in POD1 M-MDSCs than their baseline counterparts (Figure 5C, $p<0.05$). This contrasts with the S473 residue, which is not directly phosphorylated by PI3K, where no changes are observed following surgery (Figure 5D).

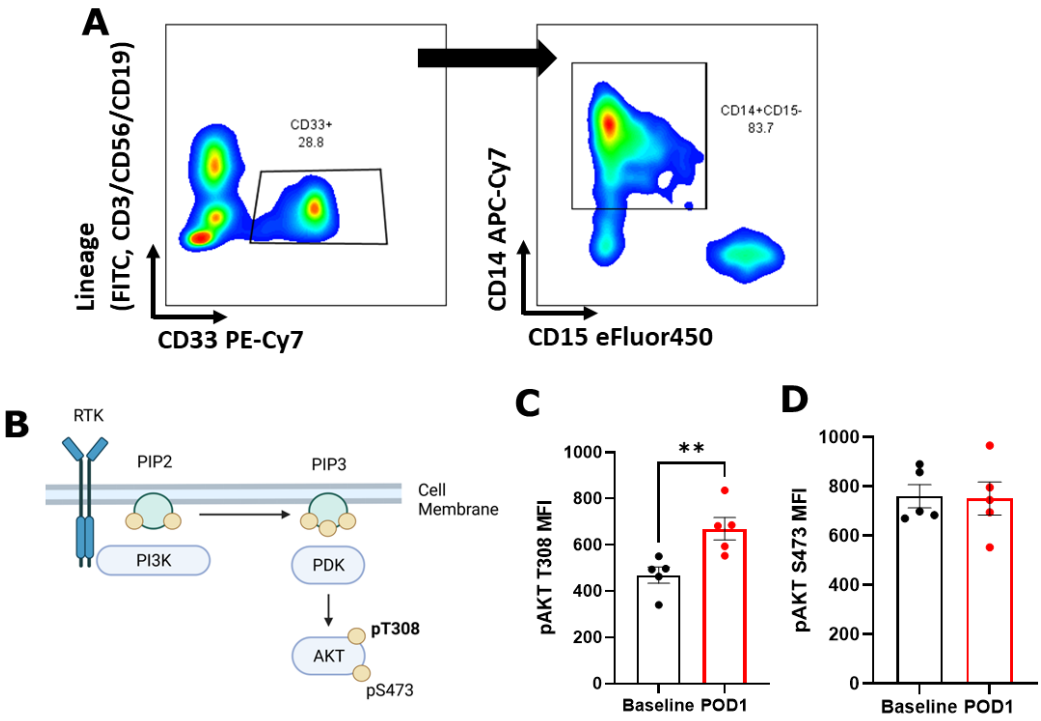

Figure 5: PI3K signalling in upregulated in postoperative MDSCs. A) sxM-MDSC ($CD14^{+}CD33^{+}CD15^{-}Lin^{-}$) were investigated by flow for phosphorylation of pAKT. MFI: Mean Fluorescence Intensity. **B)** Diagram of PI3K signalling. PI3K signalling leads to the activation of PDK1 and subsequent phosphorylation of AKT at T308 residue. Phosphorylation of S473 is mediated by MTORC, which can be independent of PI3K. Diagram was made with BioRender. **C)** Mean ± SEM of phosphorylation status (MFI) of AKT at T308 and at **D)** S473 residue measured by flow cytometry (n=5).

4.2.6 PI3Kγ inhibitors can block signalling and reduce suppression of NK cytotoxicity

Next, I explored the ability of PI3Kγ inhibitors in blocking PI3K signalling and the suppressive activity of POD1 sxMDSCs. I demonstrated that PI3Kγ inhibitor treatment (IPI-549, TG-100 or Compound 17) led to a reduction in AKT phosphorylation in a dose-dependent manner (Figure 6A, $p<0.05$), indicating a reduction in PI3Kγ signalling. This reduction in AKT phosphorylation was comparable to that of pan-PI3K inhibitor, LY294002, treatment. Moreover, this reduction in PI3Kγ signalling was coupled with a reduction in the sxMDSC-mediated suppression of NKC of target K562 cells (Figure 6B). Interestingly, IPI-549 at 1 and C17 at ≥ 1μM led to a decrease in NKC in the absence of sxMDSCs (Figure 6C).

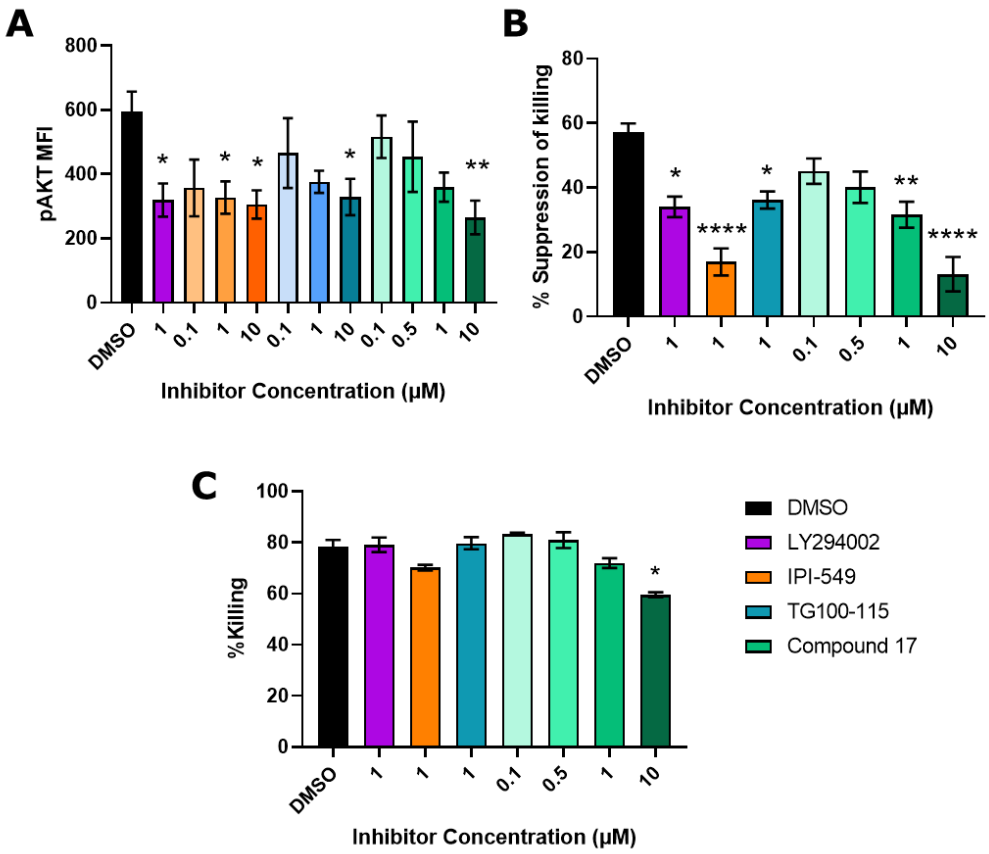

Figure 6: PI3Kγ inhibitors can block PI3K signalling and reduce suppression of NK cytotoxicity. A) Mean ± SEM dose response of AKT phosphorylation with PI3Kγ inhibitor treatment. POD1 sxMDSCs were treated with pan-PI3K inhibitor, LY294002 (purple), or PI3Kγ-specific inhibitors, IPI-549 (orange), TG100-115 (blue), or Compound 17 (green), for 3 hours at the indicated concentrations. For each drug, lighter shades of its representative colour is used to indicate lower concentrations. pAKT(T308) phosphorylation (MFI) was quantified by flow (n=6). B) Mean ± SEM effect of PI3Kγ inhibition on sxMDSC-mediated suppression of NK killing. Prior to 20 hour incubation, MDSC: NK co-culture was treated with PI3Kγ inhibitors. A suppression assay was conducted and quantified by flow (n=6). C) Mean ± SEM NK-mediated cytotoxicity of K562 targets with PI3Kγ inhibitor treatment in the absence of sxMDSCs. Signficant differences compared to DMSO control are shown.

4.2.7 SxMDSCs do not inhibit NK cells through a contact independent route

MDSCs can mediate the suppresion of NK cells through both contact dependent and independent mechanisms. Market *et al.* demonstrated the effect of postoperative TGF-β in NK cell activity inhibition, suggesting that it was a good candidate to explore in mediating sxMDSC suppression of NKC(148). MDSC-derived TGF-β can signal to NK cells through cell-to-cell contact dependent (membrane-bound TGF-β) or independent (soluble TGF-β) mechanisms (Figure 7A). Moreover, blockade of TGF-β with a monoclonal antibody or TGF-βR inhibitor, SB525334, had a similar efficacy to PI3Kγ inhibition in reducing sxMDSC-mediated suppression of NKC (Figure 7B, $p<0.05$). However, no changes in total (Figure 7B) or active TGF-β (Figure 7E) were observed comparing before and after surgery or with IPI-549 treatment. The HEK-Blue^{TM} reporter cell line was unable to detect any in MDSC supernatant (Supplemental Figure 5). Moreover, sxMDSC supernatant was unable to suppress NKC (Figure 7D).

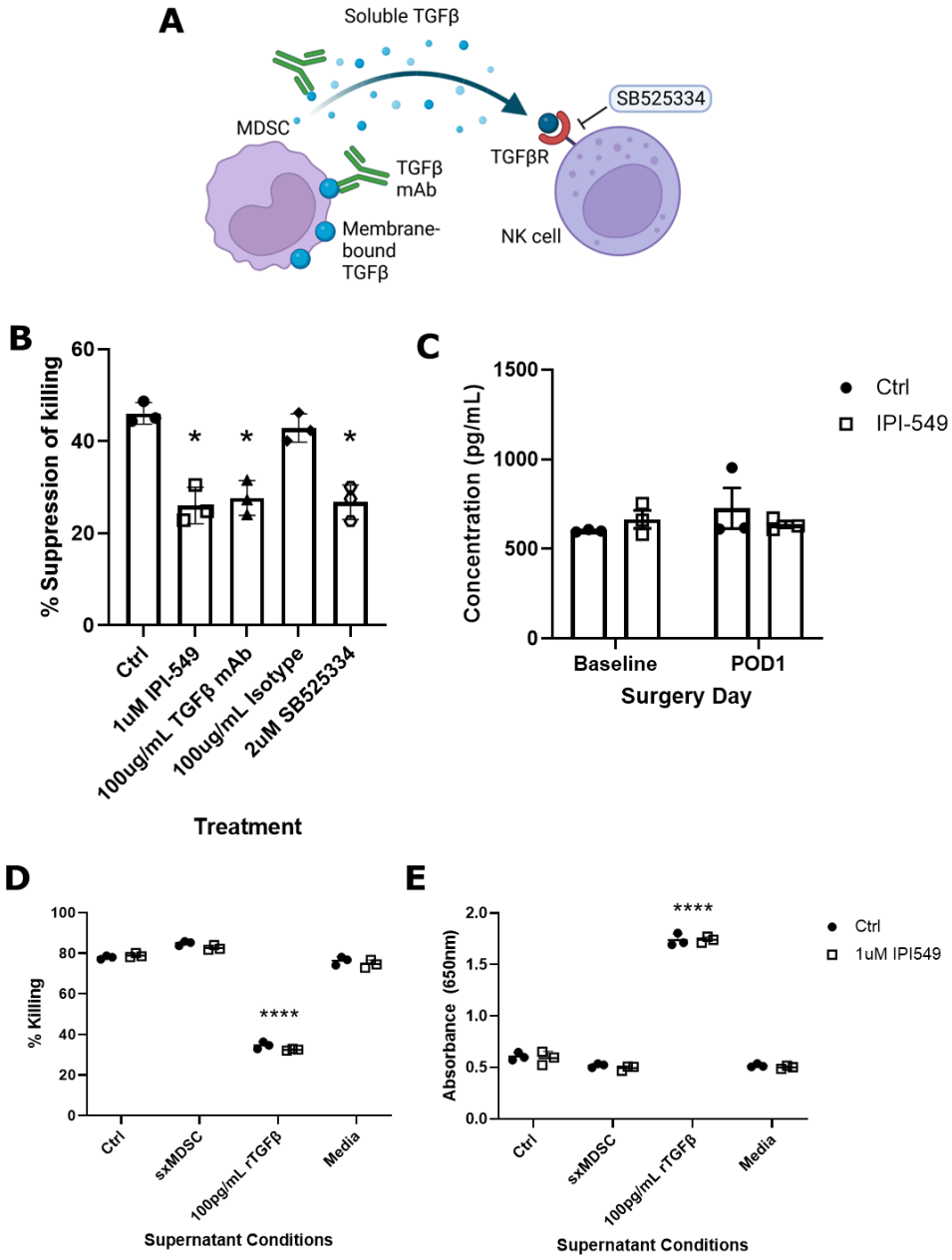

Figure 7: sxMDSCs may not secrete soluble suppressive factions. A) Schematic illustrating contact-dependent (membrane-bound) and independent (soluble) routes of MDSC-derived TGF-β expression and signalling blockade. Blockade can be achieved by a monoclonal antibody (mAb) directed against TGF-β or a TGF-β receptor (TGF-βR) small molecular inhibitor, SB525334, which prevents downstream signalling in NK cells. Both strategies can effectively block contact dependent and independent routes of TGF-β activity. Diagram was made with BioRender. B) Mean ± SEM of suppression assay comparing the efficacy of TGF-β blockade to that of PI3Kγ inhibition in reducing sxMDSC-mediated suppression of NK cells (n=3). C) Mean ± SEM of total TGF-β was measured by ELISA in isolated baseline and POD1 MDSC supernatant following 24-hour incubation in the presence or absence of 1μM IPI-549 (n=3). D) Mean ± SEM effect of PI3Kγ

inhibition on NK suppression by sxMDSC supernatant. sxMDSCs were incubated for 24 hours in the absence or presence of 1μM IPI-549. Supernatant was half diluted (50% supernatant) in fresh CRPMI and plated onto NK92 co-cultured with target K562 cells (n=3). Control baseline MDSCs supernatant (Ctrl), Media only, and 100ng/mL rTGF-β were used as controls. The killing was quantified by flow. E) A TGF-β cell-based assay was used to quantify active TGF-β. Here, HEKBlue TGF-β 293 cells were plated along with the same supernatant conditions as shown in D for a period of 24 hours. The reporter lines expressed SEAP in response to TGF-β signalling. SEAP expression is quantified by transferring the supernatant into a colorimetric alkaline phosphatase assay (QUANTI-Blue, n=3).

4.2.8 PI3Kγ controls translational and transcriptional programming in surgery-inducded MDSCs

To further understand the role of PI3Kγ in MDSC activity, I investigated the effects of inhibiting various downstream effectors. Activation of PI3Ky leads signal transduction via PDK1, and Akt, followed by activation of mTORC1, then S6K (Figure 8A). This pathway has several implications in metabolism as well as translation and protein synthesis(215). Interestingly, inhibition of PI3Kγ (IPI-549), PDK1 (GSK2334470), AKT (MK-2206), or S6K (LY2584702) all lead to a reduction in sxMDSC suppressive activity ($p < 0.05$) (Figure 9B). Given the role of S6K in initiating translation, I also investigated the role of PI3Ky in mediating the expression of immune effector mRNA transcripts. I investigated the expression of anti-inflammatory transcripts, *Arg1*, *Il10*, *Tgfb* as well as pro-inflammatory transcripts, *Il1b*, *Il12b*, and *Tnfa* in MDSCs isolated from baseline and POD1, in the presence or absence of 1μM IPI-549 (Figure 9C). Surgical stress caused a significant decrease in all pro-inflammatory transcripts, *Il1b*, *Il12b* ($p<0.01$) and *Tnfa* ($p<0.001$), while anti-inflammatory *Arg1* ($p<0.01$) was upregulated. PI3Kγ blockade with IPI-549 treatment in POD1 sxMDSCs, prevented the surgery-induced reduction of pro-inflammatory transcripts *Il1b*, and *Il12b* ($p <0.05$), however it did not rescue *Tnfa* mRNA expression.

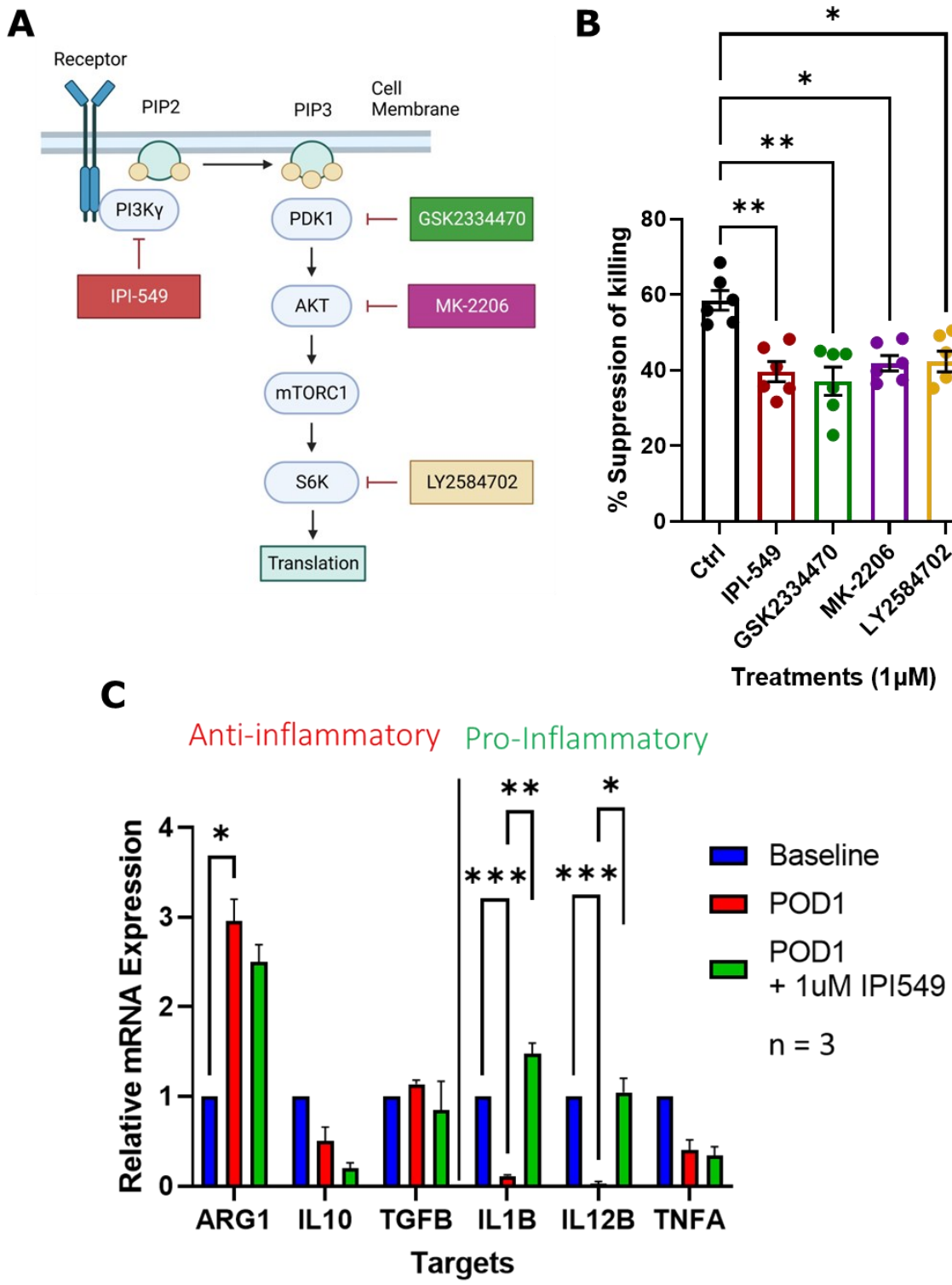

Figure 8: PI3Kγ mediates transcriptional and translational programming in sxMDSCs. A) Schematic of inhibitors targeting effectors downstream of PI3Kγ signalling. Diagram was made

with BioRender. B) Mean ± SEM of suppression assay comparing efficacy of administrating inhibitors at 1μM concentration targeting PI3Kγ (IPI-549), PDK1 (GSK2334470), AKT (MK-2206), and S6K (LY2584702) (n = 6). C) Mean ± SEM of mRNA expression of transcripts with anti- vs. pro-inflammatory effects. MDSCs were isolated on baseline and POD1 PBMCs and incubated in the presence or absence of 1μM IPI-549 for 24 hours at 37ºC. Following incubation, RNA was extracted, reverse transcibed to cDNA and qPCR was used to determine the expression of the indicated transcripts. Expression is normalized to baseline expression.

4.2.9 PI3Kγ inhibitors can block signaling in murine splenic G-MDSC and M-MDSC, *in vitro*

I wanted to move towards investigating the efficacy of PI3Kγ inhibitors in reducing postoperative metastatic burden in our murine model. Prior to this, I wanted to confirm that these inhibitors can block PI3Kγ signalling in murine MDSCs *in vitro* (Figure 9A). Splenic MDSCs were shown to respond to postoperative stress as they undergo expansion and exhibit a significant increase in immunosuppressive activity(103). Both M-MDSCs ($CD11b^+Ly6C^+$, Figure 9C) and G-MDSCs ($CD11b^+Ly6G^+$, Figure 9D) isolated from spleens showed down-regulation of AKT phosphorylation at 1μM and 10μM IPI-549 and 10μM TG100-115. IL-4 caused increased phosphorylation of AKT and served as a positive control.

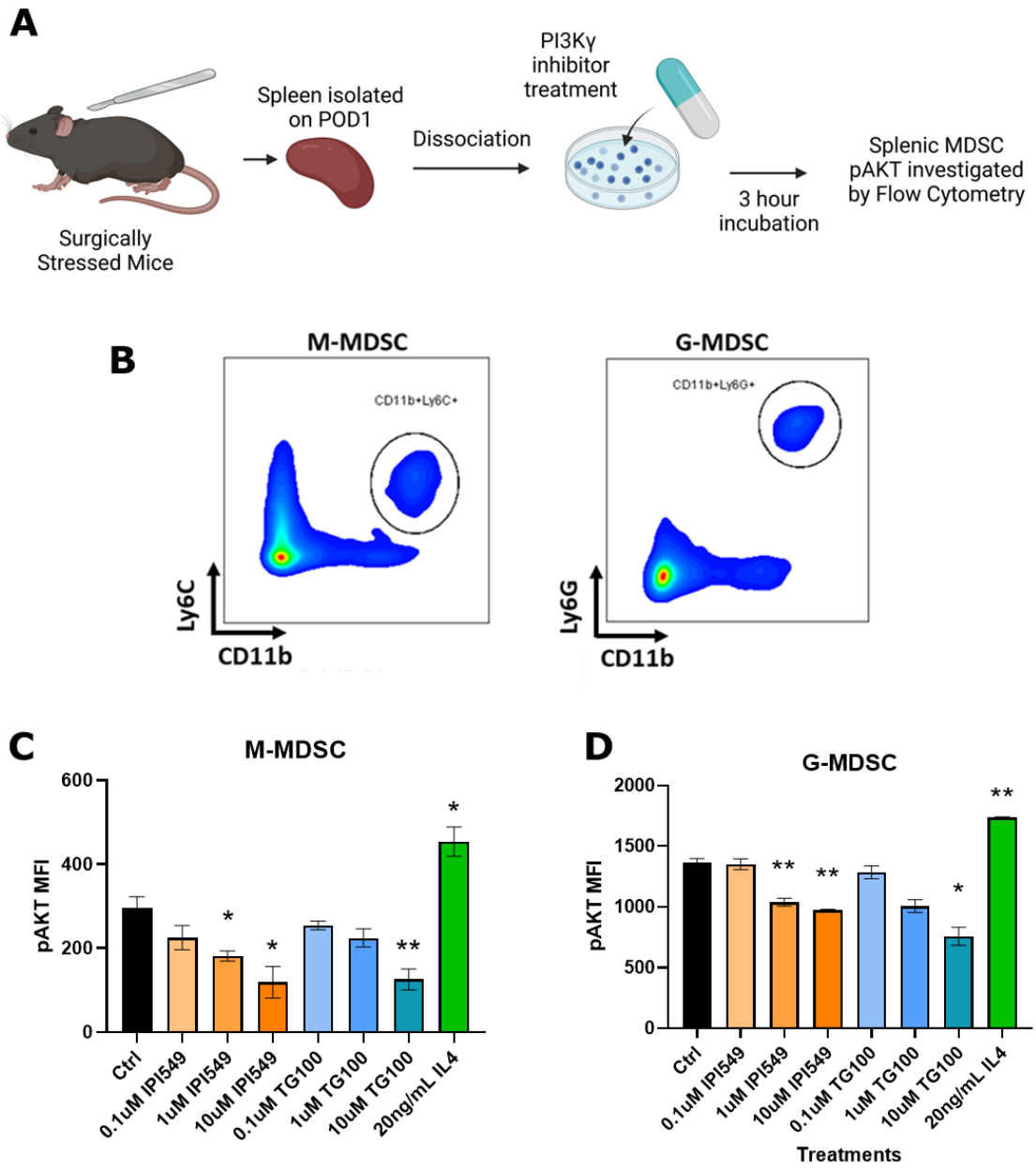

Figure 9: *In vitro* PI3Kγ inhibitor treatment blocks signalling in murine splenic MDSCs. A) Schematic of experimental workflow. Spleens were harvested on POD1 from mice that underwent surgery. Splenocytes were dissociated and treated with IPI-549 or T100-115 for 3 hours before detection of pAKT by flow. No treatment controls were included. B) Representative flow plot for murine M-MDSCs ($CD11b^{+}Ly6C^{+}$) and G-MDSCs ($CD11b^{+}Ly6G^{+}$), cell debris

was excluded, and live single cells were gated on, following by gating for Ly6C/CD11b or Ly6G/CD11b. C) Mean ± SEM phosphorylation of AKT (T308) in M-MDSCs and (D) G-MDSCs (n=3).

4.2.10 PI3Kγ inhibitors can block signalling caused by surgical stress

Next, I investigated the effects of surgical stress on PI3Kγ signalling in murine splenic MDSCs. As outlined in Figure 10A, beginning from one day before surgery to the POD1 endpoint, mice were administered either TG100-115 or IPI-549 as indicated in section 4.1.2. In both M-MDSCs (Figure 10B) and G-MDSCs (Figure 10C), the surgery caused an increase in pAKT MFI on POD1 compared to no surgery controls ($p<0.01$). Moreover, M-MDSCs had reduced pAKT MFI when surgery was conducted alongside the administration of 6mg/kg TG100-115 or 30mg/kg IPI-549 ($p<0.05$). The lower dosages of TG100-115 and IPI-549 did not affect the surgery-induced increase of pAKT MFI in M-MDSCs. However, G-MDSCs showed no reduction in pAKT MFI with either TG100 -115 or IPI-549 administration.

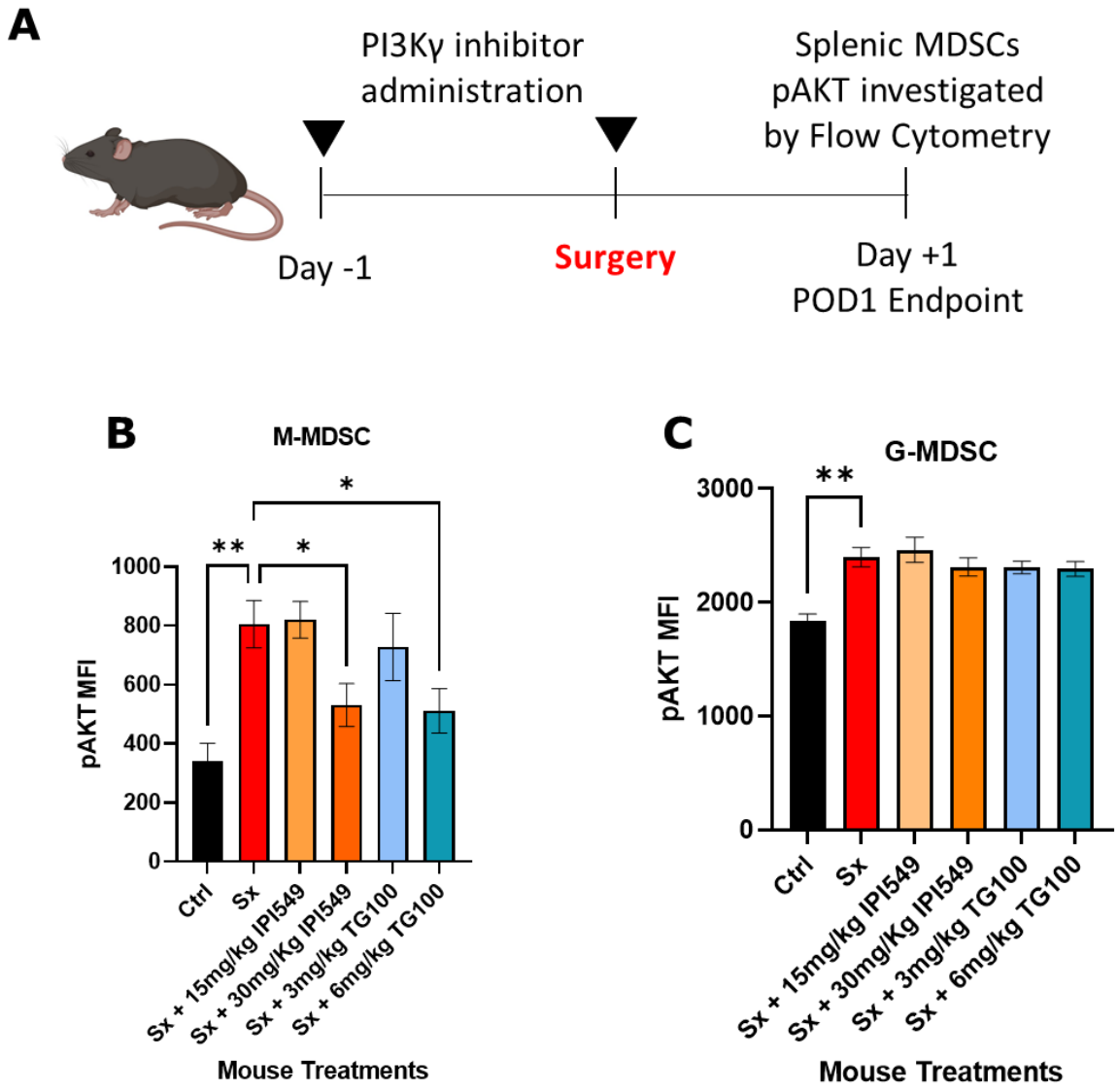

Figure 10: *In vivo* PI3Kγ blockade leads to reduction in signalling in M-MDSC only. A) Schematic of experimental workflow. Mice were administered TG100-115 (6mg/kg) or IPI-549 (30mg/kg) intraperitoneally on the specified days (▼). No treatment controls were included. The experiment was endpointed on POD1 and pAKT in splenic MDSCs and was quantified by flow. B) Mean ± SEM phosphorylation of AKT (T308) in M-MDSCs and (C) G-MDSCs (n = 3).

4.2.11 Surgical stress potentiates sxMDSC activity and postoperative metastatic burden

Alongside an increase in PI3Kγ signalling in POD1 M-MDSCs, I also demonstrated that sxMDSCs are more suppressive than baseline counterparts in an *ex vivo* suppression assay co-culture with NK cells and Yac-1 target cells (Figure 11). A significant reduction in Yac-1 target killing was observed at ratios of 4:1, 8:1 and 16:1 MDSC:NK cells in POD1 MDSCs compared to baseline MDSCs ($n = 3$, $p < 0.01$, Figure 11B). Moreover, when these sxMDSCs are transferred to healthy mice that did not receive surgery themselves, it led to a greater increase in metastatic burden than mice that received preoperative MDSCs ($n=3$, $p<0.05$, Figure 11C)

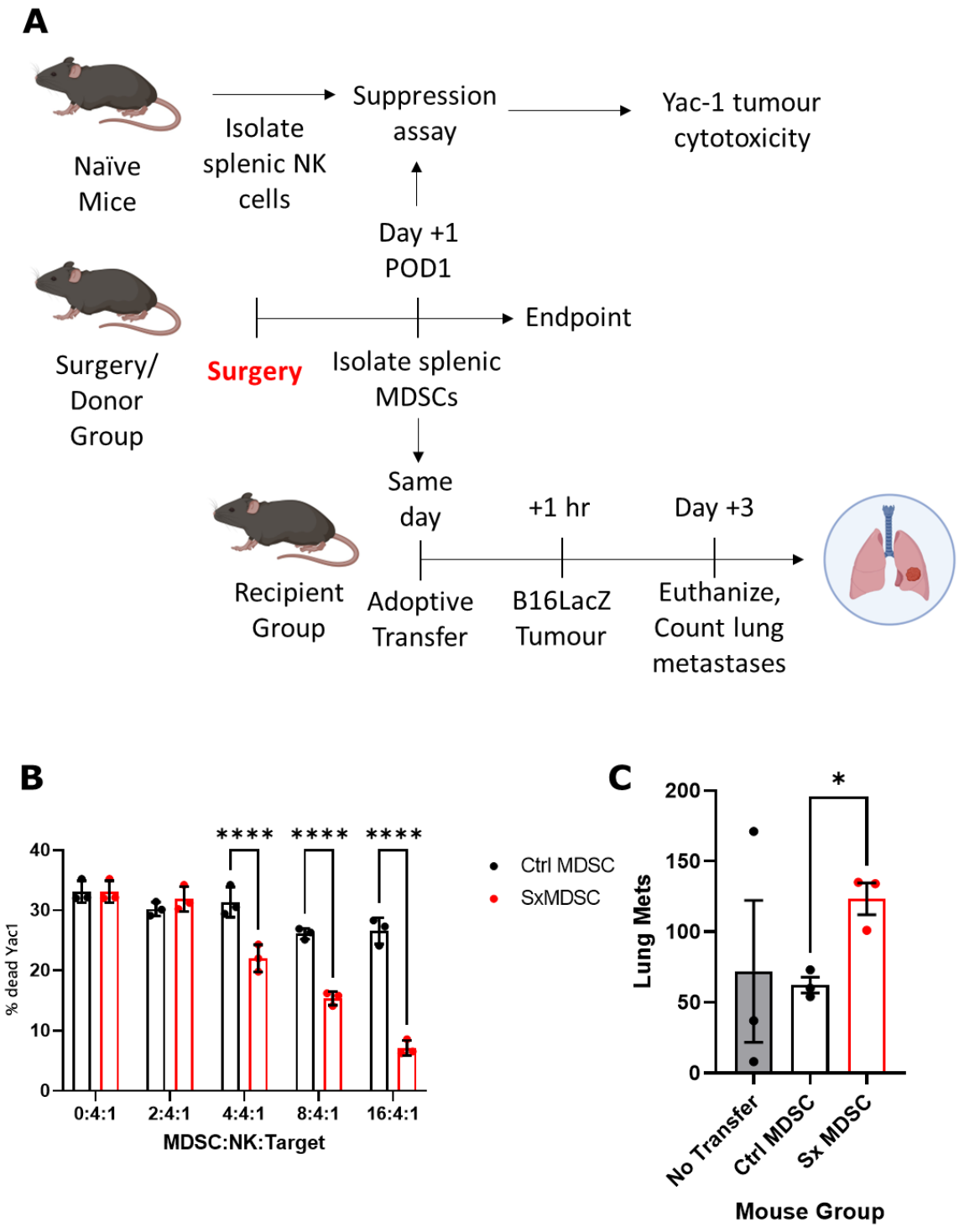

Figure 11: Surgery potentiates murine sxMDSC suppressive activity, leading to greater inhibition of NK cell cytotoxicity and postoperative metastatic burden. A) Schematic of experimental workflow. Splenic MDSCs were isolated on POD1 endpoint from mice that received surgery and co-cultured in a suppression assay with splenic NK cells isolated from naïve mice.

Cytotoxicity of Yac-1 target cells was measured by flow cytometry. Isolated sxMDSCs were adoptively transferred to recipient mice that were challenged with lung-metastases forming B16F10 LacZ tumour cells. On POD3 endpoint, lung metastases were counted following LacZ staining. B) Mean ± SEM of baseline and POD1 (red) suppression of NKC against Yac-1 targets with increasing MDSC concentration (n=3). Statistics were performed using two-way ANOVA with Šídák's multiple comparisons test, with a single pooled variance. C) Mean ± SEM of B16F10 LacZ lung metastases (n = 3) in recipient mice that received no MDSCs (no transfer), MDSCs from mice that did not receive surgery (Pre-op MDSC) or surgery induced MDSCs (sxMDSC).

4.2.12 PI3Kγ inhibition in MDSCs leads to a reduction in suppression of NK cell cytotoxicity

Next, I determined whether systemic administration of PI3Kγ inhibitors before surgery could reduce the postoperative metastatic burden. Prior experiments conducted by Dr. Angka where PI3Kγ inhibitors were administered systemically prior to surgery lead to deleterious side effects including reduced *ex vivo* NKC against Yac-1 targets as well as increased tumour metastases compared to mice that only received surgery (Supplemental Figure 6). Both observations are contradictory to our hypothesis: inhibiting PI3Kγ signalling can reduce postoperative NKC suppression and metastatic burden. This suggests that despite a beneficial reduction in sxMDSC-mediated suppression of NK activity, systemic PI3Kγ inhibition has an overall negative effect on NK-mediated anti-tumour immunity. As a result, we wanted to focus on the beneficial effects of PI3Kγ inhibition on the sxMDSC population, while excluding the deleterious effects of reduced NKC. To accomplish this, sxMDSCs were isolated from mice that were given TG100-115 or IPI-549 prior to surgery and NK cells were isolated from naïve mice that did not receive surgery or PI3Kγ inhibitors (Figure 12A). These sxMDSCs were co-cultured with the NK cells in an *ex vivo* suppression assay to determine the effects of sxMDSC-specific PI3Kγ inhibitor administration on NKC. No surgery and no treatment control MDSCs were also included in this experiment. sxMDSCs caused a significant reduction in NKC compared to no surgery control (no Sx) MDSCS (Figure 12B). Moreover, MDSC-specific treatment of TG100-115 or IPI-549 led to reduced NK cell suppression ($p<0.05$, $n = 3$).

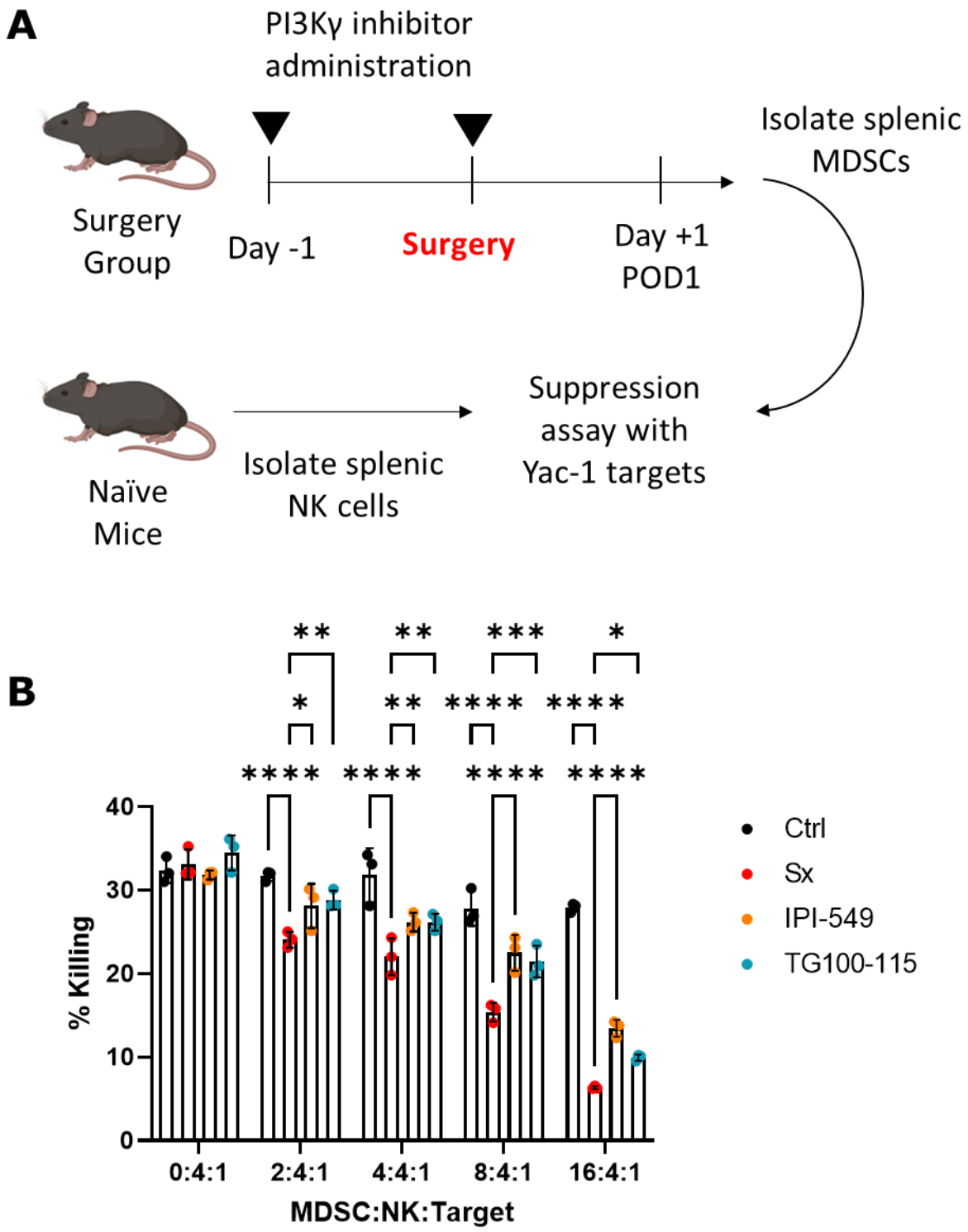

Figure 12: *In vivo* PI3Kγ blockade in sxMDSCs leads to a reduction of *ex vivo* NK suppression. A) Schematic of experimental workflow. Mice were administered TG100-115 (6mg/kg, once a day intraperitoneally) or IPI-549 (30mg/kg, twice a day by oral gavage) on the

specified days (▼) and underwent surgery. No surgery and no treatment controls were included. On POD1, MDSCs were isolated from spleens collected from surgery stressed and no surgery mice, while NK cells were also isolated from naïve (no surgery) mice. Ex-vivo suppression assay with Yac-1 targets was conducted and killing was quantified by flow. B) Yac-1 NKC following co-culture of MDSCs with NK cells with or without PI3Kγ inhibitor treatment (n=3).

4.2.13 MDSC-specific PI3Kγ inhibition reduces the postoperative metastatic burden

Next, I wanted to determine the efficacy of PI3Kγ inhibitors in reducing postoperative metastatic burden. To accomplish this, sxMDSCs from surgery stressed mice, that were treated with either TG100-115 or IPI-549, were adoptively transferred to mice that were challenged with B16LacZ tumour-forming cells. After 3 days, lung metastases were counted following LacZ staining (Figure 13A). No transfer, no surgery, and no treatment controls were also included. There was no significant difference between mice that received no MDSCs and mice that received no-surgery control MDSCs ($n = 8$, $p<0.05$, Figure 13B). Adoptive transfer of sxMDSCs caused a significant increase in lung metastases compared to no-surgery controls. sxMDSCs that were transferred from mice that also received IPI-549 treatment led to a significant reduction in lung metastases. However, in contrast, TG100-115 treatment could not reduce lung metastases.

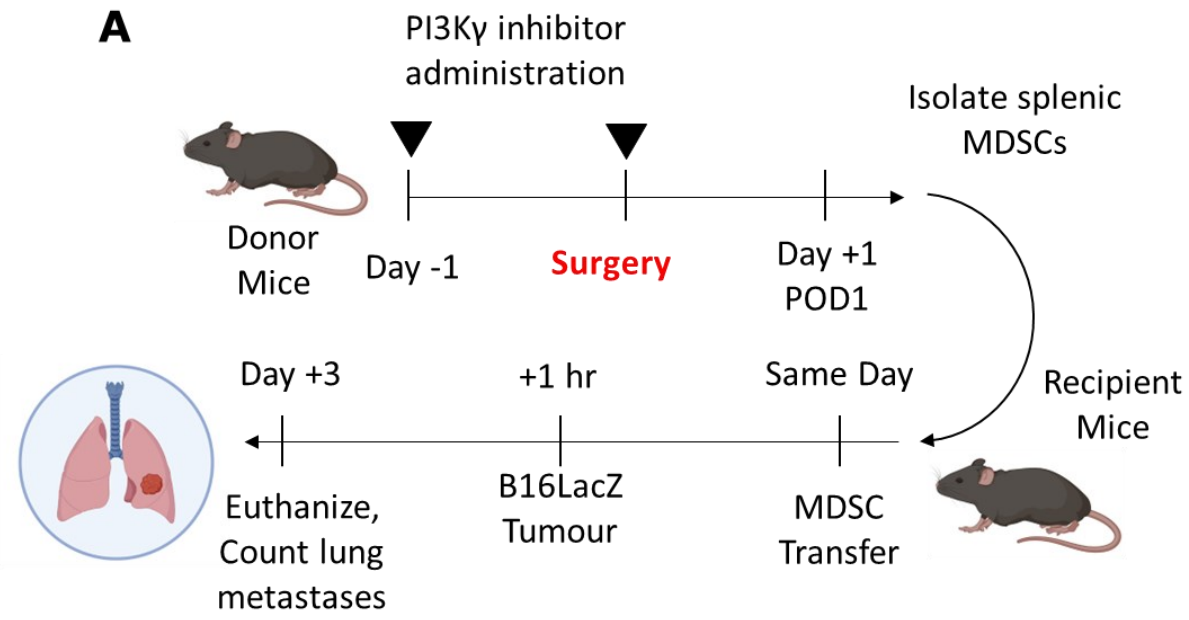
A
PI3Kγ inhibitor administration
Isolate splenic MDSCs
Donor Mice
Day -1
Surgery
Day +1 POD1
Day +3
+1 hr
Same Day
Recipient Mice
Euthanize, Count lung metastases
B16LacZ Tumour
MDSC Transfer

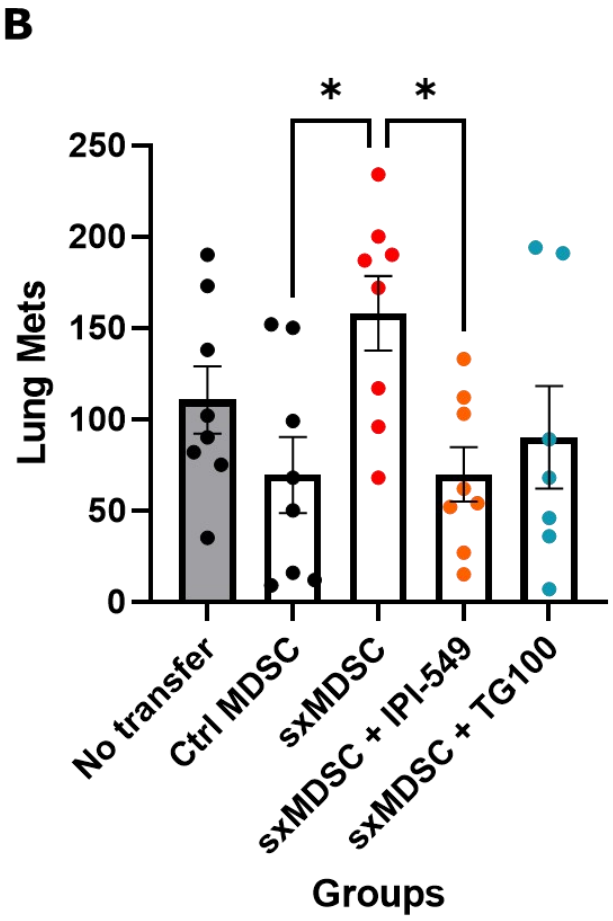
B
Lung Mets
250
200
150
100
50
0
*
*
No transfer
Ctrl MDSC
sxMDSC
sxMDSC + IPI-549
sxMDSC + TG100
Groups

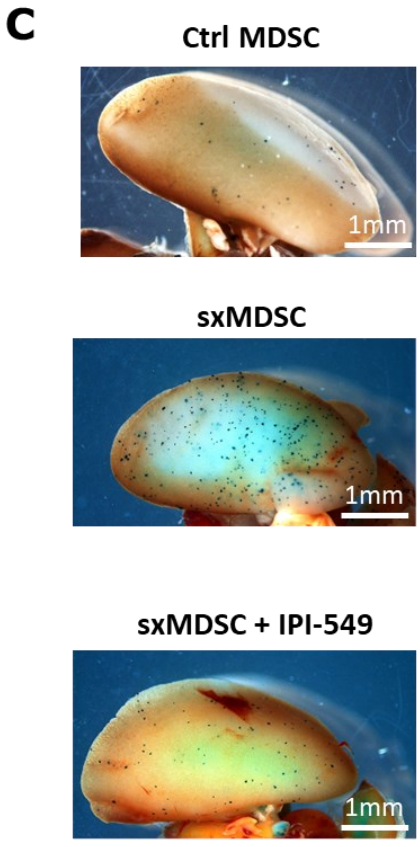
C
Ctrl MDSC
1mm
sxMDSC
1mm
sxMDSC + IPI-549
1mm

Figure 13: MDSC-specific PI3Kγ blockade leads to a reduction in metastatic tumour burden. A) Schematic of experimental workflow. Donor mice were administered TG100-115 or IPI-549 on the specified days (▼) and underwent surgery. On POD1 endpoint, spleens were collected and MDSCs were isolated. MDSCs were adoptively transferred to recipient mice that were challenged with lung metastases forming B16LacZ cells. After 3 days, lungs were collected from recipient mice, and lung metastases were counted following standardized X-gal staining protocol. No surgery and no treatment controls were included for donor mice. B) Effect of adoptive transfer of sxMDSCs with or without PI3Kγ blockade, MDSCs were not given to "no transfer" controls. Data shown is combined from 2 repeats of this experiment (n=8). C) Representative images of lung metastases from experiment groups.

4.3 Discussion

4.3.1 Surgical Stress and NK cell Suppression

Surgery is critical for curative resection of tumours in solid malignancies. However, several independent studies, as well as ones conducted at our lab, have demonstrated a clear link between surgical resection and an increased risk of cancer recurrence as well as a metastatic burden in both human(127) and murine models(103, 108). The surgery stress response, an "ebb and flow" of a crashing wave of pro-inflammatory signals immediately after the physical injury caused by surgery, followed by receding compensatory anti-inflammatory signals, which skews the postoperative environment towards a pro-tumorigenic state(68, 69). The surgical stress response releases several factors such as VEGF, PDGF, and EGF which contribute to the growth and persistence of tumour cells. MRD which is left behind from the resection margin, as well as CTCs, produced by the physical disruption of the tumour during resection benefit from these factors(216).

The surgical stress response also gives rise to several physiological responses that manifests as postoperative immunosuppression, the consequences of which is a significant impairment in anti-tumour immunity. Primarily, NK cells, which are critical for tumour surveillance are significantly suppressed in the postoperative period, regardless of surgical approach, duration of surgery, or cancer type(99, 103, 105, 217). Ultimately, studies have confirmed that surgical stress causes suppression of NK-mediated cytotoxicity and IFN-γ secretion, which contributes to increased metastatic burden and poor survival(103, 108). To further add to these studies, my results highlight the detrimental impact of surgery-induced (sx)MDSC-mediated suppression of NK cells. Importantly, I was able to recapitulate the effects of increased metastatic burden in tumour-challenged mice that had never been exposed to surgery, when I we

adoptively transferred sxMDSCs from mice that did undergo surgery (Figure 13C). This aligns with a body of work from our lab as well as others, which highlights the role of sxMDSCs as drivers of postoperative immunosuppression thereby promoting postoperative metastatic burden(103, 105, 108, 169, 218). Taken together, sxMDSCs are potent antagonists of NK-mediated anti-tumour immunity as they provide a foothold for residual cancer cells to re-establish metastatic foci in the aftermath of surgery.

4.3.2 The Surgery Stress Response Potentiates surgery-induced (sx)MDSC Activity

The surgery stress response to leads to the immediate release of several signals, such as IL-1β, IL-6, TNF-α, and IFN-γ, as well as DAMPs(91). Together, these factors causes recruitment of granulocytes and monocytes to the site of injury to initiate wound healing(219). To meet the increased demands for myeloid cells necessary for wound healing, there is a significant release of IMCs from the bone marrow through emergency myelopoiesis. These IMCs are termed MDSCs, given their potential for suppressing immune activity. We further classify these MDSCs as sxMDSCs given their enhanced ability to suppress NK-cell activity than pre-operative counterparts. I have also demonstrated that sxMDSCs expand after surgery (Figure 2). I primarily observed an expansion of sxM-MDSCs. By co-culturing pure populations of each subset with NK cells in an ex vivo suppression assay, I identified that it is sxM-MDSCs that mediate NK cell suppression, as opposed to sxG-MDSCs (Figure 4). Several studies have demonstrated that M-MDSCs are more suppressive than G-MDSCs on a per-cell basis, which is attributed to the differences in their mechanisms of suppression(220). G-MDSC primarily use reactive oxygen species (ROS) as the mechanism of immune suppression(221). In contrast, M-MDSC primarily use up-regulation of inducible nitric oxide synthase (iNOS), arginase and immune suppressive cytokines such as TGF-β and IL-10(135) to suppress various immune functions(222). The

differences in the mechanisms of suppression employed by these two subtypes suggest that those employed by sxM-MDSCs are more potent for suppressing NK cells. Indeed, studies have shown that sxG-MDSCs maybe more important for suppressing adaptive immune responses as well as promoting regulator T cell proliferation(135, 222). The implications of the expansion and potentiation of suppressive activity of M-MDSCs is concerning, as it was correlated with a lower time to recurrence and OS(127), highlighting role of this subset of MDSCs as drivers of postoperative metastatic disease. Moreover, Dr. Angka demonstrated that HLA-DR MFI is significantly lower in sxMDSCs cells than in baseline (Supplemental Figure 2). Low or no HLA-DR is an important marker of MDSCs, further indicating that surgical stress primarily causes the expansion of these suppressive cells(223).

In addition to signalling their expansion, the surgery stress response also potentiates their suppressive activity. Notably, we have demonstrated the significant expansion and activation of sxMDSCs in both human and murine models(103, 105, 108). I have confirmed that these sxMDSCs exhibit a heightened ability for suppression of NK cell activity, compared to pre-operative controls, resulting in significantly impaired NKC against both Yac-1 (Figure 11B) and K562 (Figure 3D) cells. Looking at current research, the expansion as well as increased suppressive activity may be due to the presence of DAMPs, such as HMGB1, IL-6, GM-CSF, and IFN-γ, all of which are highly abundant because of the surgery stress response(224). This highlights the role of the surgery stress response as a mechanism that promotes the activation of sxMDSCs. Ultimately, the expansion and activation of these sxMDSCs can cause postoperative metastatic burden.

Taking a step back, I want to take a moment to consider the implications of what I have discussed thus far within the context of our knowledge of metastatic disease. It is well understood that many tumours will promote their own metastatic growth. Reflecting on a long history of research in the role of the primary tumour in establishing micro-metastases, it was Piaget in 1889 who first coined this as the "seed and soil" hypothesis: host tissue is typically unfavourable for the growth of disseminated tumour cells (seed) and must undergo significant alterations to form the premetastatic niche (soil)(225). Established tumours can release factors that mediate the formation of the premetastatic niche which is necessary for the growth of disseminated tumour cells and development of metastatic foci(225). McAllister et al. described this phenomenon as "systemic instigation" when they demonstrated that a weakly metastatic tumour model was able to form persistent lung metastases only in the presence of an "instigating" primary tumour from an aggressive breast cancer cell line, with known ability to alter the local microenvironment, thereby priming the premetastatic niche(226). Although an "instigating" tumour model was not used in my study, surgery itself clearly qualifies as a "systemic instigator". My work demonstrates that the surgery stress response causes significant systemic changes that ultimately lead to the expansion and activation of sxM-MDSCs as the drivers of postoperative suppression and metastatic disease.

4.3.3 The Role of PI3Kγ in sxMDSC Activity

4.3.3.1 Identifying PI3Kγ as a potential antagonist of MDSC Activity

Our lab has demonstrated through MDSC depletion studies, that these cells play a critical role in mediating postoperative NK cell suppression, and lung metastases(108). However, this is

not feasible in cancer surgery patients due to the deleterious effects of ablating myeloid progenitors. Although MDSCs are a subset of myeloid cells that can disrupt immunosurveillance, myeloid cells as a whole are critical in the wound healing process after surgery(227). Therefore, identifying MDSC-specific therapeutics would be a more feasible approach to inhibiting their suppressive activity postoperatively. To identify potential therapeutic targets that attenuate suppression in sxMDSCs, Dr. Angka conducted a high-throughput screen of small molecules, where he identified PI3Kγ as a critical pathway in sxMDSC suppressive activity (Supplemental Figure 1). Kaneda et al. demonstrated PI3Kγ as a molecular switch that can determine the inflammatory or immunosuppressive fate in myeloid cells. PI3Kγ activity led to activation of an immunosuppressive transcription program driven by C/EBPβ, while inhibition lead to an inflammatory phenotype driven by NF-κb activation(171). Several studies have demonstrated that PI3Kγ inhibition can reduce MDSC-mediated suppression of anti-tumour immunity and tumour volume. PI3Kγ is most abundantly expressed in myeloid cells out of all other cell and tissue types. It is the dominant PI3K isoform expressed in myeloid cells(228). Both characteristics mean that targeting the PI3Kγ isoform is a potentially potent MDSC-specific strategy to prevent postoperative metastases and NK cell suppression.

4.3.3.2 PI3Kγ signalling is upregulated in postoperative MDSCs and contributes to the immunosuppressive phenotype

Activation of PI3Kγ, as well as all other isoforms, leads to PDK1-mediated phosphorylation of AKT at the T308 residue leading to its activation. Given the various roles AKT carries out within the cell, I monitored T308 phosphorylation as an indicator of PI3K signalling in MDSCs. I observed a significant increase in pAKT (T308) in sxMDSCs, compared to baseline

controls, in both humans (Figure 5C) and our murine model of surgery (Figure 10B and C). Despite the increased phosphorylation of T308 of AKT observed in sxMDSCs, compared to baseline, S473 phosphorylation remained unchanged (Figure 5D). As mentioned in section 1.2.5.2, S473 is phosphorylated by mTORC2, which can function independently of PI3K/PDK-1 activity(179). PI3Kγ-specific inhibitors, IPI-549, TG100-115, and Compound 17 were all able to reduce pAKT signalling in sxMDSC (Figure 6A). Increased PI3Kγ signalling in sxMDSCs could be caused by IL-6, PGE-2, or DAMPs such as LPS and HMGB1, all of which are highly abdundant in the postoperative environment. As mentioned prior, these factors have been shown to lead to the expansion and activation of MDSCs in a PI3Kγ-dependent manner(193, 195, 196, 229, 230). Moreover, as shown in (Figure 6B), ex vivo co-culture suppression assays demonstrated the effectiveness of PI3Kγ inhibition in reducing MDSC-mediated suppression of NKC. My findings further corroborate what was described by Kaneda *et al.*; the suppressive activity of MDSCs, both within and outside perioperative contexts, is controlled by PI3Kγ signalling. However, this signalling pathway may be even more prominent within the context of surgical stress due an overwhelming systemic abundance of soluble factors that can signal through PI3Kγ, that are typically not present in pre-operative conditions. Taken together, this suggests that upregulated PI3Kγ signalling, potentially stimulated by the surgery stress response, in sxMDSCs leads to a heightened immunosuppressive phenotype.

4.3.3.3 sxMDSC do not secrete soluble TGF-β and the role of PI3Kγ in this pathway is yet to be elucidated

Given that PI3Kγ is involved in the suppressive phenotype of sxMDSCs, I next wanted to investigate potential suppressive effector molecules released by sxMDSCs that could be mediated

by PI3Kγ. Tai et al. demonstrated the increased expression of TGF-β in postoperative plasma(103). Moreover, Market et al. demonstrated that postoperative TGF-β can inhibit NK cells. Taken together, this placed TGF-β as a potential candidate involved in sxMDSC suppressive activity(104). Moreover, it could be under the control of PI3Kγ signalling. MDSC-derived TGF-β can signal to NK cells through cell-to-cell contact dependent or independent mechanisms (Figure 7A). Membrane-bound TGF-β on MDSCs was shown to result in significant suppression of NKC, while soluble MDSC-derived TGF-β served to suppress distant NK cells(148). I was able to demonstrate that TGF-β blockade with either a monoclonal antibody or TGF-βR inhibitor, SB525334, had a similar efficacy as PI3Kγ inhibition in reducing sxMDSC-mediated suppression of NKC (Figure 7B).

Moreover, Market et al. demonstrated that TGF-β blockade in postoperative plasma reversed the suppression of NK cells. Given that the surgery stress response potentiates sxMDSC suppressive activity, I investigated the effects of surgery on MDSC-derived TGF-β. However, I was unable to detect any changes in TGF-β expression, in total (Figure 7C, active and latent) and bioactive (Figure 7E) TGF-β. It should be noted that a vast majority of TGF-β molecules are latent and are sequestered by a covalent association with the latency-associated protein (LAP) and the latent TGF-β-binding protein (LTBP)(231). Despite its abundance, latent TGF-β is not biologically active and requires proteolytic cleavage which can be mediated by an array of proteases that are present in the host circulation and on various cell surfaces. This is important to note because, all though total TGF-β can be reliably measured by ELISA, it is not an indication of the expression of active TGF-β. Unfortunately, an ELISA is not sensitive enough to be able to reliably quantify active TGF-β levels. Active TGF-β levels could potentially be changing from baseline to POD1 in MDSCs if there are differences in the expression of TGF-β activating proteases. Therefore, active

TGF-β was measured with a HEKBlueTM cell-based reporter, which produces SEAP downstream of TGF-β signalling. However, this assay was unable to detect any differences in TGF-β with or without PI3Kγ inhibition. Although the HEKBlueTM cell-based reporter was able to detect as little as 3pg/mL of rTGF-β, but unable to detect any in sxMDSC supernatant (Figure 7D). Moreover, the sxMDSC supernatant was unable to suppress NKC (Figure 7D). Therefore, TGF-β derived from MDSCs does suppress NKC, however, this is not through a contact independent mechanism. This suggests that sxMDSCs may mediate suppression via membrane-bound, rather than soluble, TGF-b. However, it is difficult to determine the role of PI3Kγ in TGF-β expression in MDSCs and it will require more work to investigate if there is a connection.

4.3.3.4 PI3Kγ controls translational and transcriptional programming in sxMDSCs

To determine a mechanistic role for PI3Kγ in sxMDSC-mediated suppression of NK cells, I investigated the effects of inhibiting downstream effectors in the signalling pathway. Activation of PI3Ky leads to signal transduction via PDK1, Akt, followed by activation of mTORC1, then S6K (Figure 8A). Inhibition of PI3Kγ (IPI-549), PDK1 (GSK2334470), AKT (MK-2206), or S6K (LY2584702) all lead to a reduction in sxMDSC suppressive activity (Figure 8B). Since the effect of reduced MDSC suppressive activity is seen with S6K inhibition, it suggests that S6K may underlie sxMDSC function. Signal transduction via S6K leads to the activation of ribosomal S6 protein, which is key for initiating translation (215). This suggests that PI3Kγ may transduce signals that lead to a translational program via S6K activation, which mediate sxMDSC immunosuppression function. Moreover, activation of S6 (by S6K) was shown to upregulate glycolysis and the TCA cycle (232). *Jian et al.* identified that MDSCs demonstrate significantly higher glycolytic activity than their normal cell counterparts. Upregulation of

glycolysis prevented excess reactive oxygen species (ROS) production by MDSCs, which protected MDSCs from apoptosis(233). ROS production from MDSCs is an important mechanism for its immunosuppressive activity (234). Therefore, increased glycolytic activity because of S6K activation may be a protective mechanism against endogenously produced ROS.

Given the role of S6K in activating translational machinery, it brought into question whether PI3Kγ may also control the expression of mRNA transcripts in sxMDSCs. I investigated the expression of anti-inflammatory transcripts, *Arg1*, *Il10*, *Tgfb* as well as pro-inflammatory transcripts*, Il1b*, *Il12b*, and *Tnfa* in MDSCs isolated from baseline and POD1, in the presence or absence of 1μM IPI-549 (Figure 8C). Surgical stress caused a significant decrease in all pro-inflammatory transcripts, *Il1b*, *Il12b* and *Tnfa,* while anti-inflammatory *Arg1* was upregulated. PI3Kγ blockade with IPI-549 treatment in POD1 sxMDSCs, prevented the surgery-induced reduction of pro-inflammatory transcripts *Il1b*, and *Il12b*, however it did not rescue *Tnfa* mRNA expression. It seems that PI3Kγ signalling in the post-operative environment causes sxMDSCs to reduce their expression of pro-inflammatory effectors IL-1β and IL-12, leading to a pre-dominantly suppressive phenotype. Indeed, *Kaneda et al.* identified PI3Kγ as a molecular switch between immune stimulation and suppression(171). Activation of PI3Kγ lead to a primarily suppressive phenotype driven by C/EBPβ activation, while blockade of this signalling pathway lead to an immunostimulatory phenotype mediated by NFκB activation. PI3Kγ therefore may play a critical role in promoting the activation of a suppressive transcriptional programming leading to the enhanced suppressive capacity of sxMDSCs.

4.3.3.5 PI3Kγ inhibition reduces signaling thereby reducing sxMDSC-mediated NK cell suppression and postoperative metastases

I used our standard model of surgical stress to determine the efficacy of PI3Kγ inhibitors in reducing postoperative metastatic burden. This model involved challenging mice with lung-metastases forming B16F10-LacZ tumour cells followed by performing a highly invasive right nephrectomy. Previous work in our lab has demonstrated that surgical stress in this model leads to a significant increase in postoperative lung metastases(103, 107, 108). This coincides with an expansion of circulating sxMDSCs with increased suppressive potency as well as dysfunctional NK cells that is observable soon after surgery, on POD1. Therefore, surgical stress in this murine model leads to a similar expansion and activation as observed in patients postoperatively. To confirm that PI3Kγ inhibitor administration can cause measurable reductions in signalling in our murine model, I monitored the phosphorylation of AKT. Indeed, IPI-549 and TG100-115 treatment reduced pAKT both *in vitro* (Figure 9) and *in vivo* (Figure 10). Interestingly, G-MDSCs did not respond to inhibitor treatment *in vivo* while M-MDSCs showed a significant reducation in pAKT (Figure 10C). Currently, we are uncertain as to what could cause this, but it may suggest a difference in the make up of isoforms that result in phosphorylation of AKT such that G-MDSCs may have lower expression of PI3Kγ than M-MDSCs. Indeed, G-MDSCs do express PI3Kγ however it is expressed at equal proportion to PI3Kα, and PI3Kδ(235). This in in contrast to M-MDSCs, where PI3Kγ is by far the most dominant isoform, and primarily relies on this isoform to mediate PI3K signalling(236).

Next, I demonstrated that in an *ex vivo* co-culture suppression assay, with sxMDSCs recovered from surgery stressed mice, induced suppression of NK cells isolated from healthy mice

(Figure 11B). Moreover, MDSCs from non-surgery stressed mice showed reduced suppressive potency than postoperative counterparts. Interestingly, PI3Kγ inhibitor treatment, namely IPI-549, either *in vitro* or *in vivo*, lead to a reduction in sxMDSC-mediated suppression of NK cells. Taken together, PI3Kγ inhibition leads to reduced MDSC suppressive potency and improved NKC.

Contradictory to our hypothesis, previously in our lab, Dr. Angka demonstrated that systemic administration of PI3Kγ inhibitors lead to an increase in tumour burden and reduced NKC (Supplemental Figure 6). Interestingly, despite the relatively low expression of PI3Kγ in NK cells, this isoform is critical for NK cell migration, development, and effector functions(237). p110γ deficiency and impairment of GPCR signaling prevented full NK cell maturation(238). Moreover, PI3Kγ is required for cytotoxicity, NK cell-target cell interaction and receptor-induced IFNγ production (238). Taken together, PI3Kγ is critical for NKC, migration and maturation.

Reflecting on our murine model, inhibiting this pathway may prevent NK-mediated clearance of B16F10 tumour cells, enabling greater tumour formation than in control surgery mice. Moreover, the fact that PI3Kγ is crucial for NK cell maturation and migration may explain why PI3Kγ inhibitor administration in the *ex vivo* co-culture suppression model showed a positive effect in reducing sxMDSC-mediated suppression of NKC. In this model, these functions may not be as important since the experimental design uses isolated mature NK cells which are already in close proximity with target cells. However, I did observe a reduction in NKC with PI3Kγ inhibition in NK cells that were co-cultured with K562s, in the absence of MDSCs (Figure 6C). This suggests that, in the *ex vivo* suppression assay, PI3Kγ inhibition can directly disrupt NK effector functions, but the benefit of inhibiting sxMDSC suppressive activity leads to an overall net improvement in NKC. In contrast, with systemic *in vivo* blockade of PI3Kγ signalling, more pathways necessary

for NK cell function, including maturation, migration, as well as NKC, are disrupted, leading to reduced tumour clearance which far outweighs the potential benefit of inhibiting sxMDSC suppressive activity. Therefore, investigating a strategy to ensure that only sxMDSCs are affected by PI3Kγ blockade is important to exclude deleterious effect on NK cell function involved with systemic administration.

Despite the efficacy of PI3Kγ inhibition in reducing sxMDSC-mediated suppression of NK cells, direct inhibition of NK cell activity with systemic *in vivo* administration presents a significant barrier in leveraging the therapeutic potential of targeting this pathway. To circumvent this confounding effect and explore the effects of sxMDSC-specific inhibition of PI3Kγ on metastatic tumour burden, we utilized an adoptive transfer model. I first confirmed that sxMDSCs isolated from surgery-stressed mice could suppress NK cells from healthy, control mice in our *ex vivo* suppression assay, and that this suppression was reversed when the surgery stressed mice were treated with PI3Kγ inhibitors prior to sxMDSC isolation.

Next, I took this a step further, as explained in section 4.1.12.4, by performing an MDSC adoptive transfer. Here, I was able to determine that adoptive transfer of sxMDSCs recapitulated the effects of postoperative stress demonstrated in previous studies(103, 108), resulting in increased metastatic burden in healthy mice that were tumour challenged (Figure 13B). This highlights that sxMDSCs are a primary driver of postoperative metastatic disease. However, IPI-549, but not TG100-115, treatment significantly reduced sxMDSC-mediated metastatic disease. Interestingly, this decrease in lung metastases was similar to that of control, non-surgery induced MDSCs, in other words, isolated from mice that were not exposed to surgery. This suggests that PI3Kγ inhibition can reverse the effects of surgical stress in activating and potentiating the suppressive

potency of sxMDSCs. Interestingly, these findings align with what was described by Kaneda *et al.*, pharmaceutical blockade of PI3Kγ signalling lead to a significant reduction in tumour burden(171). However, it is important to note that these benefits in reduced postoperative metastatic burden were observed when PI3Kγ signalling was inhibited in the sxMDSCs population specifically. With systemic administration of PI3Kγ inhibitors, there was a detrimental effect on NK cell function as well as increased postoperative metastatic burden. Therefore, this experiment highlights the importance of developing an sxMDSC-specific approach for targeting PI3Kγ signalling, thereby limiting the deleterious effect observed with systemic administration.

Taken together, Chapter 1 demonstrates that PI3Kγ signalling is upregulated in sxMDSCs. Moreover, sxMDSCs are significantly more suppressive than their preoperative counterparts. Targeting PI3Kγ signalling is a potent strategy to reduce sxMDSC-mediated suppression of NKC and metastatic burden. Despite the advantages of targeting PI3Kγ, this pathway is also important in NK anti-tumour immunity, therefore systemic administration can lead to deleterious effects resulting in NK cell suppression and increased metastatic burden. I was able to circumvent this issue using an adoptive transfer of sxMDSCs that were treated with PI3Kγ inhibitors into tumour challenged mice. From a clinical standpoint, isolating a patient's MDSCs so that they can be treated with PI3Kγ inhibitors *ex vivo* followed by autologous transfer is cumbersome and expensive. Moreover, sxMDSC expansion, and subsequent NK cell suppression, occurs rapidly within a 24-hour period(99). Therefore, an sxMDSC-specific drug delivery approach for PI3Kγ inhibition is necessary and must be administered before surgery so that it may act rapidly to counter postoperative potentiation of sxMDSCs. To circumvent these issues, Chapter 2 discusses the testing of an antibody-drug conjugate (ADC) targeting sxMDSCs with a PI3Kγ inhibitor payload.

4.3.4 Next steps

Although I have demonstrated a link between PI3Kγ signalling and the suppressive activity of sxMDSCs, there are still questions that have yet to be answered. Specifically, although I have determined that PI3Kγ causes signalling via AKT, I have yet to elucidate further downstream effectors. Kaneda *et al.* identified that inhibition of PI3Kγ signalling cause a shift in transcriptional programming, going from an immunosuppressive phenotype controlled by C/EBPβ to an inflammatory one mediated by NF-κb. A greater understanding of the transcriptional changes that occur in sxMDSCs with PI3Kγ inhibition may help to elucidate the role of this signalling pathway in mediating suppressive activity. To investigate this, I would like to perform RNA-seq on sxMDSC with or without PI3Kγ inhibition. This would allow us to understand the various transcriptional changes that occur because of PI3Kγ blockade in sxMDSCs and its implications in reducing suppressive activity.

Alongside a lack of understanding of the effect of PI3K blockade on the transcriptional programming of sxMDSCs, currently little is known about the PI3Kγ dependent mechanisms that sxMDSCs utilize to suppress NK cells. Kaneda *et al.* demonstrated that Arginase-1 expression is down-regulated with PI3Kγ inhibition(171). Arginase catalyzes the reaction of arginine into ornithine, which reduces the availability of this nutrient. This is problematic given the important role of arginine in NK cell function. As a result, MDSCs may cause a nutritional deficiency of arginine in the media, thereby inhibiting NK cell activity. As a next step, I plan to perform a proteomic screen to better understand the suppressive factors that could be expressed by MDSCs. I am currently also investigating arginase activity in baseline and postoperative MDSCs, with and without PI3Kγ inhibitor treatment. Taken together, this work may provide a better understanding of the mechanisms sxMDSCs rely on to suppress NK cells postoperatively.

Chapter 3

4.4 Introduction

Despite the potential benefits of PI3Kγ inhibition in reducing sxMDSC suppressive activity, it is plagued with deleterious side effects when administered systemically. As explained in Chapter 1, murine systemic administration of PI3Kγ inhibitors led to a reduction in NKC and increased postoperative metastatic burden. Despite the relatively low abundance of this isoform in NK cells, it plays an important role in chemotaxis and cytokine-stimulated NK effector functions(237, 238). Chapter 2 investigated the potential of an ADC as a strategy to direct a PI3Kγ inhibitor payload specifically to sxMDSCs. This would thereby eliminate the potential deleterious side effects of systemic administration while concentrating the therapeutic potential of PI3Kγ inhibition on the sxMDSC targets.

4.4.1 CD155 as a marker of postoperative MDSCs

Our first goal was to determine a potential sxMDSC marker. Previously in our lab, Dr. Angka and Dr. Martel performed a proteomic screen of N-glycosylated cell surface markers on sxMDSCs using a protocol that was developed by our collaborator, Dr. Kislinger(239). Of the 1,176 peptides discovered, 5 surface proteins were detected at high intensities on POD1 while being undetectable at baseline. Among these was CD155 (Poliovirus Receptor, PVR), which has been shown to be important for MDSC suppressive activity. Dr. Martel performed further validation by flow cytometry which established that CD155 was consistently upregulated on M-MDSCs on POD1 as compared to baseline and healthy donors (Supplemental Figure 7).

CD155, also known as poliovirus receptor (PVR) or Nectin-Like (Necl)-5, is a 70 kD trans-membrane protein belonging to the immunoglobulin superfamily(240). While its expression is very low in normal human tissue, it is overexpressed in several transformed cells and is involved in cell adhesion, movement, and proliferation, and is associated with a poor prognosis in cancer patients(241, 242). The receptor has three known ligands on NK and T cells: DNAM-1(52), TIGIT(243), and CD96 (T-cell activated increased late expression, or TACTILE)(244). While CD96 and TIGIT are considered to be immunosuppressive, DNAM-1 is an immune-activating receptor that, when bound, stimulates cytotoxicity of NK cells and T cells, and increases IFN-γ production(245, 246). Despite the importance of CD155 expression for DNAM-1 activity, research has demonstrated that chronic expression of CD155 on malignant cells results in the downregulation of DNAM-1. This down-regulation is associated with NK cell immunosuppression(247). For my undergraduate honours thesis, I demonstrated that postoperative NK cells have a marked reduction in DNAM-1 expression (Supplemental Figure 8), which is associated with reduced effector functions. Martel *et al.* has further investigated the role of CD155 on sxMDSCs in DNAM-1 down-regulation and NK cell suppression. He demonstrated that the SKII.4 monoclonal antibody, which is directed against human CD155, could block CD155-DNAM-1 interactions, thereby reducing sxMDSC-mediated NKC in an *ex vivo* co-culture suppression assay (Supplemental Figure 9). My work will capitalize on CD155 as an sxMDSC-specific marker for targeted PI3Kγ inhibitor drug delivery.

4.4.2 The Antibody-drug conjugate

ADCs are innovative biopharmaceutical products in which a monoclonal antibody is linked to a small molecule drug with a stable linker. They couple the antigen specificity of antibodies to the activity of small molecules via these cleavable linkers. Conventionally, ADCs have been

developed for cancer-specific targeting with a cytotoxic payload to kill tumor cells without harming the healthy cells. This is in comparison to chemotherapy, with its poor specificity towards tumor cells/tissues, is often associated with a poor therapeutic response and substantial toxicities to normal healthy tissues(248). However, since then, ADCs have been explored for applications in a wide variety of diseases with various payloads(249). Here, I explore the use of an ADC as a strategy to target sxMDSCs with a PI3Kγ inhibitor payload.

4.4.3 Development of an sxMDSC-specific Antibody-drug Conjugate

Our collaborators at ADMARE were able to develop an ADC using the SKII.4 monoclonal antibody (targeting CD155) linked to a PI3Kγ inhibitor payload at a 4:1 ratio (inhibitor:antibody). This payload, known as Compound 17, was first reported in the paper that also identified TG100-115 as a PI3Kγ -specific inhibitor. As a result, Compound 17 has a chemically similar structure to TG100-115(206). They both bind to the ATP binding pocket of PI3Kγ by interacting with the same protein residues. Unfortunately, the Compound 17 – CD155 ADC was the only one that was developed as attempts to conjugate IPI-549 or TG100-115 to the SKII.4 antibody led to unstable compounds.

Once the ADC has bound to CD155 expressed on sxMDSCs, it must undergo internalization via receptor-mediated endocytosis, which forms an early endosome. Endosomal trafficking is highly complex and can have multiple different fates. It could undergo cargo recycling where it is returned to the cell surface or undergo endolysosomal degradation. If the endosome is recycled back to the plasma membrane, the ADC is unable to deliver its payload thereby preventing its therapeutic activity. In contrast, internalized cargo destined for the endolysosomal degradation pathway is retained in a maturing endosome until finally being

delivered to the lysosome(250). The ADC specifically relies on this pathway to exert its therapeutic activity as it leads to the cleavage of the linker between the SKII.4 antibody and small molecular inhibitors, thereby releasing the C17 payload. This payload can then traverse through the endosomal lipid bilayer into the cytosol, where it can inhibit PI3Kγ signalling. Therefore, the acidification and maturation of the endosome containing the ADC complex is critical for the eventual processing and release of the payload(250).

This chapter will investigate the efficacy of the ADC compound in reducing sxMDSC-mediated suppression of NK.

4.5 Rationale and Hypothesis

4.5.1 Rationale

Systemic administration of PI3Kγ inhibitors lead to a deleterious reduction of NKC and increased postoperative metastatic burden compared to untreated controls. Therefore, the objective of Chapter 2 was to determine the efficacy of the αCD155-C17 ADC as an sxMDSC-specific approach for PI3Kγ inhibition. The advantage of this approach is that it can exclude the negative effects of PI3Kγ inhibition on NK-mediated tumour immunosurveillance while maximizing its therapeutic efficacy on reducing sxMDSC-mediated suppression of NKC. CD155 is upregulated on sxMDSCs and is a suitable target for cell-specific drug delivery via an ADC. As shown in Figure 5C, sxMDSCs also demonstrate increased PI3Kγ signalling which contributes to their suppressive phenotype. Taken together, an ADC that can deliver the PI3Kγ inhibitor payload, Compound 17, leading to the inhibition of this pathway in sxMDSCs can lead to a reduction in their suppressive activity.

4.5.2 Hypothesis

I hypothesize that the αCD155-C17 ADC can target CD155 expressed on sxMDSCs and can reduce their PI3Kγ signalling, thereby leading to a reduction in their suppression of NK cytotoxicity.

4.5.2.1 Aims

The aims of Chapter 2 are:

- Confirm the internalization and endolysosomal degradation of the αCD155-C17 ADC following CD155 binding
- Determine the effect of αCD155-C17 ADC on PI3Kγ signalling in sxMDSCs
- Investigate the efficacy of αCD155-C17 ADC in reducing sxMDSC-mediated suppression of NKC

4.6 Methods

All relevant methods were the same as in Chapter 4.1. The additional methods in this chapter were the internalization assay and multiple single-guide RNA (sgRNA) Cas9 CD155 knockout (KO).

4.6.1 Internalization assay

sxMDSCs were isolated as described in section 4.1.6. $5x10^5$ sxMDSCs were plated on to 2 seperate V-bottom 96 well plates designated as control and internalization. Cells were washed

with wash buffer (PBS with 1% FBS) and resuspended in a 15µg/mL dilution of mouse anti-CD155 SKII.4 mIgG1 (Biolegend) or a 15µg/mL dilution of a matched mouse mIgG1 isotype (Biolegend), followed by 1 hour incubation on ice for labelling. Samples were washed with wash buffer and resuspended in a 5µg/mL dilution of an anti-mIgG1 secondary antibody conjugated to a pH-sensitive FITC dye (pHAB, Goat α FITC mIgG1-Fc-pHAb conjugate Fc-λ, donated by ADMARE), followed by 30 minutes incubation on ice. Cells were again washed with wash buffer and the internalization plate was resuspended in CRPMI, followed by a 4-hour incubation at 37ºC in a 5% CO_2 chamber. The control plate was instead immediately stained with an MDSC ECS master mix as explained in section 4.1.5. After the 4-hour incubation, the internalization plate was washed with wash buffer and stained with the same MDSC ECS master mix. Following staining, cells were fixed, and flow cytometry was used to determine the internalization signal.

4.6.2 Multi-guide sgRNA Cas9 CD155 Knockout

4.6.2.1 Reagents and Preparation

A Gene Knockout V2 Kit containing a single tube mix of 3 pre-designed sgRNAs (1.5nmol, each 100 nucleotides long) each targeting different protospacer adjacent motif (PAM) sites on the CD155 gene, Cas9 2NLS nuclease (20µM, S. pyogenes), nuclease-free Tris-EDTA (TE, (10 mM Tris-HCl, 1 mM EDTA, pH 8.0) buffer and nuclease-free water was ordered from Synthego. A 4-D Nucleofector™ Kit V4X-2012 (optimized for K562 transfection) which contained pMAXGFP™ vector (1 µg/µL in 10 mM Tris pH 8.0) as a positive control was ordered from Lonza-Bioscience.

4.6.2.2 Electroporation of RNP complexes and confirmation of CD155 KO

Multi-guide sgRNA were prepared according to Gene Knockout V2 protocol (Synthego). Briefly, the provided 1.5nmol sgRNA were rehydrated in nuclease-free TE buffer to a final concentration of 100 µM (100 pmol/µL). The rehydrated multi guide sgRNA was then diluted to a working concentration of 30µM (30pmol/µL). Electroportaion was conducted according to the manufacturer's protocol (Lonza-Bioscience). Briefly, the provided supplement was added to the Nucleofector™ solution at a 4.5:1 ratio (Nucleofector:supplement). Cas9 2NLS (20µM) was mixed with sgRNA (30µM) at a 9:1 ratio (sgRNA:Cas9) diluted to the 25µL reaction volume with the prepared Nucleofector™ solution and incubated for 10 minutes, designated as the RNP solution. A separate transfection control was included by diluting 2µg of pMAXGFP™ vector in Nucleofector™ solution.

Cells were prepared for transfection according to the optimized Nucleofection protocol provided by Lonza-Bioscience. Briefly, K562s were replated whenever they reached $1x10^6$ cells/mL and seeded at $1x10^5$ cells/mL in a T75 flask. 2 days before electroporation, cells were subcultured at a density of $3x10^5$cells/mL. When cells were ready to be electroporated, they were harvested and washed in PBS. Cells were resuspended in prepared Nucleofector™ solution containing supplement to a final concentration of $1.33x10^7$ cells/mL. 25µL of the prepared RNP solution was added to 75µL of K562 suspension ($1x10^6$ cells) in a 100µL Nucleovette™. Electroporation was performed according to manufacturer's protocol optimized for K562 electroporation on the 4-D Nucleofector™ instrument (Lonza-Bioscience). Following electroporation, cells were plated into pre-warmed CRPMI to recover. GFP expression in

transfection control wells were determined using the EVOS™ M5000 Imaging System (Invitrogen; Waltham, MA).

After 24 hours of recovery, the bulk population was expanded and underwent limiting dilution to $0.5x10^6$ cells/mL to isolate clones. Individual cells were plated and grown out. CD155 knockout was confirmed by flow cytometry by washing the cells in PBS and resuspended in ECS Master mix containing CD155 Clone SKII.4 APC (Biolegend) and BV510 Fixable Viability dye. A matched mouse IgG1 isotype Clone MOPC-21 APC (Biolegend) was used for CD155 gating. Confirmed CD155 knockout were then sent for Sanger sequencing following DNA isolation using DNAeasy™ Kit (Qiagen; Germantown, MD), according to the manufacturer's protocol. Genetic knockout of CD155 was confirmed by Inference of CRISPR edits (ICE) analysis by Synthego(251).

4.7 Results

4.7.1 αCD155-C17 ADC undergo internalization proportional to the expression of CD155

Since an antibody drug conjugate needs to undergo internalization and lysosomal processing to deliver its drug payload, I investigated the internalization of αCD155. αCD155 or a matched mIgG1 isotype with scrambled antigen specificity was incubated with POD1 sxMDSCs. A secondary αmIgG1 antibody conjugated to a pH-sensitive dye (pHAB) is then added. As the CD155 receptor is internalized and acidified in the lysosome, the pHAB fluoresces thereby providing a measurable signal for internalization. Fluorescence is measured immediately after the addition of the secondary antibody (no internalization) or after incubating for 4 hours (Figure 14A). Fluorescent internalization signal (MFI) increased by 13.6% (left) and 37.6% (right) when

incubated with the isotype (non-specific) antibody, compared to 74.6% (left) and 86.3% (right) with αCD155 after 4 hours (Figure 14B). There was a positive correlation (R^2=0.39, Sy.x = 16.38) between the surface expression density (MFI) of CD155 on sxMDSCsvs. the internalization of CD155 in sxMDSCs (Figure 14D).

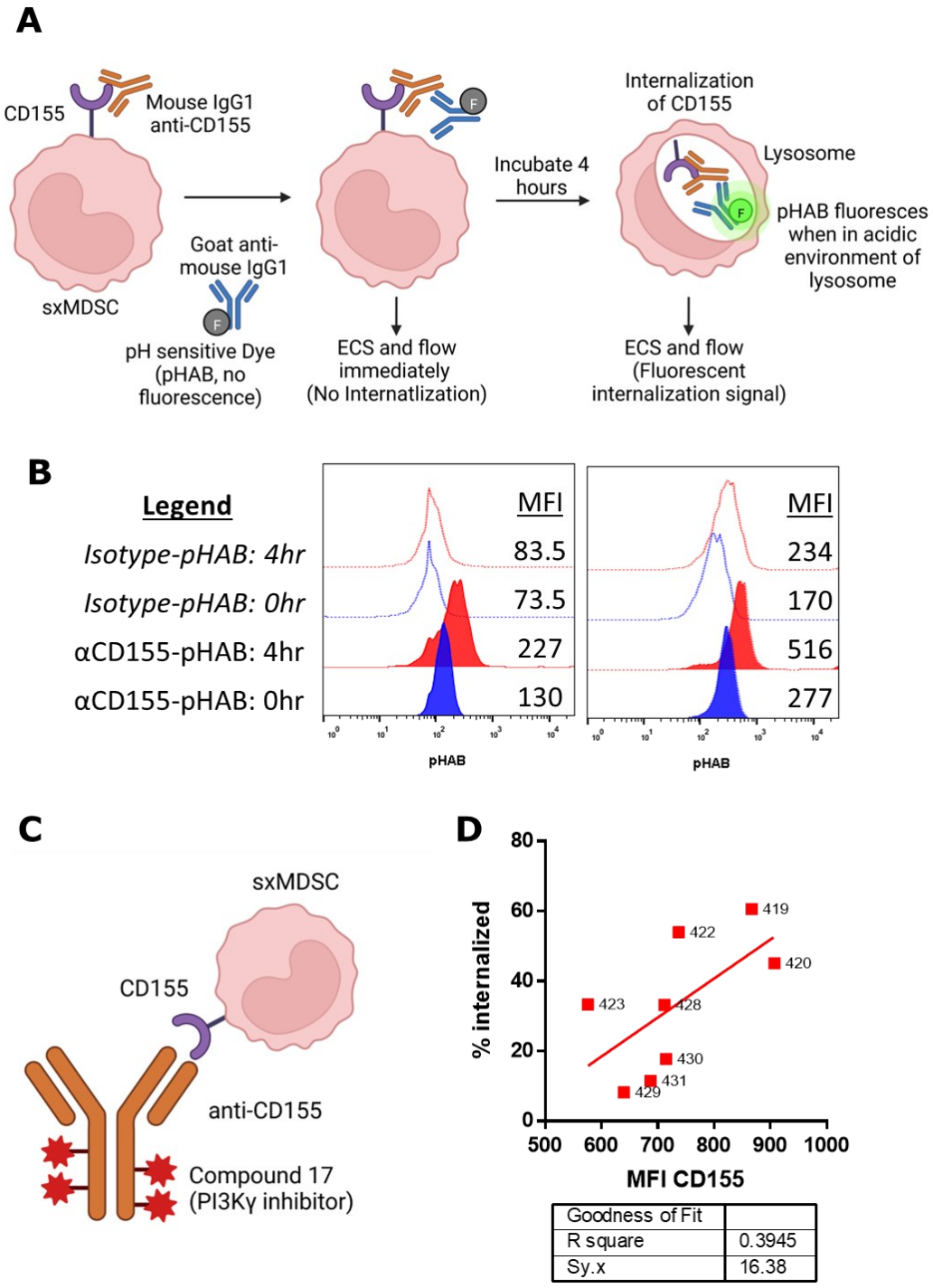

Figure 14: CD155 antibody undergoes internalization. A) Schematic of internalization assay. αCD155 primary antibody (or isotype) is incubated with sxMDSCs ($CD155^{+}$). Secondary antibody cojugated to pH-sensitive dye targets primary antibody. A subset of the sample is stained and flowed immediately to determine the "no internalization" signal. The rest of the sample is incubated for 4 hours to enable internalization of CD155. Upon acidification of the lysosome, the

pH sensitive dye becomes fluorescent which is then detected by flow. B) Representative MFI plots of two patients following internalizaton assay. Isotype is shown as a dashed line in blue (0 hr) and red (4 hr). Anti-CD155 is shown as a soild line line in blue (0 hr) and red (4 hr). C)Diagram of ADC targetting CD155 expressed on POD1 MDSCs. D)Dot plot correlation between the proportion of of MDSCs that internalized CD155 and surfacesurface expression density of CD155 (MFI) (n=8). Patient number ID is indicated.

4.7.2 αCD155-C17 ADC does not reduce sxMDSC-mediated suppression of NKC against CD155^{+} targets beyond ADC treatment alone

I investigated the efficacy of the αCD155-C17 ADC in reducing sxMDSC-mediated suppression of NK cells in our *ex vivo* suppression assay. NK cells and MDSCs were co-cultured with either DMSO, IPI-549, C17, αCD155-C17, or αCD155. 1μM IPI-549 and 0.1μM C17 lead to a significant reduction in sxMDSC suppression of NK cells compared to untreated controls ($p<0.05$, Figure 15A). 1μM C17 completely abolished MDSC suppressive activity ($p<0.01$). Both αCD155-C17 and αCD155 reduced suppressive activity ($p<0.05$), however, the αCD155-C17 ADC was unable to reduce suppressive activity beyond the effect of CD155 blockade alone. Moreover, when NK cells and K562 target cells were co-cultured without the presence of MDSCs, αCD155-C17, and αCD155 caused increased killing ($p<0.05$, Figure 15B). Alongside sxMDSCs, K562s also highly express CD155 (Figure 15C and D). This presents a possible confounding effect as the αCD155-C17 and αCD155 are capable of directly binding to the K562s which may mediate ADCC. This would explain the direct effect of αCD155-C17 and αCD155 treatment in increasing NKC of K562 cells despite the absence of sxMDSCs.

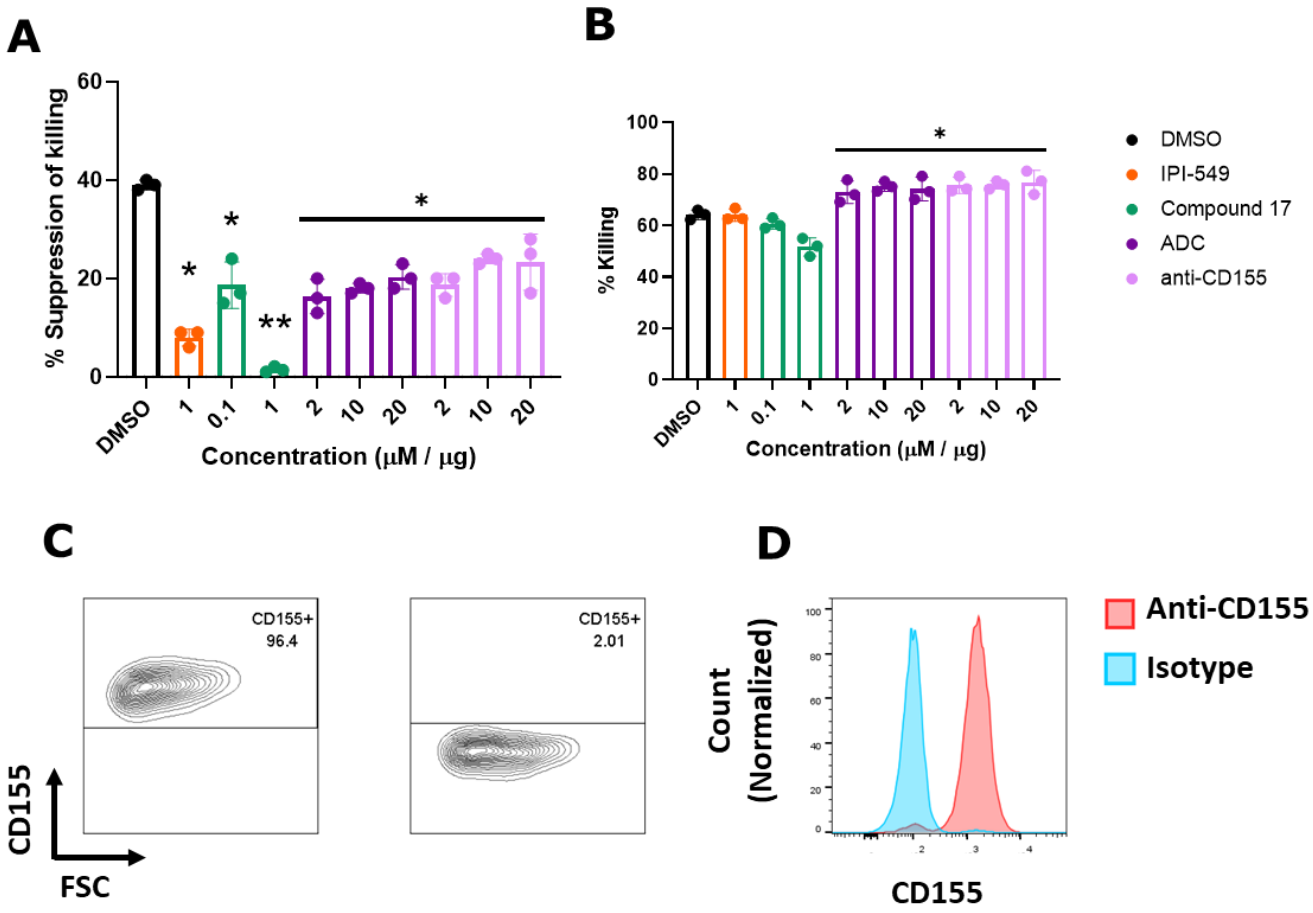

Figure 15: ADC treatment did not improve NK cell cytotoxicity beyond CD155 mAb treatment. A) Comparison of effect of ADC treatment or CD155 blockade vs PI3Kγ inhibition on suppression of NKC in MDSC:NK:K562 culture (n = 3) and (B) NK killing in NK:K562 co-culture (n=3). Significant differences compared to DMSO control are reported. C) Contour flow plot of CD155 expression on K562, anti-CD155 (left) and isotype (right). D) Histogram of anti-CD155 (red) and isotype (blue) on K562.

4.7.3 Development of a Cas9 CD155KO K562 Target cell line

Given the confounding effect of CD155 expression on K562, we wanted to develop a CD155KO cell line. Since we have standardized our suppression assay model with K562 cells, I wanted to use a CD155 genetic KO K562 cell line to test the efficacy of the ADC. A pool of 3 sgRNAs, each targeting a unique PAM site on CD155, was used which was complexed with Cas9 (Figure 16A). WT K562 cells were electroporated with this ribonucleoprotein (RNP) complex. Qualitatively, most of the cells were GFP^+ compared to mock controls, suggesting good nucleofection efficiency (Figure 16B). After 3 days, loss of CD155 surface expression was confirmed by flow, whereby both Pool #1 and Pool #2 showed a reduction in CD155 MFI compared to the mock control (Figure 16C). Given the baseline efficiency of reduction of CD155 expression in both pools, Pool #2 was used for further processing. CD155 expression continued to decrease in Pool #2 approaching that of the isotype MFI up to day 7 (Figure 16D). Following limiting dilution and clonal expansion, clone 6 was isolated from Pool #2. Clone 6 showed a complete loss of CD155 expression which was confirmed by flow (Figure 16E). Sanger sequencing, followed by ICE analysis revealed multiple indels in all three cut sites in proximity to the PAM (Supplemental Figure 10).

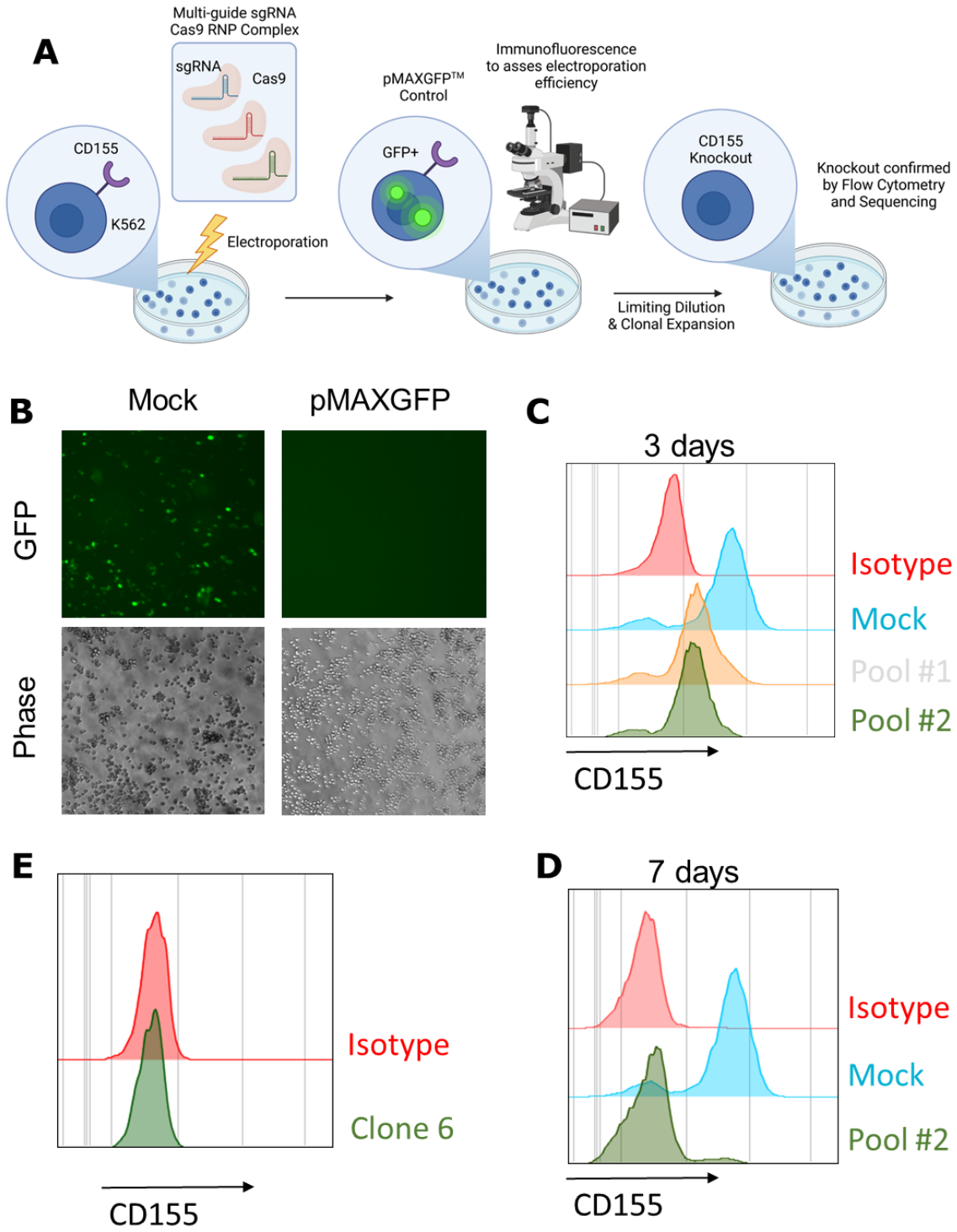

Figure 16: Development of a CD155 KO K562 Cell line. A) Schematic of workflow for knocking out CD155. K562 cells were electroporated with multiple sgRNA-Cas9 RNP complexes. pMAXGFP™ vector was used as a transfection control and efficiency was determined by IF. Pooled cells underwent limiting dilution for clonal selection, followed by expansion. CRISPR-

Cas9 mediated CD155 KO in K562 cells was confirmed by flow and gene sequencing. B) Representative IF image of GFP expression in K562 cells following nucleofection with pMAXGFP^{TM} transfection control vector (GFP^{+}) and mock. C) Histogram of expression of CD155 in K562 cells 3 and (D) 7 days after nucleofection. E) Histogram of expression of CD155 in isolated clone 6 (CD155 KO) following limiting dilution of Pool #2.

4.7.4 αCD155-C17 ADC treatment leads to a modest reduction of sxMDSC-mediated suppression of NKC against CD155KO Targets

Following knockout of CD155 in K562, MDSC-mediated suppression of NKC against CD155KO K562 targets was tested. Expectedly, 1μM IPI-549 caused a significant reduction in suppression of NKC ($p<0.01$), the same was true for 0.1μM C17 ($p<0.05$) and 1μM C17 ($p<0.01$, Figure 17A). 2 μg/mL, 10 μg/mL, 20 μg/mL of αCD155-C17 did reduce sxMDSC-mediated suppression of NKC ($p<0.05$). In contrast, αCD155 did not cause a reduction in NKC suppression. αCD155-C17 and αCD155 did not cause an increase in killing when NK92 cells were co-cultured with K562 CD155KO in the absence of sxMDSCs (Figure 17B). This suggested that the ADCC effect observed in Figure 15 was effectively abolished by CD155KO.

To confirm that αCD155-C17 could affect PI3Kγ signalling, sxMDSCs were treated with the ADC and pAKT was quantified by flow (Figure 17C). 1μM IPI-549, 0.1μM C17 and 1μM C17 caused a significant reduction in pAKT MFI ($p<0.05$). 2 μg/mL, 10 μg/mL, 20 μg/mL of αCD155-C17 also reduced pAKT levels ($p<0.05$). However, the effect did not show a dose dependent response. 2 μg/mL, 10 μg/mL, 20 μg/mL of αCD155 did not cause a reduction of pAKT levels.

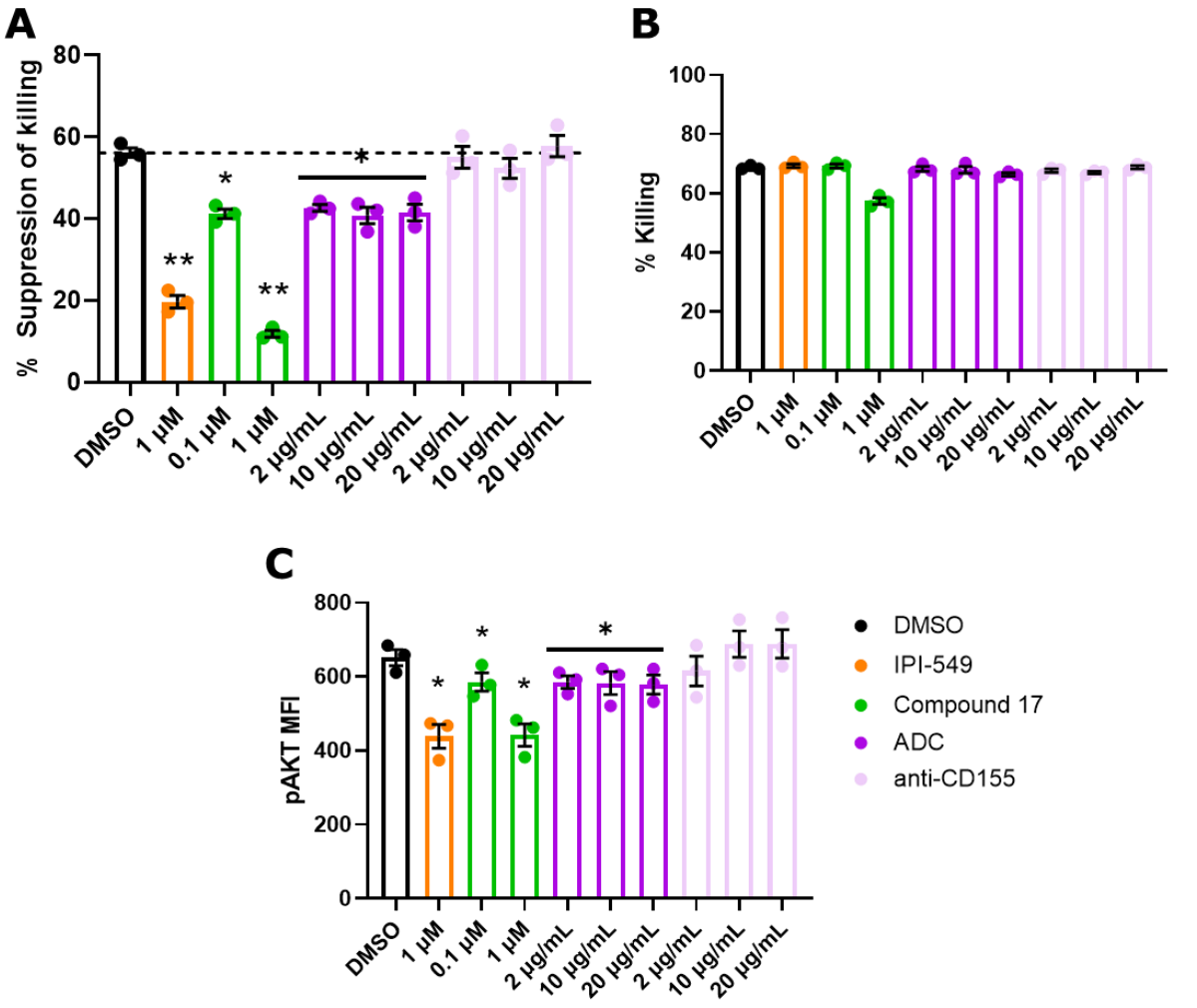

Figure 17: ADC treatment caused a modest improvement reduction of NK suppression when using K562 CD155KO targets. A) Suppression assay with MDSCs:NK: CD155KO K562 (n = 3). B) Killing assay with NK:CD155KO K562 co-culture (n = 3). C) Phosphorylation of AKT (T308) with PI3Kγ inhibitor, αCD155-C17 (ADC) or αCD155 mAb treatment (n = 3).

4.8 Discussion

Despite the potential benefits of PI3Kγ inhibition in inhibiting sxMDSC suppressive activity, it is plagued with deleterious side effects when administered systemically. As explained in 4.2.12, systemic murine administration of PI3Kγ inhibitors led to a reduction in NKC and increased postoperative metastatic burden (Supplemental Figure 6). Despite the relatively low abundance of PI3Kγ in NK cells, it plays an important role in chemotaxis and cytokine-stimulated NK effector functions(237, 238). Chapter 2 investigated the potential of utilizing an ADC as a strategy to direct a PI3Kγ inhibitor payload specifically to sxMDSCs. This would thereby eliminate the potential deleterious side effects of systemic administration while maximizing the therapeutic benefit of PI3Kγ blockade by specifically concentrating it on sxMDSC targets.

4.8.1 CD155 is a suitable target for sxMDSCs

Our first goal was to determine a potential sxMDSC marker. From a proteomic screen, Dr. Martel identified that CD155 is highly upregulated in sxMDSCs. CD155 is a Nectin-type receptor that can interact with DNAM-1, TIGIT and CD96, which are expressed on NK cells(246). This suggests that CD155 may be an important molecule in sxMDSCs that enables crosstalk between NK cells and MDSCs. Previous research has demonstrated that $TIGIT^+$ NK cells were able to interact with CD155 expressed on MDSCs, leading to their suppression(147). Blockade of the TIGIT-CD155 interaction, or by separating the cells by using a transwell, prevented MDSC-mediated NKC suppression. Previously, I had determined that postoperative NK cells demonstrate a significant reduction in DNAM-1 expression (Supplemental Figure 8), which is coupled with a reduction in effector functions(99). Research has shown that co-culturing NK cells with $CD155^+$ cells lead to a similar phenotype as surgery stress, namely the reduction in DNAM-1 expression(245). Given the upregulation of CD155 on MDSCs, a similar effect could occur in the

postoperative environment, leading to the observed reduction in DNAM-1 expression on NK cells. Dr. Martel investigated the use of the SKII.4 antibody for CD155 blockade and demonstrated a marked reduction in sxMDSC-mediated suppression of NKC (Supplemental Figure 9). My work focused on targeting CD155 as a unique marker of sxMDSCs for ADC-mediated PI3Kγ inhibitor, Compound 17, drug delivery (αCD155-C17). Thus, I wanted to investigate its potential in targeting PI3Kγ signalling in MDSCs, thereby reducing the suppression of NKC.

4.8.2 αCD155 undergoes internalization in the endolysosomal degradation pathway, which is critical for ADC-mediated therapeutic activity

As described by Chalouni *et al.* ADC internalization, and processing is an important step for its therapeutic activity(252). Therefore, for the C17 small-molecular inhibitor to carry out its function, following CD155 binding, the ADC must be internalized and undergo acidification as part of endolysosomal degradation. We investigated the internalization of αCD155 by using the workflow described in 4.6.1. Briefly, antibody binding to CD155 causes receptor-mediated endocytosis which forms an early endosome. The αCD155-C17ADC specifically relies on the endolysosomal degradation pathway as it leads to the cleavage of the linker between αCD155 and the drug thereby releasing the C17 payload. This payload can traverse through the endosomal lipid bilayer into the cytosol, where it can inhibit PI3Kγ signalling. We confirmed that the ADC undergoes endolysosomal degradation by using a pH-sensitive dye which fluoresces as the endosome acidifies. Acidification is not present in endosome trafficking that leads to the receptor being recycled back to the cell surface and is exclusive to the endolysosomal degradation pathway. Therefore, this pHAB allowed us to quantify CD155 internalization events that will specifically undertake the critical endolysosomal degradation pathway, which is necessary for ADC function. We determined that CD155 does undergo internalization following SKII.4 binding, compared to a

non-specific, isotype-matched control antibody (Figure 14B). Notably, CD155 internalization was directly correlated with the expression of CD155 on MDSCs. This is important to note since internalization does not seem to plateau where it reaches a fixed upper rate limit, instead, it suggests that internalization is only limited by the magnitude of CD155 expression on sxMDSCs.

However, this protocol does not capture some key pieces of information. DeVay *et al.* demonstrated target receptors for ADCs can have different affinity for endosomal trafficking(253). Some targets were more likely to undergo endolysosomal degradation, thereby bolstering therapeutic efficacy, while other targets preferentially were recycled back to the cell surface. It is important to be able to investigate the preferential trafficking of CD155 upon ADC binding, and whether that is skewed towards endolysosomal degradation or not(253). Moreover, although these results indicate proper internalisation and processing of the ADC, it does not indicate whether the payload is efficiently cleaved and released. In the next section, I attempted to determine the release of the payload from the endolysosome to exert its therapeutic effects by investigating the effects of the ADC on sxMDSC-mediated suppression of NK cells and phosphorylation of AKT as an indicator of PI3Kγ signalling.

4.8.3 αCD155-C17 was not as effective as C17 alone in reducing sxMDSC-mediated suppression of NKC and inhibiting PI3Kγ signalling

Having confirmed that αCD155-C17 can undergo internalization, I have attempted to determine the efficacy of αCD155-C17 in reducing sxMDSC-mediated suppression of NKC. Although αCD155-C17 treatment improved NKC compared to DMSO controls it was unable to surpass the effect of CD155 blockade alone (Figure 15A). Moreover, both αCD155-C17 and αCD155 increased NKC against K562s in the absence of sxMDSCs (Figure 15B). Alongside

sxMDSCs, K562s also highly express CD155 (Figure 15C and D). This presents a possible confounding effect as the αCD155-C17 and αCD155 are capable of directly binding to the K562s which may mediate ADCC. This would explain the direct effect of αCD155-C17 and αCD155 treatment in increasing NKC cells despite the absence of sxMDSCs.

This led to the development of a $CD155^{-/-}$ K562 cell line (Figure 16). Although this approach enabled the determination of PI3Kγ inhibitor payload mediated reduction of sxMDSC activity, the effect was modest. It should be noted that 5μg/mL, 10μg/mL, and 20μg/mL concentration of αCD155-C17 provides approximately 0.1uM, 0.2μM and 0.4μM concentration of C17, respectively. The highest concentration, 20μg/mL of αCD155-C17, had a similar efficacy to 0.1μM of the unconjugated C17 drug, despite delivering approximately 4 times the concentration (0.4μM of C17) (Figure 17A). This suggests that conjugating C17 to the αCD155 led to an overall reduction in efficacy when it was administered in the form of an ADC.

This was further confirmed by investigating phosphorylation of AKT, as an indicator of PI3Kγ signalling, following αCD155-C17, C17 or aCD155 treatment. Although αCD155-C17 had a greater ability to inhibit PI3Kγ signalling by reducing pAKT compared to αCD155, its efficacy was not as potent as the effect of the unconjugated C17 at 0.1μM (Figure 17C). Given the observation that both inhibition of sxMDSC suppressive activity and PI3Kγ signalling does not exhibit a dose-dependent response to αCD155-C17 treatment, it suggests that there is a potential rate limiting step that is reducing the overall efficacy of the C17 compound when administered in the form of an ADC. In this *ex vivo* model, there are 2 major steps needed to deliver the C17 payload from the ADC. First, αCD155-C17 must bind to CD155 and undergo internalization. Next, following endolysosomal processing, the C17 payload must be cleaved from its linker so that the

small molecular inhibitor can exert its effect on the sxMDSC. In section 4.7.1, I concluded that ADC internalization is only limited by the magnitude of CD155 expression on the sxMDSC. In all instances, patients show highly upregulated CD155 expression (Supplemental Figure 7) following surgery which would be sufficient for αCD155-C17 internalization. In follow up discussions with Admare, they indicated that they faced a great deal of difficulty in preparing a stable ADC conjugate with the C17 inhibitor. As a result, they had to make use of a linker which is known for its high stability which may potentially come at the cost of reduced cleavage efficiency. They suggested that following internalization, the linker may not be cleaved effectively, preventing the release of the C17 inhibitor. This conclusion does corroborate with the observations made: despite proper internalization of the ADC, the release of the C17 could be a rate limiting step, thereby preventing its activity in targeting PI3Kγ. Unfortunately, the instruments and expertise needed to confirm the poor performance of the αCD155-C17 ADC is beyond the scope of this thesis. Despite this, the potential for inhibiting PI3Kγ in sxMDSCs shows promise and we are already considering alternative approaches for sxMDSC-specific targeting.

4.8.4 Alternative approach to target MDSCs

Reflecting on the results, it is disappointing that the ADC did not show efficacy in reducing PI3Kγ-mediated suppression of NKC, beyond the C17 compound on its own. If anything, this was an important learning moment for me: as scientists, we are left to make amends with the fact that even the most valiant of efforts may be unfruitful. Yet there is an unspoken curiosity of results that do not align with expected results, that stokes the fires of creativity, as we search for the silver lining to carry us forward in our research efforts. For me, after reviewing the available literature, that silver lining is recognizing that this was the first time ever that an ADC has been developed to target sxMDSCs. Our partners at Admare went through significant hurdles to identify an appropriate PI3Kγ inhibitor payload and linker to develop this

truly one-of-a-kind therapeutic product. Given the novelty of this research, it is important to view it as a "first attempt", for what could be a powerful strategy to target sxMDSCs and prevent postoperative immunosuppression. As such, it prompted me to consider alternative approaches for an MDSC-specific strategy to target PI3Kγ.

As mentioned, CD155 is the poliovirus (PV) receptor, which PV binds to undergo cell entry. PV was shown to bind to the membrane-distal, N-terminal domain known as "D1" of CD155 which interacts with specific residues on the PV capsid(254). This binding process causes changes in the structural conformation of PV which causes the virus to "unzip" thereby releasing its genetic code for replication upon entry. The PV capsid consists of 60 copies of each of the VP1, VP2, VP3, and VP4 proteins, which forms 5 icosahedral axes. Belnap *et al.* utilized a crystal structure of PV complexed with soluble CD155 to determine the binding regions(255). They identified that D1 binds to the viral canyon, a narrow depression around each of the icosahedral axes. Importantly, specific residues in the interface between the VP1, VP2, and VP3 subunits interact with the D1 domain of CD155 in the viral canyon(254). Mutational studies demonstrated that residues on VP1, and not VP2 or VP3, were critical for CD155 binding(256). Taken together, VP1 could be used as a ligand to direct MDSC-specific therapeutic by targeting CD155 expression. This could include linking VP1 with a PI3Kγ inhibitor payload or loading an exosome with this payload and coating it with VP1 particles(257). This approach provides an entirely new approach to targeting MDSCs, separate to an ADC-based platform.

Conclusion

Despite the importance of surgery for tumour resection, the full benefits of this curative procedure cannot be realized due to the consequences of postoperative suppression of tumour immunosurveillance. Therefore, perioperative research which attempt to reduce the counter-

productive side effects of surgery will ultimately lead to improved patient outcomes. Surgery causes activation of the surgery stress response which is marked by two clashing forces, an inflammatory phase, and the CAR. The physical trauma that is induced by surgery causes an overwhelming release of DAMPs. These DAMPs activate neutrophils which are a key promoter of the acute inflammatory phase, while anti-inflammatory cytokines dominate the CAR. The CAR is responsible for significant suppression of NK cells. This may provide a window of opportunity for residual tumour cells to re-establish themselves and manifest as postoperative metastatic disease. Moreover, several effectors of the surgery stress response promote the expansion, migration, and activation of MDSCs. DAMPs signals emergency myelopoiesis from the bone marrows which leads to the rapid expansion of immature myeloid cells (MDSCs). Factors that are highly expressed during the CAR potentiate the suppressive activity of MDSCs. So much so, that we have termed these unique, highly suppressive immunoregulatory cell as surgery induced MDSCs (sxMDSCs). This prompted the search for potential sxMDSC antagonists.

Previously in our lab, Dr. Angka identified PI3K as a target for reducing sxMDSC-mediated suppression of NKC. Given its role as a master regulator of many pathways, targeting PI3Kγ may serve to impact several of these suppressive mechanisms simultaneously. As highlighted by Zhu *et al.*(258), PI3Kγ inhibition is already undergoing investigations in Phase 2 clinical trials for its efficacy in treating advanced solid tumors head and neck squamous cell carcinoma, triple negative break cancer, renal cell carcinoma and urothelial carcinoma(259–261). However, its application in the perioperative space, had yet to be investigated. I have demonstrated that PI3Kγ inhibition shows efficacy in reversing the effects of surgical stress in inducing the suppressive activity of sxMDSCs thereby reducing postoperative inhibition of NKC and metastatic burden. However, the benefits of PI3Kγ inhibition are countered by its potentially deleterious

effects on NKC with systemic administration. In fact, systemic PI3Kγ blockade led to a significant increase in postoperative metastatic burden. This presents a troubling implication for the suitability of PI3Kγ inhibitors in a clinical setting, as it may inadvertently lead to worse patient outcomes and greater metastatic disease. As mentioned prior, PI3Kγ inhibitors are currently being tested in Phase 2 clinical trials so it is important that we better understand the "double edged" nature of blocking this pathway to ensure the best possible patient outcomes and addressing the potential for negative side effects.

These findings prompted us to consider a sxMDSC-specific approach to targeting PI3Kγ signalling. As a preliminary experiment, sxMDSCs were isolated from donor mice that underwent surgery in the presence or absence of PI3Kγ inhibition. These sxMDSCs were transferred to tumour challenged recipient mice. This ensured that only the adoptively transferred sxMDSCs were exposed to surgery-induced stress and PI3Kγ blockade. This sxMDSC-specific approach to determine the effects of PI3Kγ blockade allowed us to exclude the deleterious side effects on anti-tumour immunity associated with systemic PI3Kγ inhibition in the recipient mice. I was able to determine that adoptive transfer of sxMDSCs to recipient mice recapitulated the effects of postoperative metastatic burden, leading to greater metastases. However, blockade of PI3Kγ signalling in the sxMDSCs, prior to adoptive transfer, prevented this increased metastatic burden. Therefore, this experiment served as an important steppingstone to confirm the necessity of an sxMDSC-specific approach for PI3Kγ blockade, to maximize the therapeutic benefits, while minimizing its deleterious effects on anti-tumour immunity mediated by NK cells. Chapter 2 discussed the development of an sxMDSC-specific MDSCs.

Previously in our lab, Dr. Martel and Dr. Angka identified that CD155 was a viable candidate as a sxMDSC marker, given its significant upregulation postoperatively in this cell population. While its expression is very low in normal human tissue, it is overexpressed in several transformed cells and is involved in cell adhesion, movement, and proliferation, and is associated with a poor prognosis in cancer patients(241, 242). Dr. Martel investigated the role of CD155 on sxMDSCs in NK cell suppression. He demonstrated that the commercially available SKII.4 monoclonal antibody, which is directed against human CD155, blocked interactions between sxMDSCs and NK cells, thereby reducing sxMDSC-mediated NKC in an *ex vivo* co-culture suppression model. My work capitalized on this unique expression profile of CD155 to directly target sxMDSCs. Using this information, Admare, our collaborators developed an ADC, named αCD155-C17, which conjugated the SKII.4 antibody-mediated targeting of $CD155^{+}$ sxMDSCs with a PI3Kγ inhibitor payload (called C17) via a cleavable linker. I confirmed that the SKII.4 antibody used for the αCD155-C17 undergoes internalization and endolysosomal degradation in sxMDSCs, following CD155 binding. Endolysosomal degradation is important as it enables the release of the PI3Ks inhibitor payload from the ADC via cleavage. However, the use of a clinically actionable ADC targeting sxMDSCs with a PI3Kγ inhibitor payload was not effective in reducing sxMDSC-mediated suppression of NKC. Moreover, it did not impact pAKT signalling to a greater degree than C17 compound alone. In fact, it seemed that conjugating the C17 compound to the SKII.4 antibody to form αCD155-C17 significantly reduced its therapeutic efficacy. We believe this is most likely due to ineffective cleavage of the linker, thereby preventing release of the C17 payload to exert a therapeutic effect within the sxMDSC. Therefore, this inefficient cleavage acts a rate limiting step, preventing effective blockade of PI3Kγ signalling. As such, further investigation into new strategies for targeting sxMDSCs will be required. Notably, PV ligands that

binds to CD155 and mediate internalization are well characterized. This could offer an entirely new platform for sxMDSC-specific targeting separate to ADC-based treatments. Regardless, my work has highlighted the current gap in addressing the critical perioperative period that contributes to the risk of cancer recurrence in patients following surgery. Targeting PI3Kγ in sxMDSCs could be an important strategy to help reduce this risk.

Final Thoughts and the Importance of this Work

Patients who undergo cancer surgery have hope to be free of the burden that this disease places on them and their loved ones. Sadly, cancer recurrence, especially after curative surgery, is a devastating reality that many face. Currently, cancer surgery may seem like a double-edged sword as its negatives seek to undermine the therapeutic benefits it can have on a patient's clinical outcomes. Research such as this shows compelling evidence that perioperative therapies are an overlooked, yet important area of research that has the potential to generate novel, targeted approaches that complement and improve surgical outcomes. I hope that our efforts one day ensure that patients undergoing curative surgery are truly free of the burden of cancer.

References

1. Little MP. 2010. Cancer models, genomic instability and somatic cellular Darwinian evolution. Biol Direct 5:19.

2. Huang S. 2012. Tumor progression: Chance and necessity in Darwinian and Lamarckian somatic (mutationless) evolution. Prog Biophys Mol Biol 110:69–86.

3. Cooper GM. 2000. The Development and Causes of Cancer. Cell Mol Approach 2nd Ed.

4. Knox SS. 2010. From “omics” to complex disease: a systems biology approach to gene-environment interactions in cancer. Cancer Cell Int 10:11.

5. Munhoz RR, Postow MA. 2016. Recent advances in understanding antitumor immunity. F1000Research 5:2545.

6. Egen JG, Ouyang W, Wu LC. 2020. Human Anti-tumor Immunity: Insights from Immunotherapy Clinical Trials. Immunity 52:36–54.

7. Kinker GS, Vitiello GAF, Ferreira WAS, Chaves AS, Cordeiro de Lima VC, Medina T da S. 2021. B Cell Orchestration of Anti-tumor Immune Responses: A Matter of Cell Localization and Communication. Front Cell Dev Biol 9.

8. Greaves M, Maley CC. 2012. CLONAL EVOLUTION IN CANCER. Nature 481:306–313.

9. Greaves M. 2015. Evolutionary Determinants of Cancer. Cancer Discov 5:806–820.

10. Vineis P, Berwick M. 2006. The population dynamics of cancer: a Darwinian perspective. Int J Epidemiol 35:1151–1159.

11. Hanahan D, Weinberg RA. 2000. The Hallmarks of Cancer. Cell 100:57–70.

12. Tran KB, Lang JJ, Compton K, Xu R, Acheson AR, Henrikson HJ, Kocarnik JM, Penberthy L, Aali A, Abbas Q, Abbasi B, Abbasi-Kangevari M, Abbasi-Kangevari Z, Abbastabar H, Abdelmasseh M, Abd-Elsalam S, Abdelwahab AA, Abdoli G, Abdulkadir HA, Abedi A, Abegaz KH, Abidi H, Aboagye RG, Abolhassani H, Absalan A, Abtew YD, Ali HA, Abu-Gharbieh E, Achappa B, Acuna JM, Addison D, Addo IY, Adegboye OA, Adesina MA, Adnan M, Adnani QES, Advani SM, Afrin S, Afzal MS, Aggarwal M, Ahinkorah BO, Ahmad AR, Ahmad R, Ahmad S, Ahmad S, Ahmadi S, Ahmed H, Ahmed LA, Ahmed MB, Rashid TA, Aiman W, Ajami M, Akalu GT, Akbarzadeh-Khiavi M, Aklilu A, Akonde M, Akunna CJ, Hamad HA, Alahdab F, Alanezi FM, Alanzi TM, Alessy SA, Algammal AM, Al-Hanawi MK, Alhassan RK, Ali BA, Ali L, Ali SS, Alimohamadi Y, Alipour V, Aljunid SM, Alkhayyat M, Al-Maweri SAA, Almustanyir S, Alonso N, Alqalyoobi S, Al-Raddadi RM, Al-Rifai RHH, Al-Sabah SK, Al-Tammemi AB, Altawalah H, Alvis-Guzman N, Amare F, Ameyaw EK, Dehkordi JJA, Amirzade-Iranaq MH, Amu H, Amusa GA, Ancuceanu R, Anderson JA, Animut YA, Anoushiravani A, Anoushirvani AA, Ansari-Moghaddam A, Ansha MG, Antony B, Antwi MH, Anwar SL, Anwer R, Anyasodor AE, Arabloo J, Arab-Zozani M, Aremu O, Argaw AM, Ariffin H, Aripov T, Arshad M, Artaman A, Arulappan J, Aruleba RT, Aryannejad A, Asaad M, Asemahagn MA, Asemi Z, Asghari-Jafarabadi M, Ashraf T, Assadi R, Athar M, Athari SS, Atout MMW, Attia S, Aujayeb A, Ausloos M, Avila-Burgos L, Awedew AF, Awoke MA, Awoke T, Quintanilla BPA, Ayana TM, Ayen SS, Azadi D, Azadnajafabad S, Azami-Aghdash S, Azanaw MM, Azangou-Khyavy M, Jafari AA, Azizi H, Azzam AYY, Babajani A, Badar M, Badiye AD, Baghcheghi N, Bagheri N, Bagherieh S, Bahadory S, Baig AA, Baker JL, Bakhtiari A, Bakshi RK, Banach M, Banerjee I, Bardhan M, Barone-Adesi F, Barra F, Barrow A, Bashir NZ, Bashiri A, Basu S, Batiha A-MM, Begum A, Bekele AB, Belay AS, Belete MA, Belgaumi UI, Bell AW, Belo L, Benzian H, Berhie AY, Bermudez ANC, Bernabe E, Bhagavathula AS, Bhala N, Bhandari BB, Bhardwaj N, Bhardwaj P, Bhattacharyya K, Bhojaraja VS, Bhuyan SS, Bibi S,

Bilchut AH, Bintoro BS, Biondi A, Birega MGB, Birhan HE, Bjørge T, Blyuss O, Bodicha BBA, Bolla SR, Boloor A, Bosetti C, Braithwaite D, Brauer M, Brenner H, Briko AN, Briko NI, Buchanan CM, Bulamu NB, Bustamante-Teixeira MT, Butt MH, Butt NS, Butt ZA, Santos FLC dos, Cámera LA, Cao C, Cao Y, Carreras G, Carvalho M, Cembranel F, Cerin E, Chakraborty PA, Charalampous P, Chattu VK, Chimed-Ochir O, Chirinos-Caceres JL, Cho DY, Cho WCS, Christopher DJ, Chu D-T, Chukwu IS, Cohen AJ, Conde J, Cortés S, Costa VM, Cruz-Martins N, Culbreth GT, Dadras O, Dagnaw FT, Dahlawi SMA, Dai X, Dandona L, Dandona R, Daneshpajouhnejad P, Danielewicz A, Dao ATM, Soltani RDC, Darwesh AM, Das S, Davitoiu DV, Esmaeili ED, Hoz FPD la, Debela SA, Dehghan A, Demisse B, Demisse FW, Denova-Gutiérrez E, Derakhshani A, Molla MD, Dereje D, Deribe KS, Desai R, Desalegn MD, Dessalegn FN, Dessalegni SAA, Dessie G, Desta AA, Dewan SMR, Dharmaratne SD, Dhimal M, Dianatinasab M, Diao N, Diaz D, Digesa LE, Dixit SG, Doaei S, Doan LP, Doku PN, Dongarwar D, Santos WM dos, Driscoll TR, Dsouza HL, Durojaiye OC, Edalati S, Eghbalian F, Ehsani-Chimeh E, Eini E, Ekholuenetale M, Ekundayo TC, Ekwueme DU, Tantawi ME, Elbahnasawy MA, Elbarazi I, Elghazaly H, Elhadi M, El-Huneidi W, Emamian MH, Bain LE, Enyew DB, Erkhembayar R, Eshetu T, Eshrati B, Eskandarieh S, Espinosa-Montero J, Etaee F, Etemadimanesh A, Eyayu T, Ezeonwumelu IJ, Ezzikouri S, Fagbamigbe AF, Fahimi S, Fakhradiyev IR, Faraon EJA, Fares J, Farmany A, Farooque U, Farrokhpour H, Fasanmi AO, Fatehizadeh A, Fatima W, Fattahi H, Fekadu G, Feleke BE, Ferrari AA, Ferrero S, Desideri LF, Filip I, Fischer F, Foroumadi R, Foroutan M, Fukumoto T, Gaal PA, Gad MM, Gadanya MA, Gaipov A, Galehdar N, Gallus S, Garg T, Fonseca MG, Gebremariam YH, Gebremeskel TG, Gebremichael MA, Geda YF, Gela YY, Gemeda BNB, Getachew M, Getachew ME, Ghaffari K, Ghafourifard M, Ghamari S-H, Nour MG, Ghassemi F, Ghimire A, Ghith N, Gholamalizadeh M, Navashenaq JG, Ghozy S, Gilani SA, Gill PS, Ginindza TG, Gizaw ATT, Glasbey JC, Godos J, Goel A, Golechha M, Goleij P, Golinelli D, Golitaleb M, Gorini G, Goulart BNG, Grosso G, Guadie HA, Gubari MIM, Gudayu TW, Guerra MR,

Gunawardane DA, Gupta B, Gupta S, Gupta VB, Gupta VK, Gurara MK, Guta A, Habibzadeh P, Avval AH, Hafezi-Nejad N, Ali AH, Haj-Mirzaian A, Halboub ES, Halimi A, Halwani R, Hamadeh RR, Hameed S, Hamidi S, Hanif A, Hariri S, Harlianto NI, Haro JM, Hartono RK, Hasaballah AI, Hasan SMM, Hasani H, Hashemi SM, Hassan AM, Hassanipour S, Hayat K, Heidari G, Heidari M, Heidarymeybodi Z, Herrera-Serna BY, Herteliu C, Hezam K, Hiraike Y, Hlongwa MM, Holla R, Holm M, Horita N, Hoseini M, Hossain MM, Hossain MBH, Hosseini M-S, Hosseinzadeh A, Hosseinzadeh M, Hostiuc M, Hostiuc S, Househ M, Huang J, Hugo FN, Humayun A, Hussain S, Hussein NR, Hwang B-F, Ibitoye SE, Iftikhar PM, Ikuta KS, Ilesanmi OS, Ilic IM, Ilic MD, Immurana M, Innos K, Iranpour P, Irham LM, Islam MS, Islam RM, Islami F, Ismail NE, Isola G, Iwagami M, J LM, Jaiswal A, Jakovljevic M, Jalili M, Jalilian S, Jamshidi E, Jang S-I, Jani CT, Javaheri T, Jayarajah UU, Jayaram S, Jazayeri SB, Jebai R, Jemal B, Jeong W, Jha RP, Jindal HA, John-Akinola YO, Jonas JB, Joo T, Joseph N, Joukar F, Jozwiak JJ, Jürisson M, Kabir A, Kacimi SEO, Kadashetti V, Kahe F, Kakodkar PV, Kalankesh LR, Kalankesh LR, Kalhor R, Kamal VK, Kamangar F, Kamath A, Kanchan T, Kandaswamy E, Kandel H, Kang H, Kanno GG, Kapoor N, Kar SS, Karanth SD, Karaye IM, Karch A, Karimi A, Kassa BG, Katoto PD, Kauppila JH, Kaur H, Kebede AG, Keikavoosi-Arani L, Kejela GG, Bohan PMK, Keramati M, Keykhaei M, Khajuria H, Khan A, Khan AAK, Khan EA, Khan G, Khan MN, Khan MA, Khanali J, Khatab K, Khatatbeh MM, Khatib MN, Khayamzadeh M, Kashani HRK, Tabari MAK, Khezeli M, Khodadost M, Kim MS, Kim YJ, Kisa A, Kisa S, Klugar M, Klugarová J, Kolahi A-A, Kolkhir P, Kompani F, Koul PA, Laxminarayana SLK, Koyanagi A, Krishan K, Krishnamoorthy Y, Bicer BK, Kugbey N, Kulimbet M, Kumar A, Kumar GA, Kumar N, Kurmi OP, Kuttikkattu A, Vecchia CL, Lahiri A, Lal DK, Lám J, Lan Q, Landires I, Larijani B, Lasrado S, Lau J, Lauriola P, Ledda C, Lee S, Lee SWH, Lee W-C, Lee YY, Lee YH, Legesse SM, Leigh J, Leong E, Li M-C, Lim SS, Liu G, Liu J, Lo C-H, Lohiya A, Lopukhov PD, Lorenzovici L, Lotfi M, Loureiro JA, Lunevicius R, Madadizadeh F, Mafi AR, Magdeldin S, Mahjoub S, Mahmoodpoor A, Mahmoudi M, Mahmoudimanesh M, Mahumud RA,

Majeed A, Majidpoor J, Makki A, Makris KC, Rad EM, Malekpour M-R, Malekzadeh R, Malik AA, Mallhi TH, Mallya SD, Mamun MA, Manda AL, Mansour-Ghanaei F, Mansouri B, Mansournia MA, Mantovani LG, Martini S, Martorell M, Masoudi S, Masoumi SZ, Matei CN, Mathews E, Mathur MR, Mathur V, McKee M, Meena JK, Mehmood K, Nasab EM, Mehrotra R, Melese A, Mendoza W, Menezes RG, Mengesha SiD, Mensah LG, Mentis A-FA, Mera-Mamián AYM, Meretoja TJ, Merid MW, Mersha AG, Meselu BT, Meshkat M, Mestrovic T, Jonasson JM, Miazgowski T, Michalek IM, Mijena GFW, Miller TR, Mir SA, Mirinezhad SK, Mirmoeeni S, Mirza-Aghazadeh-Attari M, Mirzaei H, Mirzaei HR, Misganaw AS, Misra S, Mohammad KA, Mohammadi E, Mohammadi M, Mohammadian-Hafshejani A, Mohammadpourhodki R, Mohammed A, Mohammed S, Mohan S, Mohseni M, Moka N, Mokdad AH, Molassiotis A, Molokhia M, Momenzadeh K, Momtazmanesh S, Monasta L, Mons U, Montasir AA, Montazeri F, Montero A, Moosavi MA, Moradi A, Moradi Y, Sarabi MM, Moraga P, Morawska L, Morrison SD, Morze J, Mosapour A, Mostafavi E, Mousavi SM, Isfahani HM, Khaneghah AM, Mpundu-Kaambwa C, Mubarik S, Mulita F, Munblit D, Munro SB, Murillo-Zamora E, Musa J, Nabhan AF, Nagarajan AJ, Nagaraju SP, Nagel G, Naghipour M, Naimzada MD, Nair TS, Naqvi AA, Swamy SN, Narayana AI, Nassereldine H, Natto ZS, Nayak BP, Ndejjo R, Nduaguba SO, Negash WW, Nejadghaderi SA, Nejati K, Kandel SN, Nguyen HVN, Niazi RK, Noor NM, Noori M, Noroozi N, Nouraei H, Nowroozi A, Nuñez-Samudio V, Nzoputam CI, Nzoputam OJ, Oancea B, Odukoya OO, Oghenetega OB, Ogunsakin RE, Oguntade AS, Oh I-H, Okati-Aliabad H, Okekunle AP, Olagunju AT, Olagunju TO, Olakunde BO, Olufadewa II, Omer E, Omonisi AEE, Ong S, Onwujekwe OE, Orru H, Otstavnov SS, Oulhaj A, Oumer B, Owopetu OF, Oyinloye BE, A MP, Padron-Monedero A, Padubidri JR, Pakbin B, Pakshir K, Pakzad R, Palicz T, Pana A, Pandey A, Pandey A, Pant S, Pardhan S, Park E-C, Park E-K, Park S, Patel J, Pati S, Paudel R, Paudel U, Paun M, Toroudi HP, Peng M, Pereira J, Pereira RB, Perna S, Perumalsamy N, Pestell RG, Pezzani R, Piccinelli C, Pillay JD, Piracha ZZ, Pischon T, Postma MJ, Langroudi AP, Pourshams A,

Pourtaheri N, Prashant A, Qadir MMF, Syed ZQ, Rabiee M, Rabiee N, Radfar A, Radhakrishnan RA, Radhakrishnan V, Raeisi M, Rafiee A, Rafiei A, Raheem N, Rahim F, Rahman MO, Rahman M, Rahman MA, Rahmani AM, Rahmani S, Rahmanian V, Rajai N, Rajesh A, Ram P, Ramezanzadeh K, Rana J, Ranabhat K, Ranasinghe P, Rao CR, Rao SJ, Rashedi S, Rashidi A, Rashidi M, Rashidi M-M, Ratan ZA, Rawaf DL, Rawaf S, Rawal L, Rawassizadeh R, Razeghinia MS, Rehman AU, Rehman I ur, Reitsma MB, Renzaho AMN, Rezaei M, Rezaei N, Rezaei N, Rezaei N, Rezaei S, Rezaeian M, Rezapour A, Riad A, Rikhtegar R, Rios-Blancas M, Roberts TJ, Rohloff P, Romero-Rodríguez E, Roshandel G, Rwegerera GM, S M, Saber-Ayad MM, Saberzadeh-Ardestani B, Sabour S, Saddik B, Sadeghi E, Saeb MR, Saeed U, Safaei M, Safary A, Sahebazzamani M, Sahebkar A, Sahoo H, Sajid MR, Salari H, Salehi S, Salem MR, Salimzadeh H, Samodra YL, Samy AM, Sanabria J, Sankararaman S, Sanmarchi F, Santric-Milicevic MM, Saqib MAN, Sarveazad A, Sarvi F, Sathian B, Satpathy M, Sayegh N, Schneider IJC, Schwarzinger M, Šekerija M, Senthilkumaran S, Sepanlou SG, Seylani A, Seyoum K, Sha F, Shafaat O, Shah PA, Shahabi S, Shahid I, Shahrbaf MA, Shahsavari HR, Shaikh MA, Shaka MF, Shaker E, Shannawaz M, Sharew MMS, Sharifi A, Sharifi-Rad J, Sharma P, Shashamo BB, Sheikh A, Sheikh M, Sheikhbahaei S, Sheikhi RA, Sheikhy A, Shepherd PR, Shetty A, Shetty JK, Shetty RS, Shibuya K, Shirkoohi R, Shirzad-Aski H, Shivakumar KM, Shivalli S, Shivarov V, Shobeiri P, Varniab ZS, Shorofi SA, Shrestha S, Sibhat MM, Malleshappa SKS, Sidemo NB, Silva DAS, Silva LMLR, Julian GS, Silvestris N, Simegn W, Singh AD, Singh A, Singh G, Singh H, Singh JA, Singh JK, Singh P, Singh S, Sinha DN, Sinke AH, Siraj MS, Sitas F, Siwal SS, Skryabin VY, Skryabina AA, Socea B, Soeberg MJ, Sofi-Mahmudi A, Solomon Y, Soltani-Zangbar MS, Song S, Song Y, Sorensen RJD, Soshnikov S, Sotoudeh H, Sowe A, Sufiyan MB, Suk R, Suleman M, Abdulkader RS, Sultana S, Sur D, Szócska M, Tabaeian SP, Tabarés-Seisdedos R, Tabatabaei SM, Tabuchi T, Tadbiri H, Taheri E, Taheri M, Soodejani MT, Takahashi K, Talaat IM, Tampa M, Tan K-K, Tat NY, Tat VY, Tavakoli A, Tavakoli A, Tehrani-Banihashemi A, Tekalegn Y, Tesfay FH, Thapar R, Thavamani A,

Chandrasekar VT, Thomas N, Thomas NK, Ticoalu JHV, Tiyuri A, Tollosa DN, Topor-Madry R, Touvier M, Tovani-Palone MR, Traini E, Tran MTN, Tripathy JP, Ukke GG, Ullah I, Ullah S, Ullah S, Unnikrishnan B, Vacante M, Vaezi M, Tahbaz SV, Valdez PR, Vardavas C, Varthya SB, Vaziri S, Velazquez DZ, Veroux M, Villeneuve PJ, Violante FS, Vladimirov SK, Vlassov V, Vo B, Vu LG, Wadood AW, Waheed Y, Walde MT, Wamai RG, Wang C, Wang F, Wang N, Wang Y, Ward P, Waris A, Westerman R, Wickramasinghe ND, Woldemariam M, Woldu B, Xiao H, Xu S, Xu X, Yadav L, Jabbari SHY, Yang L, Yazdanpanah F, Yeshaw Y, Yismaw Y, Yonemoto N, Younis MZ, Yousefi Z, Yousefian F, Yu C, Yu Y, Yunusa I, Zahir M, Zaki N, Zaman BA, Zangiabadian M, Zare F, Zare I, Zareshahrabadi Z, Zarrintan A, Zastrozhin MS, Zeineddine MA, Zhang D, Zhang J, Zhang Y, Zhang Z-J, Zhou L, Zodpey S, Zoladl M, Vos T, Hay SI, Force LM, Murray CJL. 2022. The global burden of cancer attributable to risk factors, 2010–19: a systematic analysis for the Global Burden of Disease Study 2019. The Lancet 400:563–591.

13. Biemar F, Foti M. 2013. Global progress against cancer—challenges and opportunities. Cancer Biol Med 10:183–186.

14. Nagai H, Kim YH. 2017. Cancer prevention from the perspective of global cancer burden patterns. J Thorac Dis 9:448–451.

15. Fares J, Fares MY, Khachfe HH, Salhab HA, Fares Y. 2020. Molecular principles of metastasis: a hallmark of cancer revisited. 1. Signal Transduct Target Ther 5:1–17.

16. Guan X. 2015. Cancer metastases: challenges and opportunities. Acta Pharm Sin B 5:402–418.

17. Riihimäki M, Thomsen H, Hemminki A, Sundquist K, Hemminki K. 2013. Comparison of survival of patients with metastases from known versus unknown primaries: survival in metastatic cancer. BMC Cancer 13:36.

18. Sugiura H, Yamada K, Sugiura T, Hida T, Mitsudomi T. 2008. Predictors of Survival in Patients With Bone Metastasis of Lung Cancer. Clin Orthop 466:729–736.

19. He L, Wang X, Liu X, Jia Y, Zhao W, Jia X, Zhu Y, Meng W, Tong Z. 2022. Analysis of Clinical Characteristics, Treatment, and Prognostic Factors of 106 Breast Cancer Patients With Solitary Pulmonary Nodules. Front Surg 9.

20. Hosseini H, Obradović MMS, Hoffmann M, Harper KL, Sosa MS, Werner-Klein M, Nanduri LK, Werno C, Ehrl C, Maneck M, Patwary N, Haunschild G, Gužvić M, Reimelt C, Grauvogl M, Eichner N, Weber F, Hartkopf AD, Taran F-A, Brucker SY, Fehm T, Rack B, Buchholz S, Spang R, Meister G, Aguirre-Ghiso JA, Klein CA. 2016. Early dissemination seeds metastasis in breast cancer. 7634. Nature 540:552–558.

21. Ring A, Spataro M, Wicki A, Aceto N. 2022. Clinical and Biological Aspects of Disseminated Tumor Cells and Dormancy in Breast Cancer. Front Cell Dev Biol 10.

22. Riggio AI, Varley KE, Welm AL. 2021. The lingering mysteries of metastatic recurrence in breast cancer. 1. Br J Cancer 124:13–26.

23. Wells A, Griffith L, Wells JZ, Taylor DP. 2013. The dormancy dilemma: Quiescence versus balanced proliferation. Cancer Res 73:3811–3816.

24. Roche J. 2018. The Epithelial-to-Mesenchymal Transition in Cancer. Cancers 10:52.

25. Fokas E, Engenhart-Cabillic R, Daniilidis K, Rose F, An HX. 2007. Metastasis: The seed and soil theory gains identity. Cancer Metastasis Rev 26:705–715.

26. López-Soto A, Gonzalez S, Smyth MJ, Galluzzi L. 2017. Control of Metastasis by NK Cells. Cancer Cell 32:135–154.

27. Kim YR, Yoo JK, Jeong CW, Choi JW. 2018. Selective killing of circulating tumor cells prevents metastasis and extends survival. J Hematol OncolJ Hematol Oncol 11:114.

28. Li Y, Wu S, Bai F. 2018. Molecular characterization of circulating tumor cells—from bench to bedside. Semin Cell Dev Biol 75:88–97.

29. Economos C, Morrissey C, Vessella RL. 2012. Circulating tumor cells as a marker of response: implications for determining treatment efficacy and evaluating new agents. Curr Opin Urol 22:190–196.

30. Vivier E, Tomasello E, Baratin M, Walzer T, Ugolini S. 2008. Functions of natural killer cells. Nat Immunol 9:503–510.

31. Paul S, Lal G. 2017. The Molecular Mechanism of Natural Killer Cells Function and Its Importance in Cancer Immunotherapy. Front Immunol 8:1124.

32. Zhang Y, Wallace DL, de Lara CM, Ghattas H, Asquith B, Worth A, Griffin GE, Taylor GP, Tough DF, Beverley PCL, Macallan DC. 2007. In vivo kinetics of human natural killer cells: the effects of ageing and acute and chronic viral infection. Immunology 121:258–265.

33. Sordo-Bahamonde C, Lorenzo-Herrero S, Payer ÁR, Gonzalez S, López-Soto A. 2020. Mechanisms of Apoptosis Resistance to NK Cell-Mediated Cytotoxicity in Cancer. Int J Mol Sci 21:3726.

34. Lo Nigro C, Macagno M, Sangiolo D, Bertolaccini L, Aglietta M, Merlano MC. 2019. NK-mediated antibody-dependent cell-mediated cytotoxicity in solid tumors: biological evidence and clinical perspectives. Ann Transl Med 7:105.

35. Mavilio D, Hosmalin A, Scott-Algara D. 2010. Chapter Thirty-Six - Natural killer cells and human immunodeficiency virus, p. 481–497. *In* Lotze, MT, Thomson, AW (eds.), Natural Killer Cells. Academic Press, San Diego.

36. Lin Q, Rong L, Jia X, Li R, Yu B, Hu J, Luo X, Badea SR, Xu C, Fu G, Lai K, Lee M, Zhang B, Gong H, Zhou N, Chen XL, Lin S, Fu G, Huang J-D. 2021. IFN-γ-dependent NK cell activation is essential to metastasis suppression by engineered Salmonella. 1. Nat Commun 12:2537.

37. 1996. Interferon gamma production by natural killer (NK) cells and NK1.1+ T cells upon NKR-P1 cross-linking. J Exp Med 183:2391–2396.

38. Schroder K, Hertzog PJ, Ravasi T, Hume DA. 2004. Interferon-gamma: an overview of signals, mechanisms and functions. J Leukoc Biol 75:163–189.

39. Ikeda H, Old LJ, Schreiber RD. 2002. The roles of IFN gamma in protection against tumor development and cancer immunoediting. Cytokine Growth Factor Rev 13:95–109.

40. 'T-cell-ness' of NK cells: unexpected similarities between NK cells and T cells | International Immunology | Oxford Academic. https://academic.oup.com/intimm/article/23/7/427/675088. Retrieved 10 December 2022.

41. Gonzalez S, González-Rodríguez AP, Suárez-Álvarez B, López-Soto A, Huergo-Zapico L, Lopez-Larrea C. 2011. Conceptual aspects of self and nonself discrimination. Self Nonself 2:19–25.

42. Sivori S, Vacca P, Del Zotto G, Munari E, Mingari MC, Moretta L. 2019. Human NK cells: surface receptors, inhibitory checkpoints, and translational applications. Cell Mol Immunol 16:430–441.

43. Barrow AD, Martin CJ, Colonna M. 2019. The Natural Cytotoxicity Receptors in Health and Disease. Front Immunol 10.

44. Shifrin N, Raulet DH, Ardolino M. 2014. NK cell self tolerance, responsiveness and missing self recognition. Semin Immunol 26:138–144.

45. Wu J, Cherwinski H, Spies T, Phillips JH, Lanier LL. 2000. Dap10 and Dap12 Form Distinct, but Functionally Cooperative, Receptor Complexes in Natural Killer Cells. J Exp Med 192:1059–1068.

46. Lanier LL. 2009. DAP10- and DAP12-associated receptors in innate immunity. Immunol Rev 227:150–160.

47. Ben-Shmuel A, Sabag B, Biber G, Barda-Saad M. 2021. The Role of the Cytoskeleton in Regulating the Natural Killer Cell Immune Response in Health and Disease: From Signaling Dynamics to Function. Front Cell Dev Biol 9:609532.

48. Gilfillan S, Chan CJ, Cella M, Haynes NM, Rapaport AS, Boles KS, Andrews DM, Smyth MJ, Colonna M. 2008. DNAM-1 promotes activation of cytotoxic lymphocytes by nonprofessional antigen-presenting cells and tumors. J Exp Med 205:2965–2973.

49. Xiong P, Sang H-W, Zhu M. 2015. Critical roles of co-activation receptor DNAX accessory molecule-1 in natural killer cell immunity. Immunology 146:369–378.

50. Pende D, Bottino C, Castriconi R, Cantoni C, Marcenaro S, Rivera P, Spaggiari GM, Dondero A, Carnemolla B, Reymond N, Mingari MC, Lopez M, Moretta L, Moretta A. 2005. PVR (CD155) and Nectin-2 (CD112) as ligands of the human DNAM-1 (CD226) activating receptor: involvement in tumor cell lysis. Mol Immunol 42:463–469.

51. Zhang Z, Wu N, Lu Y, Davidson D, Colonna M, Veillette A. 2015. DNAM-1 controls NK cell activation via an ITT-like motif. J Exp Med 212:2165–2182.

52. Tahara-Hanaoka S, Shibuya K, Onoda Y, Zhang H, Yamazaki S, Miyamoto A, Honda S-I, Lanier LL, Shibuya A. 2004. Functional characterization of DNAM-1 (CD226) interaction with its ligands PVR (CD155) and nectin-2 (PRR-2/CD112). Int Immunol 16:533–538.

53. Gao J, Zheng Q, Xin N, Wang W, Zhao C. 2017. CD155, an onco-immunologic molecule in human tumors. Cancer Sci 108:1934–1938.

54. Okumura G, Iguchi-Manaka A, Murata R, Yamashita-Kanemaru Y, Shibuya A, Shibuya K. 2020. Tumor-derived soluble CD155 inhibits DNAM-1–mediated antitumor activity of natural killer cells. J Exp Med 217:e20191290.

55. Killer Ig-Like Receptors (KIRs): Their Role in NK Cell Modulation and Developments Leading to Their Clinical Exploitation - PMC. https://www.ncbi.nlm.nih.gov/pmc/articles/PMC6558367/. Retrieved 11 December 2022.

56. Kärre K. 2002. NK Cells, MHC Class I Molecules and the Missing Self. Scand J Immunol 55:221–228.

57. Borrego F. 2006. The First Molecular Basis of the “Missing Self” Hypothesis. J Immunol 177:5759–5760.

58. Dhatchinamoorthy K, Colbert JD, Rock KL. 2021. Cancer Immune Evasion Through Loss of MHC Class I Antigen Presentation. Front Immunol 12:636568.

59. Purdy AK, Campbell KS. 2009. Natural killer cells and cancer: regulation by the killer cell Ig-like receptors (KIR). Cancer Biol Ther 8:13–22.

60. Ishigami S, Natsugoe S, Tokuda K, Nakajo A, Che X, Iwashige H, Aridome K, Hokita S, Aikou T. 2000. Prognostic value of intratumoral natural killer cells in gastric carcinoma. Cancer 88:577–583.

61. Coca S, Perez-Piqueras J, Martinez D, Colmenarejo A, Saez MA, Vallejo C, Martos JA, Moreno M. 1997. The prognostic significance of intratumoral natural killer cells in patients with colorectal carcinoma. Cancer 79:2320–2328.

62. Donskov F, von der Maase H. 2006. Impact of immune parameters on long-term survival in metastatic renal cell carcinoma. J Clin Oncol Off J Am Soc Clin Oncol 24:1997–2005.

63. Gannon PO, Poisson AO, Delvoye N, Lapointe R, Mes-Masson A-M, Saad F. 2009. Characterization of the intra-prostatic immune cell infiltration in androgen-deprived prostate cancer patients. J Immunol Methods 348:9–17.

64. Tong L, Jiménez-Cortegana C, Tay AHM, Wickström S, Galluzzi L, Lundqvist A. 2022. NK cells and solid tumors: therapeutic potential and persisting obstacles. Mol Cancer 21:206.

65. Imai K, Matsuyama S, Miyake S, Suga K, Nakachi K. 2000. Natural cytotoxic activity of peripheral-blood lymphocytes and cancer incidence: an 11-year follow-up study of a general population. The Lancet 356:1795–1799.

66. Filip S, Vymetalkova V, Petera J, Vodickova L, Kubecek O, John S, Cecka F, Krupova M, Manethova M, Cervena K, Vodicka P. 2020. Distant Metastasis in Colorectal Cancer Patients—Do We Have New Predicting Clinicopathological and Molecular Biomarkers? A Comprehensive Review. Int J Mol Sci 21:5255.

67. Retsky M, Demicheli R. 2014. Multimodal Hazard Rate for Relapse in Breast Cancer: Quality of Data and Calibration of Computer Simulation. Cancers 6:2343–2355.

68. Onuma AE, Zhang H, Gil L, Huang H, Tsung A. 2020. Surgical Stress Promotes Tumor Progression: A Focus on the Impact of the Immune Response. J Clin Med 9:4096.

69. Tohme S, Simmons RL, Tsung A. 2017. Surgery for Cancer: A Trigger for Metastases. Cancer Res 77:1548–1552.

70. Park Y, Jun HR, Choi HW, Hwang DW, Lee JH, Song KB, Lee W, Kwon J, Ha SH, Jun E, Kim SC. 2021. Circulating tumour cells as an indicator of early and systemic recurrence after surgical resection in pancreatic ductal adenocarcinoma. 1. Sci Rep 11:1644.

71. Tachtsidis A, McInnes LM, Jacobsen N, Thompson EW, Saunders CM. 2016. Minimal residual disease in breast cancer: an overview of circulating and disseminated tumour cells. Clin Exp Metastasis 33:521–550.

72. Coffey J, Wang J, Smith M, Bouchier-Hayes D, Cotter T, Redmond H. Excisional surgery for cancer cure: therapy at a cost 9.

73. Horowitz M, Neeman E, Sharon E, Ben-Eliyahu S. 2015. Exploiting the critical perioperative period to improve long-term cancer outcomes. Nat Rev Clin Oncol 12:213–226.

74. Finnerty CC, Mabvuure NT, Ali A, Kozar RA, Herndon DN. 2013. The Surgically Induced Stress Response. JPEN J Parenter Enteral Nutr 37:21S-29S.

75. Dąbrowska AM, Słotwiński R. 2014. The immune response to surgery and infection. Cent-Eur J Immunol 39:532–537.

76. Raytis JL, Lew MW. 2013. Surgical Stress Response and Cancer Metastasis: The Potential Benefit of Perioperative Beta BlockadeMadame Curie Bioscience Database [Internet]. Landes Bioscience. https://www.ncbi.nlm.nih.gov/books/NBK169223/. Retrieved 11 December 2022.

77. Angka L, Khan ST, Kilgour MK, Xu R, Kennedy MA, Auer RC. 2017. Dysfunctional Natural Killer Cells in the Aftermath of Cancer Surgery. Int J Mol Sci 18:E1787.

78. Mancuso ME, Santagostino E. 2017. Platelets: much more than bricks in a breached wall. Br J Haematol 178:209–219.

79. Mokbel K, Choy C, Engledow A. 2000. The effect of surgical wounding on tumour development. Eur J Surg Oncol. W.B. Saunders Ltd https://doi.org/10.1053/ejso.1999.0771.

80. Stuelten CH, Barbul A, Busch JI, Sutton E, Katz R, Sato M, Wakefield LM, Roberts AB, Niederhuber JE. 2008. Acute wounds accelerate tumorigenesis by a T cell-dependent mechanism. Cancer Res 68:7278–7282.

81. Yokoi K, Sasaki T, Bucana CD, Fan D, Baker CH, Kitadai Y, Kuwai T, Abbruzzese JL, Fidler IJ. 2005. Simultaneous Inhibition of EGFR, VEGFR and PDGFR Signaling Combined with Gemcitabine Produces Therapy of Human Pancreatic Carcinoma and Prolongs Survival in an Orthotopic Nude Mouse Model. Cancer Res 65:10371–10380.

82. Nagano H, Tomida C, Yamagishi N, Teshima-Kondo S. 2019. VEGFR-1 Regulates EGF-R to Promote Proliferation in Colon Cancer Cells. Int J Mol Sci 20:5608.

83. Rybinski B, Franco-Barraza J, Cukierman E. 2014. The wound healing, chronic fibrosis, and cancer progression triad. Physiol Genomics. American Physiological Society https://doi.org/10.1152/physiolgenomics.00158.2013.

84. Muliaditan T, Caron J, Okesola M, Opzoomer JW, Kosti P, Georgouli M, Gordon P, Lall S, Kuzeva DM, Pedro L, Shields JD, Gillett CE, Diebold SS, Sanz-Moreno V, Ng T, Hoste E, Arnold JN. 2018. Macrophages are exploited from an innate wound healing response to facilitate cancer metastasis. Nat Commun 9.

85. Wicherska-Pawłowska K, Wróbel T, Rybka J. 2021. Toll-Like Receptors (TLRs), NOD-Like Receptors (NLRs), and RIG-I-Like Receptors (RLRs) in Innate Immunity. TLRs, NLRs, and RLRs Ligands as Immunotherapeutic Agents for Hematopoietic Diseases. Int J Mol Sci 22:13397.

86. Sharma B, McLeland CB, Potter TM, Stern ST, Adiseshaiah PP. 2018. Assessing NLRP3 inflammasome activation by nanoparticles, p. 135–147. *In* Methods in Molecular Biology. Humana Press Inc.

87. Ershaid N, Sharon Y, Doron H, Raz Y, Shani O, Cohen N, Monteran L, Leider-Trejo L, Ben-Shmuel A, Yassin M, Gerlic M, Ben-Baruch A, Pasmanik-Chor M, Apte R, Erez N. 2019. NLRP3 inflammasome in fibroblasts links tissue damage with inflammation in breast cancer progression and metastasis. Nat Commun 10.

88. Chen X, Wang L, Li P, Song M, Qin G, Gao Q, Zhang Z, Yue D, Wang D, Nan S, Qi Y, Li F, Yang L, Huang L, Zhang M, Zhang B, Gao Y, Zhang Y. 2018. Dual TGF-β and PD-1 blockade synergistically enhances MAGE-A3-specific CD8+ T cell response in esophageal squamous cell carcinoma. Int J Cancer 143:2561–2574.

89. Kim EY, Song KY. 2020. The preoperative and the postoperative neutrophil-to-lymphocyte ratios both predict prognosis in gastric cancer patients. World J Surg Oncol 18:293.

90. Pathogen Recognition and Inflammatory Signaling in Innate Immune Defenses - PMC. https://www.ncbi.nlm.nih.gov/pmc/articles/PMC2668232/. Retrieved 11 December 2022.

91. Alazawi W, Pirmadjid N, Lahiri R, Bhattacharya S. 2016. Inflammatory and Immune Responses to Surgery and Their Clinical Impact. Ann Surg 264:73–80.

92. Ng CSH, Lee TW, Wan S, Wan IYP, Sihoe ADL, Arifi AA, Yim APC. 2005. Thoracotomy is associated with significantly more profound suppression in lymphocytes and natural killer cells than video-assisted thoracic surgery following major lung resections for cancer. J Investig Surg Off J Acad Surg Res 18:81–88.

93. Narita S, Tsuchiya N, Kumazawa T, Maita S, Numakura K, Obara T, Tsuruta H, Saito M, Inoue T, Horikawa Y, Satoh S, Habuchi T. 2013. Comparison of surgical stress in patients undergoing open versus laparoscopic radical prostatectomy by measuring perioperative serum cytokine levels. J Laparoendosc Adv Surg Tech A 23:33–37.

94. Paruk F, Chausse JM. 2019. Monitoring the post surgery inflammatory host response. 0. J Emerg Crit Care Med 3.

95. Gabay C. 2006. Interleukin-6 and chronic inflammation. Arthritis Res Ther 8:S3.

96. Immune perturbations in patients along the perioperative period: alterations in cell surface markers and leukocyte subtypes before and after surgery - PubMed. https://pubmed.ncbi.nlm.nih.gov/19254757/. Retrieved 11 December 2022.

97. Landén NX, Li D, Ståhle M. 2016. Transition from inflammation to proliferation: a critical step during wound healing. Cell Mol Life Sci 73:3861–3885.

98. Weledji EP. 2021. The role of cytokines in enhanced recovery after surgery. IJS Short Rep 6:e21.

99. Angka L, Martel AB, Kilgour M, Jeong A, Sadiq M, de Souza CT, Baker L, Kennedy MA, Kekre N, Auer RC. 2018. Natural Killer Cell IFNγ Secretion is Profoundly Suppressed Following Colorectal Cancer Surgery. Ann Surg Oncol 25:3747–3754.

100. Market M, Tennakoon G, Auer RC. 2021. Postoperative Natural Killer Cell Dysfunction: The Prime Suspect in the Case of Metastasis Following Curative Cancer Surgery. Int J Mol Sci 22:11378.

101. Reinhardt R, Pohlmann S, Kleinertz H, Hepner-Schefczyk M, Paul A, Flohé SB. 2015. Invasive Surgery Impairs the Regulatory Function of Human CD56bright Natural Killer Cells in Response to Staphylococcus aureus. Suppression of Interferon-γ Synthesis. PLOS ONE 10:e0130155.

102. Zhou C, Wang Z, Jiang B, Di J, Su X. 2022. Monitoring Pre- and Post-Operative Immune Alterations in Patients With Locoregional Colorectal Cancer Who Underwent Laparoscopy by Single-Cell Mass Cytometry. Front Immunol 13.

103. Tai L-H, de Souza CT, Bélanger S, Ly L, Alkayyal AA, Zhang J, Rintoul JL, Ananth AA, Lam T, Breitbach CJ, Falls TJ, Kirn DH, Bell JC, Makrigiannis AP, Auer RA. 2013. Preventing postoperative metastatic disease by inhibiting surgery-induced dysfunction in natural killer cells. Cancer Res 73:97–107.

104. Market M, Tennakoon G, Scaffidi M, Cook DP, Angka L, Ng J, Tanese de Souza C, Kennedy MA, Vanderhyden BC, Auer RC. 2022. Preventing Surgery-Induced NK Cell Dysfunction Using Anti-TGF-β Immunotherapeutics. 23. Int J Mol Sci 23:14608.

105. Angka L, Souza CT de, Baxter KE, Khan ST, Market M, Martel AB, Tai L-H, Kennedy MA, Bell JC, Auer RC. 2022. Perioperative arginine prevents metastases by accelerating natural killer cell recovery after surgery. Mol Ther 30:3270–3283.

106. Bi J, Tian Z. 2019. NK Cell Dysfunction and Checkpoint Immunotherapy. Front Immunol 10.

107. Tai L-H, Zhang J, Auer RC. 2013. Preventing surgery-induced NK cell dysfunction and cancer metastases with influenza vaccination. OncoImmunology 2:e26618.

108. Tai L-H, Alkayyal AA, Leslie AL, Sahi S, Bennett S, Tanese de Souza C, Baxter K, Angka L, Xu R, Kennedy MA, Auer RC. 2018. Phosphodiesterase-5 inhibition reduces postoperative metastatic disease by targeting surgery-induced myeloid derived suppressor cell-dependent inhibition of Natural Killer cell cytotoxicity. Oncoimmunology 7:e1431082.

109. Seth R, Tai L-H, Falls T, de Souza CT, Bell JC, Carrier M, Atkins H, Boushey R, Auer RA. 2013. Surgical Stress Promotes the Development of Cancer Metastases by a Coagulation-Dependent Mechanism Involving Natural Killer Cells in a Murine Model. Ann Surg 258:158–168.

110. Iannone F, Porzia A, Peruzzi G, Birarelli P, Milana B, Sacco L, Dinatale G, Peparini N, Prezioso G, Battella S, Caronna R, Morrone S, Palmieri G, Mainiero F, Chirletti P. 2015. Effect of surgery on pancreatic tumor-dependent lymphocyte asset: modulation of natural killer cell frequency and cytotoxic function. Pancreas 44:386–393.

111. Velásquez JF, Ramírez MF, Ai DI, Lewis V, Cata JP. 2015. Impaired Immune Function in Patients Undergoing Surgery for Bone Cancer. Anticancer Res 35:5461–5466.

112. Decker D, Tolba R, Springer W, Lauschke H, Hirner A, von Ruecker A. 2005. Abdominal surgical interventions: local and systemic consequences for the immune system--a prospective study on elective gastrointestinal surgery. J Surg Res 126:12–18.

113. Scheid C, Young R, McDermott R, Fitzsimmons L, Scarffe JH, Stern PL. 1994. Immune function of patients receiving recombinant human interleukin-6 (IL-6) in a phase I clinical study: induction of

C-reactive protein and IgE and inhibition of natural killer and lymphokine-activated killer cell activity. Cancer Immunol Immunother CII 38:119–126.

114. Inhibition of natural killer cell cytotoxicity by interleukin-6: implications for the pathogenesis of macrophage activation syndrome. - Google Search. https://www.google.com/search?client=firefox-b-d&q=Inhibition+of+natural+killer+cell+cytotoxicity+by+interleukin-6%3A+implications+for+the+pathogenesis+of+macrophage+activation+syndrome. Retrieved 12 December 2022.

115. Kang Y-J, Jeung IC, Park A, Park Y-J, Jung H, Kim T-D, Lee HG, Choi I, Yoon SR. 2014. An increased level of IL-6 suppresses NK cell activity in peritoneal fluid of patients with endometriosis via regulation of SHP-2 expression. Hum Reprod Oxf Engl 29:2176–2189.

116. Vredevoe DL, Widawski M, Fonarow GC, Hamilton M, Martínez-Maza O, Gage JR. 2004. Interleukin-6 (IL-6) expression and natural killer (NK) cell dysfunction and anergy in heart failure. Am J Cardiol 93:1007–1011.

117. Joshi PC, Zhou X, Cuchens M, Jones Q. 2001. Prostaglandin E2 suppressed IL-15-mediated human NK cell function through down-regulation of common gamma-chain. J Immunol Baltim Md 1950 166:885–891.

118. Slattery K, Woods E, Zaiatz-Bittencourt V, Marks S, Chew S, Conroy M, Goggin C, MacEochagain C, Kennedy J, Lucas S, Finlay DK, Gardiner CM. 2021. TGFβ drives NK cell metabolic dysfunction in human metastatic breast cancer. J Immunother Cancer 9:e002044.

119. Viel S, Marçais A, Guimaraes FS-F, Loftus R, Rabilloud J, Grau M, Degouve S, Djebali S, Sanlaville A, Charrier E, Bienvenu J, Marie JC, Caux C, Marvel J, Town L, Huntington ND, Bartholin L, Finlay D, Smyth MJ, Walzer T. 2016. TGF-β inhibits the activation and functions of NK cells by repressing the mTOR pathway. Sci Signal 9:ra19.

120. Regis S, Dondero A, Caliendo F, Bottino C, Castriconi R. 2020. NK Cell Function Regulation by TGF-β-Induced Epigenetic Mechanisms. Front Immunol 11.

121. Lazarova M, Steinle A. 2019. Impairment of NKG2D-Mediated Tumor Immunity by TGF-β. Front Immunol 10:2689.

122. Han B, Mao F, Zhao Y, Lv Y, Teng Y, Duan M, Chen W, Cheng P, Wang T, Liang Z, Zhang J, Liu Y, Guo G, Zou Q, Zhuang Y, Peng L. 2018. Altered NKp30, NKp46, NKG2D, and DNAM-1 Expression on Circulating NK Cells Is Associated with Tumor Progression in Human Gastric Cancer. J Immunol Res 2018:1–9.

123. Park YP, Choi S-C, Kiesler P, Gil-Krzewska A, Borrego F, Weck J, Krzewski K, Coligan JE. 2011. Complex regulation of human NKG2D-DAP10 cell surface expression: opposing roles of the γc cytokines and TGF-β1. Blood 118:3019–27.

124. Zhang XL, Topley N, Ito T, Phillips A. 2005. Interleukin-6 regulation of transforming growth factor (TGF)-beta receptor compartmentalization and turnover enhances TGF-beta1 signaling. J Biol Chem 280:12239–12245.

125. Ulich TR, Yin S, Guo K, Yi ES, Remick D, del Castillo J. 1991. Intratracheal injection of endotoxin and cytokines. II. Interleukin-6 and transforming growth factor beta inhibit acute inflammation. Am J Pathol 138:1097–1101.

126. Turner M, Chantry D, Feldmann M. 1990. Transforming growth factor beta induces the production of interleukin 6 by human peripheral blood mononuclear cells. Cytokine 2:211–216.

127. Gao X-H, Tian L, Wu J, Ma X-L, Zhang C-Y, Zhou Y, Sun Y-F, Hu B, Qiu S-J, Zhou J, Fan J, Guo W, Yang X-R. 2017. Circulating CD14+ HLA-DR-/low myeloid-derived suppressor cells predicted early recurrence of hepatocellular carcinoma after surgery. Hepatol Res Off J Jpn Soc Hepatol 47:1061–1071.

128. Furusawa J, Mizoguchi I, Chiba Y, Hisada M, Kobayashi F, Yoshida H, Nakae S, Tsuchida A, Matsumoto T, Ema H, Mizuguchi J, Yoshimoto T. 2016. Promotion of Expansion and Differentiation of Hematopoietic Stem Cells by Interleukin-27 into Myeloid Progenitors to Control Infection in Emergency Myelopoiesis. PLOS Pathog 12:e1005507.

129. Cuenca AG, Cuenca AL, Gentile LF, Efron PA, Islam S, Moldawer LL, Kays DW, Larson SD. 2015. Delayed emergency myelopoiesis following polymicrobial sepsis in neonates. Innate Immun 21:386–391.

130. O'Driscoll DN. 2022. Emergency myelopoiesis in critical illness: lessons from the COVID-19 pandemic. Ir J Med Sci 1–2.

131. Shibata J, Ishihara S, Tada N, Kawai K, Tsuno NH, Yamaguchi H, Sunami E, Kitayama J, Watanabe T. 2015. Surgical stress response after colorectal resection: a comparison of robotic, laparoscopic, and open surgery. Tech Coloproctology 19:275–280.

132. Gaudillière B, Fragiadakis GK, Bruggner RV, Nicolau M, Finck R, Tingle M, Silva J, Ganio EA, Yeh CG, Maloney WJ, Huddleston JI, Goodman SB, Davis MM, Bendall SC, Fantl WJ, Angst MS, Nolan

GP. 2014. Clinical recovery from surgery correlates with single-cell immune signatures. Sci Transl Med 6:255ra131.

133. Bronte V, Brandau S, Chen S-H, Colombo MP, Frey AB, Greten TF, Mandruzzato S, Murray PJ, Ochoa A, Ostrand-Rosenberg S, Rodriguez PC, Sica A, Umansky V, Vonderheide RH, Gabrilovich DI. 2016. Recommendations for myeloid-derived suppressor cell nomenclature and characterization standards. 1. Nat Commun 7:12150.

134. Zhao Y, Wu T, Shao S, Shi B, Zhao Y. 2015. Phenotype, development, and biological function of myeloid-derived suppressor cells. Oncoimmunology 5:e1004983.

135. Gabrilovich DI, Nagaraj S. 2009. Myeloid-derived suppressor cells as regulators of the immune system. Nat Rev Immunol 9:162–174.

136. Huang B, Pan PY, Li Q, Sato AI, Levy DE, Bromberg J, Divino CM, Chen SH. 2006. Gr-1+CD115+ immature myeloid suppressor cells mediate the development of tumor-induced T regulatory cells and T-cell anergy in tumor-bearing host. Cancer Res 66:1123–1131.

137. Wang PF, Song SY, Wang TJ, Ji WJ, Li SW, Liu N, Yan CX. 2018. Prognostic role of pretreatment circulating MDSCs in patients with solid malignancies: A meta-analysis of 40 studies. OncoImmunology. Taylor and Francis Inc. https://doi.org/10.1080/2162402X.2018.1494113.

138. Veglia F, Perego M, Gabrilovich D. 2018. Myeloid-derived suppressor cells coming of age. Nat Immunol 19:108–119.

139. Wang P-F, Song S-Y, Wang T-J, Ji W-J, Li S-W, Liu N, Yan C-X. 2018. Prognostic role of pretreatment circulating MDSCs in patients with solid malignancies: A meta-analysis of 40 studies. Oncoimmunology 7:e1494113.

140. Gunes EG, Rosen ST, Querfeld C. 2020. The Role of Myeloid Derived Suppressor Cells in Hematologic Malignancies. Curr Opin Oncol 32:518–526.

141. Ahn A, Park C-J, Kim M, Cho Y-U, Jang S, Bae MH, Lee J-H, Lee J-H, Koh K-N, Im HJ. 2021. Granulocytic and Monocytic Myeloid-Derived Suppressor Cells are Functionally and Prognostically Different in Patients with Chronic Myeloid Leukemia. Ann Lab Med 41:479–484.

142. Weber R, Fleming V, Hu X, Nagibin V, Groth C, Altevogt P, Utikal J, Umansky V. 2018. Myeloid-Derived Suppressor Cells Hinder the Anti-Cancer Activity of Immune Checkpoint Inhibitors. Front Immunol 9:1310.

143. Nausch N, Galani IE, Schlecker E, Cerwenka A. 2008. Mononuclear myeloid-derived “suppressor” cells express RAE-1 and activate natural killer cells. Blood 112:4080–4089.

144. Sceneay J, Chow MT, Chen A, Halse HM, Wong CSF, Andrews DM, Sloan EK, Parker BS, Bowtell DD, Smyth MJ, Möller A. 2012. Primary tumor hypoxia recruits CD11b+/Ly6Cmed/Ly6G+ immune suppressor cells and compromises NK cell cytotoxicity in the premetastatic niche. Cancer Res 72:3906–3911.

145. Sarhan D, Wang J, Arvindam US, Hallstrom C, Verneris MR, Grzywacz B, Warlick E, Blazar BR, Miller JS. 2020. Mesenchymal stromal cells shape the MDS microenvironment by inducing suppressive monocytes that dampen NK cell function. JCI Insight 5.

146. Hoechst B, Voigtlaender T, Ormandy L, Gamrekelashvili J, Zhao F, Wedemeyer H, Lehner F, Manns MP, Greten TF, Korangy F. 2009. Myeloid derived suppressor cells inhibit natural killer cells in patients with hepatocellular carcinoma via the NKp30 receptor. Hepatology 50:799–807.

147. Sarhan D, Cichocki F, Zhang B, Yingst A, Spellman SR, Cooley S, Verneris MR, Blazar BR, Miller JS. 2016. Adaptive NK Cells with Low TIGIT Expression Are Inherently Resistant to Myeloid-Derived Suppressor Cells. Cancer Res 76:5696–5706.

148. Li H, Han Y, Guo Q, Zhang M, Cao X. 2009. Cancer-expanded myeloid-derived suppressor cells induce anergy of NK cells through membrane-bound TGF-beta 1. J Immunol Baltim Md 1950 182:240–249.

149. Bronte V, Zanovello P. 2005. Regulation of immune responses by L-arginine metabolism. Nat Rev Immunol. Nat Rev Immunol https://doi.org/10.1038/nri1668.

150. Geiger R, Rieckmann JC, Wolf T, Basso C, Feng Y, Fuhrer T, Kogadeeva M, Picotti P, Meissner F, Mann M, Zamboni N, Sallusto F, Lanzavecchia A. 2016. L-Arginine Modulates T Cell Metabolism and Enhances Survival and Anti-tumor Activity. Cell 167:829-842.e13.

151. Lamas B, Vergnaud-Gauduchon J, Goncalves-Mendes N, Perche O, Rossary A, Vasson MP, Farges MC. 2012. Altered functions of natural killer cells in response to L-Arginine availability. Cell Immunol 280:182–190.

152. Ohl K, Tenbrock K. 2018. Reactive Oxygen Species as Regulators of MDSC-Mediated Immune Suppression. Front Immunol. NLM (Medline) https://doi.org/10.3389/fimmu.2018.02499.

153. Stiff A, Trikha P, Mundy-Bosse B, McMichael E, Mace TA, Benner B, Kendra K, Campbell A, Gautam S, Abood D, Landi I, Hsu V, Duggan M, Wesolowski R, Old M, Howard JH, Yu L, Stasik N, Olencki T, Muthusamy N, Tridandapani S, Byrd JC, Caligiuri M, Carson WE. 2018. Nitric Oxide Production by Myeloid-Derived Suppressor Cells Plays a Role in Impairing Fc Receptor–Mediated Natural Killer Cell Function. Clin Cancer Res 24:1891–1904.

154. Tumino N, Besi F, Martini S, Di Pace AL, Munari E, Quatrini L, Pelosi A, Fiore PF, Fiscon G, Paci P, Scordamaglia F, Covesnon MG, Bogina G, Mingari MC, Moretta L, Vacca P. 2022. Polymorphonuclear Myeloid-Derived Suppressor Cells Are Abundant in Peripheral Blood of Cancer Patients and Suppress Natural Killer Cell Anti-Tumor Activity. Front Immunol 12:803014.

155. Angka L, Martel AB, Kilgour M, Jeong A, Sadiq M, de Souza CT, Baker L, Kennedy MA, Kekre N, Auer RC. 2018. Natural Killer Cell IFNγ Secretion is Profoundly Suppressed Following Colorectal Cancer Surgery. Ann Surg Oncol 25:3747–3754.

156. Wang J, Su X, Yang L, Qiao F, Fang Y, Yu L, Yang Q, Wang Y, Yin Y, Chen R, Hong Z. 2016. The influence of myeloid-derived suppressor cells on angiogenesis and tumor growth after cancer surgery. Int J Cancer 138:2688–2699.

157. Tengesdal IW, Dinarello A, Powers NE, Burchill MA, Joosten LAB, Marchetti C, Dinarello CA. 2021. Tumor NLRP3-Derived IL-1β Drives the IL-6/STAT3 Axis Resulting in Sustained MDSC-Mediated Immunosuppression. Front Immunol 12.

158. Elkabets M, Ribeiro VSG, Dinarello CA, Ostrand-Rosenberg S, Di Santo JP, Apte RN, Vosshenrich CAJ. 2010. IL-1β regulates a novel myeloid-derived suppressor cell subset that impairs NK cell development and function. Eur J Immunol 40:3347–3357.

159. Li W, Wu K, Zhao E, Shi L, Li R, Zhang P, Yin Y, Shuai X, Wang G, Tao K. 2013. HMGB1 recruits myeloid derived suppressor cells to promote peritoneal dissemination of colon cancer after resection. Biochem Biophys Res Commun 436:156–161.

160. Ha H, Debnath B, Neamati N. 2017. Role of the CXCL8-CXCR1/2 Axis in Cancer and Inflammatory Diseases. Theranostics 7:1543–1588.

161. Han Z-J, Li Y-B, Yang L-X, Cheng H-J, Liu X, Chen H. 2021. Roles of the CXCL8-CXCR1/2 Axis in the Tumor Microenvironment and Immunotherapy. Molecules 27:137.

162. Tai L-H, Alkayyal AA, Leslie AL, Sahi S, Bennett S, Tanese de Souza C, Baxter K, Angka L, Xu R, Kennedy MA, Auer RC. 2018. Phosphodiesterase-5 inhibition reduces postoperative metastatic disease by targeting surgery-induced myeloid derived suppressor cell-dependent inhibition of Natural Killer cell cytotoxicity. Oncoimmunology 7.

163. 雅史立花. 2018. Hmgb1-Tlr4シグナルによる骨髄由来免疫抑制細胞の機能制御. Yakugaku Zasshi 138:143–148.

164. Sinha P, Clements VK, Fulton AM, Ostrand-Rosenberg S. 2007. Prostaglandin E2 promotes tumor progression by inducing myeloid-derived suppressor cells. Cancer Res 67:4507–4513.

165. Tomić S, Joksimović B, Bekić M, Vasiljević M, Milanović M, Čolić M, Vučević D. 2019. Prostaglanin-E2 Potentiates the Suppressive Functions of Human Mononuclear Myeloid-Derived Suppressor Cells and Increases Their Capacity to Expand IL-10-Producing Regulatory T Cell Subsets. Front Immunol 10.

166. Li J, Sun J, Rong R, Li L, Shang W, Song D, Feng G, Luo F. 2017. HMGB1 promotes myeloid-derived suppressor cells and renal cell carcinoma immune escape. Oncotarget 8:63290–63298.

167. Patel H, Le Marer N, Wharton RQ, Khan ZAJ, Araia R, Glover C, Henry MM, Allen-Mersh TG. 2002. Clearance of Circulating Tumor Cells After Excision of Primary Colorectal Cancer. Ann Surg 235:226–231.

168. Tamminga M, de Wit S, van de Wauwer C, van den Bos H, Swennenhuis JF, Klinkenberg TJ, Hiltermann TJN, Andree KC, Spierings DCJ, Lansdorp PM, van den Berg A, Timens W, Terstappen

LWMM, Groen HJM. 2020. Analysis of Released Circulating Tumor Cells During Surgery for Non-Small Cell Lung Cancer. Clin Cancer Res 26:1656–1666.

169. Zhu S, Zhao Y, Quan Y, Ma X. 2021. Targeting Myeloid-Derived Suppressor Cells Derived From Surgical Stress: The Key to Prevent Post-surgical Metastasis. Front Surg 8:783218.

170. Menezes AS, Barnes A, Scheer AS, Martel G, Moloo H, Boushey RP, Sabri E, Auer RC. 2013. Clinical research in surgical oncology: an analysis of ClinicalTrials.gov. Ann Surg Oncol 20:3725–3731.

171. Kaneda MM, Messer KS, Ralainirina N, Li H, Leem CJ, Gorjestani S, Woo G, Nguyen AV, Figueiredo CC, Foubert P, Schmid MC, Pink M, Winkler DG, Rausch M, Palombella VJ, Kutok J, McGovern K, Frazer KA, Wu X, Karin M, Sasik R, Cohen EEW, Varner JA. 2016. PI3Kγ is a molecular switch that controls immune suppression. Nature 539:437–442.

172. Liu P, Cheng H, Roberts TM, Zhao JJ. 2009. Targeting the phosphoinositide 3-kinase (PI3K) pathway in cancer. Nat Rev Drug Discov 8:627–644.

173. Vanhaesebroeck B, Guillermet-Guibert J, Graupera M, Bilanges B. 2010. The emerging mechanisms of isoform-specific PI3K signalling. Nat Rev Mol Cell Biol 11:329–341.

174. Rathinaswamy MK, Dalwadi U, Fleming KD, Adams C, Stariha JTB, Pardon E, Baek M, Vadas O, DiMaio F, Steyaert J, Hansen SD, Yip CK, Burke JE. 2021. Structure of the phosphoinositide 3-kinase (PI3K) p110γ-p101 complex reveals molecular mechanism of GPCR activation. Sci Adv 7:eabj4282.

175. Chaib M, Chauhan SC, Makowski L. 2020. Friend or Foe? Recent Strategies to Target Myeloid Cells in Cancer. Front Cell Dev Biol 8.

176. Williams O, Houseman BT, Kunkel EJ, Aizenstein B, Hoffman R, Knight ZA, Shokat KM. 2010. Discovery of dual inhibitors of the immune cell PI3Ks p110δ and p110γ: a prototype for new anti-inflammatory drugs. Chem Biol 17:123–134.

177. Nürnberg B, Beer-Hammer S. 2019. Function, Regulation and Biological Roles of PI3Kγ Variants. Biomolecules 9:427.

178. Ras is an indispensable coregulator of the class IB phosphoinositide 3-kinase p87/p110γ | PNAS. https://www.pnas.org/doi/10.1073/pnas.0905506106. Retrieved 13 December 2022.

179. VADLAKONDA L, Dash A, Pasupuleti M, Kotha AK, Reddanna P. 2013. The Paradox of Akt-mTOR Interactions. Front Oncol 3.

180. Vincent EE, Elder DJE, Thomas EC, Phillips L, Morgan C, Pawade J, Sohail M, May MT, Hetzel MR, Tavaré JM. 2011. Akt phosphorylation on Thr308 but not on Ser473 correlates with Akt protein kinase activity in human non-small cell lung cancer. Br J Cancer 104:1755–1761.

181. Alessi DR, Andjelkovic M, Caudwell B, Cron P, Morrice N, Cohen P, Hemmings BA. 1996. Mechanism of activation of protein kinase B by insulin and IGF-1. EMBO J 15:6541–6551.

182. Pérez-Tenorio G, Stål O, Southeast Sweden Breast Cancer Group. 2002. Activation of AKT/PKB in breast cancer predicts a worse outcome among endocrine treated patients. Br J Cancer 86:540–545.

183. Dai DL, Martinka M, Li G. 2005. Prognostic significance of activated Akt expression in melanoma: a clinicopathologic study of 292 cases. J Clin Oncol Off J Am Soc Clin Oncol 23:1473–1482.

184. Immuno-analysis of phospho-Akt in primary human breast cancers. https://www.spandidos-publications.com/10.3892/ijo_00000432. Retrieved 13 December 2022.

185. Vanhaesebroeck B, Alessi DR. 2000. The PI3K-PDK1 connection: more than just a road to PKB. Biochem J 346:561–576.

186. Tsurutani J, Fukuoka J, Tsurutani H, Shih JH, Hewitt SM, Travis WD, Jen J, Dennis PA. 2006. Evaluation of two phosphorylation sites improves the prognostic significance of Akt activation in non-small-cell lung cancer tumors. J Clin Oncol Off J Am Soc Clin Oncol 24:306–314.

187. Gallay N, Dos Santos C, Cuzin L, Bousquet M, Simmonet Gouy V, Chaussade C, Attal M, Payrastre B, Demur C, Récher C. 2009. The level of AKT phosphorylation on threonine 308 but not on serine 473 is associated with high-risk cytogenetics and predicts poor overall survival in acute myeloid leukaemia. Leukemia 23:1029–1038.

188. Sancak Y, Thoreen CC, Peterson TR, Lindquist RA, Kang SA, Spooner E, Carr SA, Sabatini DM. 2007. PRAS40 Is an Insulin-Regulated Inhibitor of the mTORC1 Protein Kinase. Mol Cell 25:903–915.

189. HUANG J, MANNING BD. 2008. The TSC1–TSC2 complex: a molecular switchboard controlling cell growth. Biochem J 412:179–190.

190. Guertin DA, Stevens DM, Thoreen CC, Burds AA, Kalaany NY, Moffat J, Brown M, Fitzgerald KJ, Sabatini DM. 2006. Ablation in mice of the mTORC components raptor, rictor, or mLST8 reveals that mTORC2 is required for signaling to Akt-FOXO and PKCalpha, but not S6K1. Dev Cell 11:859–871.

191. Vadlakonda L, Pasupuleti M, Pallu R. 2013. Role of PI3K-AKT-mTOR and Wnt Signaling Pathways in Transition of G1-S Phase of Cell Cycle in Cancer Cells. Front Oncol 3:85.

192. Xu W, Hua H, Chiu Y-H, Li G, Zhi H, Yu Z, Ren F, Luo Y, Cui W. 2019. CD146 Regulates Growth Factor-Induced mTORC2 Activity Independent of the PI3K and mTORC1 Pathways. Cell Rep 29:1311-1322.e5.

193. Schmid MC, Franco I, Kang SW, Hirsch E, Quilliam LA, Varner JA. 2013. PI3-Kinase γ Promotes Rap1a-Mediated Activation of Myeloid Cell Integrin α4β1, Leading to Tumor Inflammation and Growth. PLOS ONE 8:e60226.

194. Liu Y, Xu C, Xiao X, Chen Y, Wang X, Liu W, Tan Y, Zhu W, Hu J, Liang J, Yan G, Lin Y, Cai J. 2022. Overcoming resistance to oncolytic virus M1 by targeting PI3K-γ in tumor-associated myeloid cells. Mol Ther J Am Soc Gene Ther 30:3677–3693.

195. Schmidt C, Schneble-Löhnert N, Lajqi T, Wetzker R, Müller JP, Bauer R. 2021. PI3Kγ Mediates Microglial Proliferation and Cell Viability via ROS. 10. Cells 10:2534.

196. Kuehn HS, Jung M-Y, Beaven MA, Metcalfe DD, Gilfillan AM. 2011. Prostaglandin E2 Activates and Utilizes mTORC2 as a Central Signaling Locus for the Regulation of Mast Cell Chemotaxis and Mediator Release. J Biol Chem 286:391–402.

197. Foubert P, Kaneda MM, Varner JA. 2017. PI3Kγ Activates Integrin α4 and Promotes Immune Suppressive Myeloid Cell Polarization during Tumor Progression. Cancer Immunol Res 5:957–968.

198. Li M, Li M, Yang Y, Liu Y, Xie H, Yu Q, Tian L, Tang X, Ren K, Li J, Zhang Z, He Q. 2020. Remodeling tumor immune microenvironment via targeted blockade of PI3K-γ and CSF-1/CSF-1R pathways in tumor associated macrophages for pancreatic cancer therapy. J Control Release Off J Control Release Soc 321:23–35.

199. Rynkiewicz NK, Anderson KE, Suire S, Collins DM, Karanasios E, Vadas O, Williams R, Oxley D, Clark J, Stephens LR, Hawkins PT. 2020. Gβγ is a direct regulator of endogenous p101/p110γ and p84/p110γ PI3Kγ complexes in mouse neutrophils. Sci Signal 13:eaaz4003.

200. Davis RJ, Moore EC, Clavijo PE, Friedman J, Cash H, Chen Z, Silvin C, Van Waes C, Allen C. 2017. Anti-PD-L1 Efficacy Can Be Enhanced by Inhibition of Myeloid-Derived Suppressor Cells with a Selective Inhibitor of PI3Kδ/γ. Cancer Res 77:2607–2619.

201. Zhang X, Shen L, Liu Q, Hou L, Huang L. 2019. Inhibiting PI3 kinase-γ in both myeloid and plasma cells remodels the suppressive tumor microenvironment in desmoplastic tumors. J Control Release Off J Control Release Soc 309:173–180.

202. Cohen E, Postow M, Sullivan R, Hong D, Yeckes-Rodin H, McCarter J, Zizlsperger N, Kutok J, O'Connell B, Page K, Roberts J, Zhang H, Chmielowski B. 2020. 352 Updated clinical data from the squamous cell carcinoma of the head and neck (SCCHN) expansion cohort of an ongoing Ph1/1b Study of eganelisib (formerly IPI-549) in combination with nivolumab. J Immunother Cancer 8.

203. Hogan BV, Peter MB, Shenoy HG, Horgan K, Hughes TA. 2011. Surgery induced immunosuppression. Surg J R Coll Surg Edinb Irel 9:38–43.

204. Sullivan RJ, Hong DS, Tolcher AW, Patnaik A, Shapiro G, Chmielowski B, Ribas A, Brail LH, Roberts J, Lee L, O'Connell B, Kutok JL, Mahabhashyam S, Dansky Ullmann C, Postow MA, Wolchok JD. 2018. Initial results from first-in-human study of IPI-549, a tumor macrophage-targeting agent, combined with nivolumab in advanced solid tumors. J Clin Oncol 36:3013–3013.

205. Tolcher AW, Hong DS, Sullivan RJ, Mier JW, Shapiro G, Pearlberg J, Brail LH, Kharidia J, Han L, Dansky Ullmann C, Stern HM, Wolchok JD. 2016. IPI-549-01-A phase 1/1b first in human study of

IPI-549, a PI3K-γ inhibitor, as monotherapy and in combination with pembrolizumab in subjects with advanced solid tumors. J Clin Oncol 34:TPS3111–TPS3111.

206. Palanki MSS, Dneprovskaia E, Doukas J, Fine RM, Hood J, Kang X, Lohse D, Martin M, Noronha G, Soll RM, Wrasidlo W, Yee S, Zhu H. 2007. Discovery of 3,3‘-(2,4-Diaminopteridine-6,7-diyl)diphenol as an Isozyme-Selective Inhibitor of PI3K for the Treatment of Ischemia Reperfusion Injury Associated with Myocardial Infarction. J Med Chem 50:4279–4294.

207. Bøyum A. 1976. Isolation of Lymphocytes, Granulocytes and Macrophages. Scand J Immunol 5:9–15.

208. Mandruzzato S, Brandau S, Britten CM, Bronte V, Damuzzo V, Gouttefangeas C, Maurer D, Ottensmeier C, van der Burg SH, Welters MJP, Walter S. 2016. Toward harmonized phenotyping of human myeloid-derived suppressor cells by flow cytometry: results from an interim study. Cancer Immunol Immunother 65:161–169.

209. Human PBMCs. https://www.bdbiosciences.com/en-ca/resources/protocols/human-pbmcs. Retrieved 16 January 2023.

210. CD33 MicroBeads, human | Granulocytes and myeloid cells | MicroBeads and Isolation Kits | Cell separation reagents | MACS Cell Separation | Products | Miltenyi Biotec | Canada. https://www.miltenyibiotec.com/CA-en/products/cd33-microbeads-human.html. Retrieved 16 January 2023.

211. Human/Mouse/Rat/Porcine/Canine TGF-beta 1 Quantikine ELISA. www.rndsystems.com. https://www.rndsystems.com/products/human-mouse-rat-porcine-canine-tgf-beta-1-quantikine-elisa_db100b. Retrieved 16 January 2023.

212. 2016. TGF-β Reporter HEK 293 Cells. InvivoGen. https://www.invivogen.com/hek-blue-tgfb. Retrieved 31 January 2023.

213. 2016. QUANTI-Blue™. InvivoGen. https://www.invivogen.com/quanti-blue. Retrieved 31 January 2023.

214. Myeloid-Derived Suppressor Cell Isolation Kit, mouse | Granulocytes and myeloid cells | MicroBeads and Isolation Kits | Cell separation reagents | MACS Cell Separation | Products | Miltenyi Biotec | Canada. https://www.miltenyibiotec.com/CA-en/products/myeloid-derived-suppressor-cell-isolation-kit-mouse.html. Retrieved 16 January 2023.

215. Magnuson B, Ekim B, Fingar DC. 2012. Regulation and function of ribosomal protein S6 kinase (S6K) within mTOR signalling networks. Biochem J 441:1–21.

216. Agresti R, Triulzi T, Sasso M, Ghirelli C, Aiello P, Rybinska I, Campiglio M, Sfondrini L, Tagliabue E, Bianchi F. 2019. Wound Healing Fluid Reflects the Inflammatory Nature and Aggressiveness of Breast Tumors. Cells 8:181.

217. Ramirez MF, Ai D, Bauer M, Vauthey J-N, Gottumukkala V, Kee S, Shon D, Truty M, Kuerer HM, Kurz A, Hernandez M, Cata JP. 2015. Innate immune function after breast, lung, and colorectal cancer surgery. J Surg Res 194:185–193.

218. Ananth AA, Tai L-H, Lansdell C, Alkayyal AA, Baxter KE, Angka L, Zhang J, Tanese de Souza C, Stephenson KB, Parato K, Bramson JL, Bell JC, Lichty BD, Auer RC. 2016. Surgical Stress Abrogates Pre-Existing Protective T Cell Mediated Anti-Tumor Immunity Leading to Postoperative Cancer Recurrence. PloS One 11:e0155947.

219. Spahn JH, Kreisel D. 2014. Monocytes in sterile inflammation: recruitment and functional consequences. Arch Immunol Ther Exp (Warsz) 62:187–194.

220. Gabrilovich DI, Ostrand-Rosenberg S, Bronte V. 2012. Coordinated regulation of myeloid cells by tumours. 4. Nat Rev Immunol 12:253–268.

221. Youn J-I, Nagaraj S, Collazo M, Gabrilovich DI. 2008. Subsets of Myeloid-Derived Suppressor Cells in Tumor Bearing Mice. J Immunol Baltim Md 1950 181:5791–5802.

222. Peranzoni E, Zilio S, Marigo I, Dolcetti L, Zanovello P, Mandruzzato S, Bronte V. 2010. Myeloid-derived suppressor cell heterogeneity and subset definition. Curr Opin Immunol 22:238–244.

223. Hassan M, Raslan HM, Eldin HG, Mahmoud E, Elwajed HAA. 2018. CD33+ HLA-DR– Myeloid-Derived Suppressor Cells Are Increased in Frequency in the Peripheral Blood of Type1 Diabetes Patients with Predominance of CD14+ Subset. Open Access Maced J Med Sci 6:303–309.

224. Parker KH, Beury DW, Ostrand-Rosenberg S. 2015. Myeloid-Derived Suppressor Cells: Critical Cells Driving Immune Suppression in the Tumor Microenvironment. Adv Cancer Res 128:95–139.

225. Liu Q, Zhang H, Jiang X, Qian C, Liu Z, Luo D. 2017. Factors involved in cancer metastasis: a better understanding to “seed and soil” hypothesis. Mol Cancer 16:176.

226. McAllister SS. 2011. Systemic Instigation: A Mouse Model to Study Breast Cancer as a Systemic Disease, p. 145–162. *In* Brakebusch, C, Pihlajaniemi, T (eds.), Mouse as a Model Organism: From Animals to Cells. Springer Netherlands, Dordrecht.

227. Joshi N, Pohlmeier L, Ben-Yehuda Greenwald M, Haertel E, Hiebert P, Kopf M, Werner S. 2020. Comprehensive characterization of myeloid cells during wound healing in healthy and healing-impaired diabetic mice. Eur J Immunol 50:1335–1349.

228. Marvel D, Gabrilovich DI. 2015. Myeloid-derived suppressor cells in the tumor microenvironment: expect the unexpected. J Clin Invest 125:3356–3364.

229. König C, Ebersberger A, Eitner A, Wetzker R, Schaible H-G. Prostaglandin EP3 receptor activation is antinociceptive in sensory neurons via PI3Kγ, AMPK and GRK2. Br J Pharmacol n/a.

230. Cahill CM, Rogers JT. 2008. Interleukin (IL) 1β Induction of IL-6 Is Mediated by a Novel Phosphatidylinositol 3-Kinase-dependent AKT/IκB Kinase α Pathway Targeting Activator Protein-1*. J Biol Chem 283:25900–25912.

231. Buscemi L, Ramonet D, Klingberg F, Formey A, Smith-Clerc J, Meister J-J, Hinz B. 2011. The Single-Molecule Mechanics of the Latent TGF-β1 Complex. Curr Biol 21:2046–2054.

232. Fujinaga A, Hirashita T, Hirashita Y, Sakai K, Kawamura M, Masuda T, Endo Y, Ohta M, Murakami K, Inomata M. 2023. Glucose metabolic upregulation via phosphorylation of S6 ribosomal protein affects tumor progression in distal cholangiocarcinoma. BMC Gastroenterol 23:157.

233. Jian S-L, Chen W-W, Su Y-C, Su Y-W, Chuang T-H, Hsu S-C, Huang L-R. 2017. Glycolysis regulates the expansion of myeloid-derived suppressor cells in tumor-bearing hosts through prevention of ROS-mediated apoptosis. Cell Death Dis 8:e2779.

234. Ohl K, Tenbrock K. 2018. Reactive Oxygen Species as Regulators of MDSC-Mediated Immune Suppression. Front Immunol 9:2499.

235. Martin KJS, Muessel MJ, Pullar CE, Willars GB, Wardlaw AJ. 2015. The Role of Phosphoinositide 3-Kinases in Neutrophil Migration in 3D Collagen Gels. PLOS ONE 10:e0116250.

236. Joshi S, Singh AR, Zulcic M, Durden DL. 2014. A Macrophage-Dominant PI3K Isoform Controls Hypoxia-Induced HIF1α and HIF2α Stability and Tumor Growth, Angiogenesis, and Metastasis. Mol Cancer Res 12:1520–1531.

237. Saudemont A, Garçon F, Yadi H, Roche-Molina M, Kim N, Segonds-Pichon A, Martín-Fontecha A, Okkenhaug K, Colucci F. 2009. p110gamma and p110delta isoforms of phosphoinositide 3-kinase differentially regulate natural killer cell migration in health and disease. Proc Natl Acad Sci U S A 106:5795–5800.

238. Tassi I, Cella M, Gilfillan S, Turnbull I, Diacovo TG, Penninger JM, Colonna M. 2007. p110gamma and p110delta phosphoinositide 3-kinase signaling pathways synergize to control development and functions of murine NK cells. Immunity 27:214–227.

239. Macklin A, Khan S, Kislinger T. 2020. Recent advances in mass spectrometry based clinical proteomics: applications to cancer research. Clin Proteomics 17:17.

240. Wu B, Zhong C, Lang Q, Liang Z, Zhang Y, Zhao X, Yu Y, Zhang H, Xu F, Tian Y. 2021. Poliovirus receptor (PVR)-like protein cosignaling network: new opportunities for cancer immunotherapy. J Exp Clin Cancer Res CR 40:267.

241. Molfetta R, Zitti B, Lecce M, Milito ND, Stabile H, Fionda C, Cippitelli M, Gismondi A, Santoni A, Paolini R. 2020. CD155: A Multi-Functional Molecule in Tumor Progression. Int J Mol Sci 21:922.

242. Tumor CD155 Expression Is Associated with Resistance to Anti-PD1 Immunotherapy in Metastatic Melanoma | Clinical Cancer Research | American Association for Cancer Research. https://aacrjournals.org/clincancerres/article/26/14/3671/10183/Tumor-CD155-Expression-Is-Associated-with. Retrieved 24 January 2023.

243. Tahara-Hanaoka S, Shibuya K, Kai H, Miyamoto A, Morikawa Y, Ohkochi N, Honda S, Shibuya A. 2006. Tumor rejection by the poliovirus receptor family ligands of the DNAM-1 (CD226) receptor. Blood 107:1491–1496.

244. Fuchs A, Cella M, Giurisato E, Shaw AS, Colonna M. 2004. Cutting edge: CD96 (tactile) promotes NK cell-target cell adhesion by interacting with the poliovirus receptor (CD155). J Immunol Baltim Md 1950 172:3994–3998.

245. Tumor-derived soluble CD155 inhibits DNAM-1–mediated antitumor activity of natural killer cells | Journal of Experimental Medicine | Rockefeller University Press. https://rupress.org/jem/article/217/4/e20191290/133708/Tumor-derived-soluble-CD155-inhibits-DNAM-1. Retrieved 24 January 2023.

246. Sanchez-Correa B, Valhondo I, Hassouneh F, Lopez-Sejas N, Pera A, Bergua JM, Arcos MJ, Bañas H, Casas-Avilés I, Durán E, Alonso C, Solana R, Tarazona R. 2019. DNAM-1 and the TIGIT/PVRIG/TACTILE Axis: Novel Immune Checkpoints for Natural Killer Cell-Based Cancer Immunotherapy. Cancers 11:877.

247. Carlsten M, Norell H, Bryceson YT, Poschke I, Schedvins K, Ljunggren H-G, Kiessling R, Malmberg K-J. 2009. Primary Human Tumor Cells Expressing CD155 Impair Tumor Targeting by Down-Regulating DNAM-1 on NK Cells1. J Immunol 183:4921–4930.

248. Fu Z, Li S, Han S, Shi C, Zhang Y. 2022. Antibody drug conjugate: the “biological missile” for targeted cancer therapy. Signal Transduct Target Ther 7:93.

249. Zhao P, Zhang Y, Li W, Jeanty C, Xiang G, Dong Y. 2020. Recent advances of antibody drug conjugates for clinical applications. Acta Pharm Sin B 10:1589–1600.

250. Ritchie M, Tchistiakova L, Scott N. 2013. Implications of receptor-mediated endocytosis and intracellular trafficking dynamics in the development of antibody drug conjugates. mAbs 5:13.

251. Conant D, Hsiau T, Rossi N, Oki J, Maures T, Waite K, Yang J, Joshi S, Kelso R, Holden K, Enzmann BL, Stoner R. 2022. Inference of CRISPR Edits from Sanger Trace Data. CRISPR J 5:123–130.

252. Chalouni C, Doll S. 2018. Fate of Antibody-Drug Conjugates in Cancer Cells. J Exp Clin Cancer Res 37:20.

253. DeVay RM, Delaria K, Zhu G, Holz C, Foletti D, Sutton J, Bolton G, Dushin R, Bee C, Pons J, Rajpal A, Liang H, Shelton D, Liu S-H, Strop P. 2017. Improved Lysosomal Trafficking Can Modulate the Potency of Antibody Drug Conjugates. Bioconjug Chem 28:1102–1114.

254. He Y, Mueller S, Chipman PR, Bator CM, Peng X, Bowman VD, Mukhopadhyay S, Wimmer E, Kuhn RJ, Rossmann MG. 2003. Complexes of Poliovirus Serotypes with Their Common Cellular Receptor, CD155. J Virol 77:4827–4835.

255. Three-dimensional structure of poliovirus receptor bound to poliovirus | PNAS. https://www.pnas.org/doi/10.1073/pnas.97.1.73. Retrieved 25 January 2023.

256. Zhang P, Mueller S, Morais MC, Bator CM, Bowman VD, Hafenstein S, Wimmer E, Rossmann MG. 2008. Crystal structure of CD155 and electron microscopic studies of its complexes with polioviruses. Proc Natl Acad Sci 105:18284–18289.

257. Luan X, Sansanaphongpricha K, Myers I, Chen H, Yuan H, Sun D. 2017. Engineering exosomes as refined biological nanoplatforms for drug delivery. Acta Pharmacol Sin 38:754–763.

258. Zhu J, Li K, Yu L, Chen Y, Cai Y, Jin J, Hou T. 2021. Targeting phosphatidylinositol 3-kinase gamma (PI3Kγ): Discovery and development of its selective inhibitors. Med Res Rev 41:1599–1621.

259. Cohen E. 2022. Phase 2 Window of Opportunity Study of IPI-549 in Patients With Locally Advanced HPV+ and HPV- Head and Neck Squamous Cell Carcinoma. NCT03795610. Clinical trial registration. clinicaltrials.gov.

260. Infinity Pharmaceuticals, Inc. 2022. A Phase 2, Multi-arm, Multicenter, Open-label Study to Evaluate the Efficacy and Safety of IPI-549 Administered in Combination With Front-line Treatment Regimens in Patients With Locally Advanced and/or Metastatic Triple-Negative Breast Cancer or Renal Cell Carcinoma. NCT03961698. Clinical trial registration. clinicaltrials.gov.

261. Infinity Pharmaceuticals, Inc. 2022. A Phase 2, Multicenter, Randomized, Double-Blind, Active-Control Study to Evaluate the Efficacy and Safety of Nivolumab Administered in Combination With IPI-549 Compared to Nivolumab Monotherapy in the Treatment of Patients With Immune Therapy-Naïve, Advanced Urothelial Carcinoma. NCT03980041. Clinical trial registration. clinicaltrials.gov.

Contribution of Collaborators

In this section, I would like to acknowledge the work and assistance of a few specific collaborators. Please note that the legends of specific experiments indicate if the data was produced and analyzed by someone other than me. Instead, this section will acknowledge the work that went on behind the scenes that can`t acknowledged in figure legends. Christiano T. de Souza played an instrumental role in the planning and completion of my murine experiments. He was the one who did all the surgeries and PI3K inhibitor drug administrations for the murine models used within this thesis. As well, he performed the IV injections for B16F10LacZ tumour challenges, as well as MDSC adoptive transfer. He also performed the murine euthanasia by lethal buprenorphine injections and cervical dislocation. Dr. Leonard Angka was critical for the

success of this project. He identified PI3K as a pathway to target in sxMDSCs from a high-throughput drug screen. Moreover, he identified inhibiting PI3Kγ was a viable substitute to target pan-PI3K. He also conducted the initial mouse experiments shown in the supplementary figures. I would like to thank Dr. Rafeah Alam, and Dr. Alice Lau for their guidance on experiments as well as for editing this thesis. I would also like to acknowledge the tremendous amount of work done by our collaborators at Admare who synthesized Compound 17, produced the ADC and validated it. Unless stated otherwise in the figure legend, all other figures are results entirely from my own experiments.

Appendix

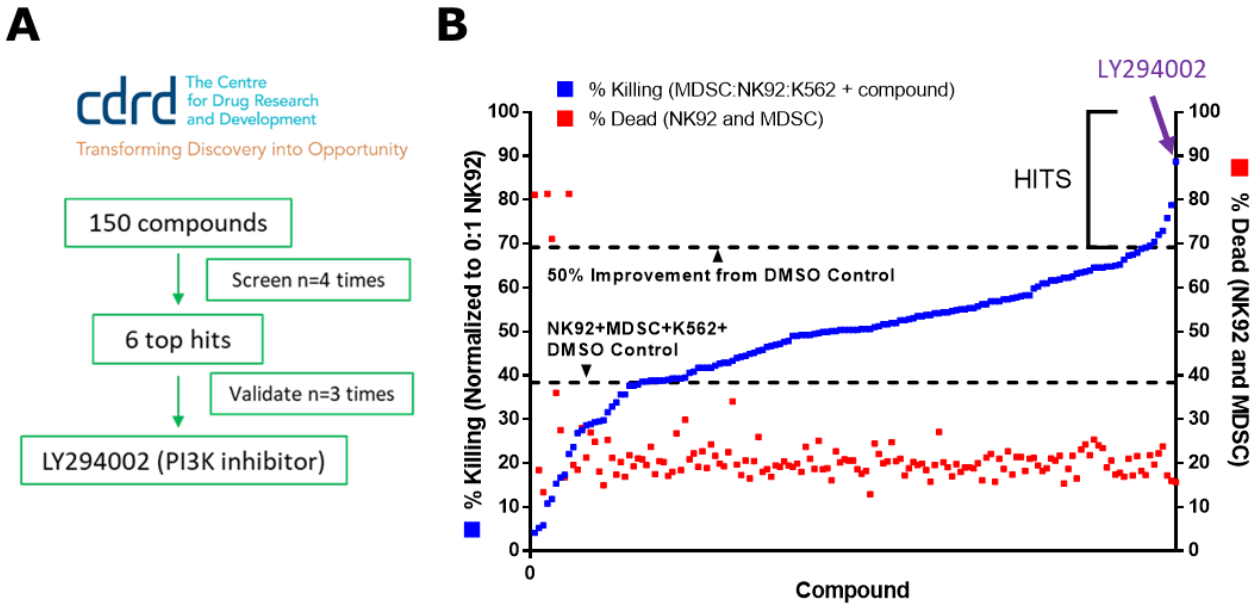

Supplemental Figure 1: Identification of PI3K inhibitor, LY294002, as a potent sxMDSC antagonist. A) Schematic of 150 compound library screen (donated by ADMARE) which was used in a high throughput *ex vivo* sxMDSC:NK92 co-culture suppression assay. sxMDSC:NK92 co-cultures were treated with 1μM of each compound for 20 hours, followed by addition of fluorescently-labelled NK-sensitive K562 target cells. NK-mediated K562 cytotoxicity was measured by viability dye using flow cytometry. Screen was conducted 4 times. B) Representative results from 150 compound screen. Compounds that improved NK cell cytotoxicity (blue, left y-axis) by >50% from DMSO control (black dotted line), without impacting NK cell viability (red, right y-axis), were considered hits. LY294002 (indicated in purple) improved cytotoxicity in all screens and was the top hit in 3/4 screens. This experiment was conducted and analyzed by Dr. Leonard Angka.

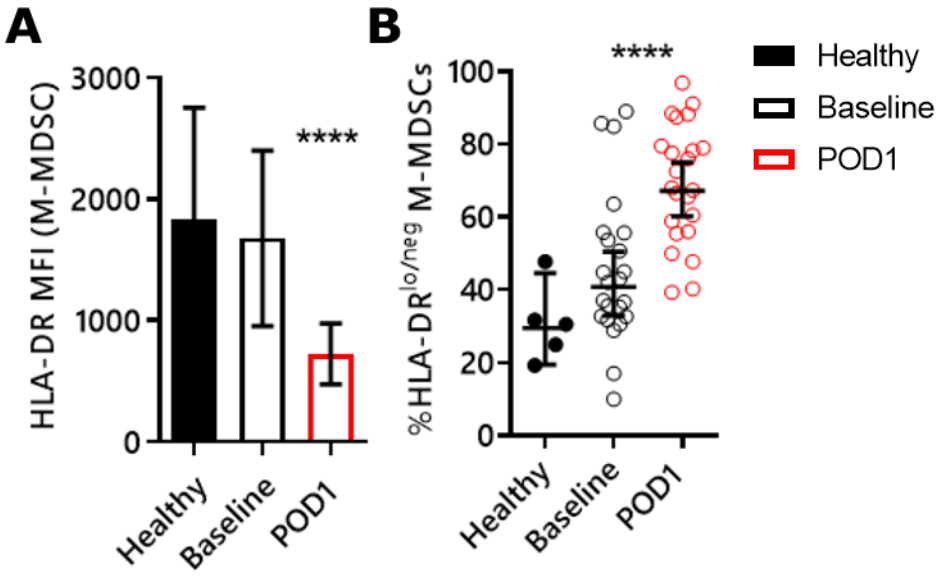

Supplemental Figure 2: HLA-DR$^{Lo/neg}$ M-MDSCs expand postoperatively. A) MFI of HLA-DR in M-MDSCs (n=20). B) proportion of HLA-DR$^{Lo/neg}$ M-MDSCs (CD14^{+}CD15^{-}CD33^{+}CD56^{-} CD3^{-}CD19^{-}) in Healthy, Baseline and POD1 PBMCs (n=20). This experiment was conducted and analyzed by Dr. Leonard Angka.

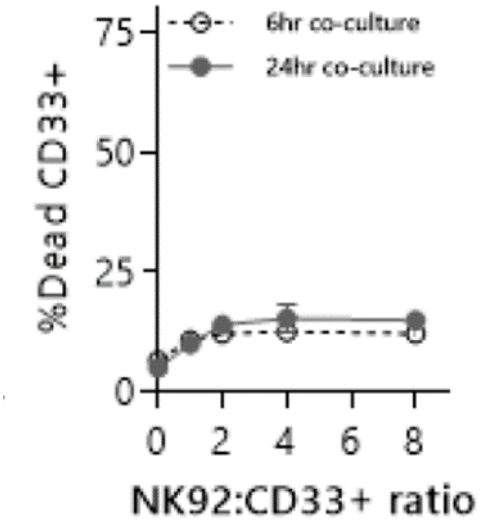

Supplemental Figure 3: NK92s are not cytotoxic against CD33^{+} (MDSCs). NK92s were co-cultured with MDSCs at increasing ratios for 6 hour or 24 hours. NK-mediated cytotoxicity against MDSCs was determined by a fluorescent viability dye using flow cytometry (n=3). This experiment was conducted and analyzed by Dr. Leonard Angka.

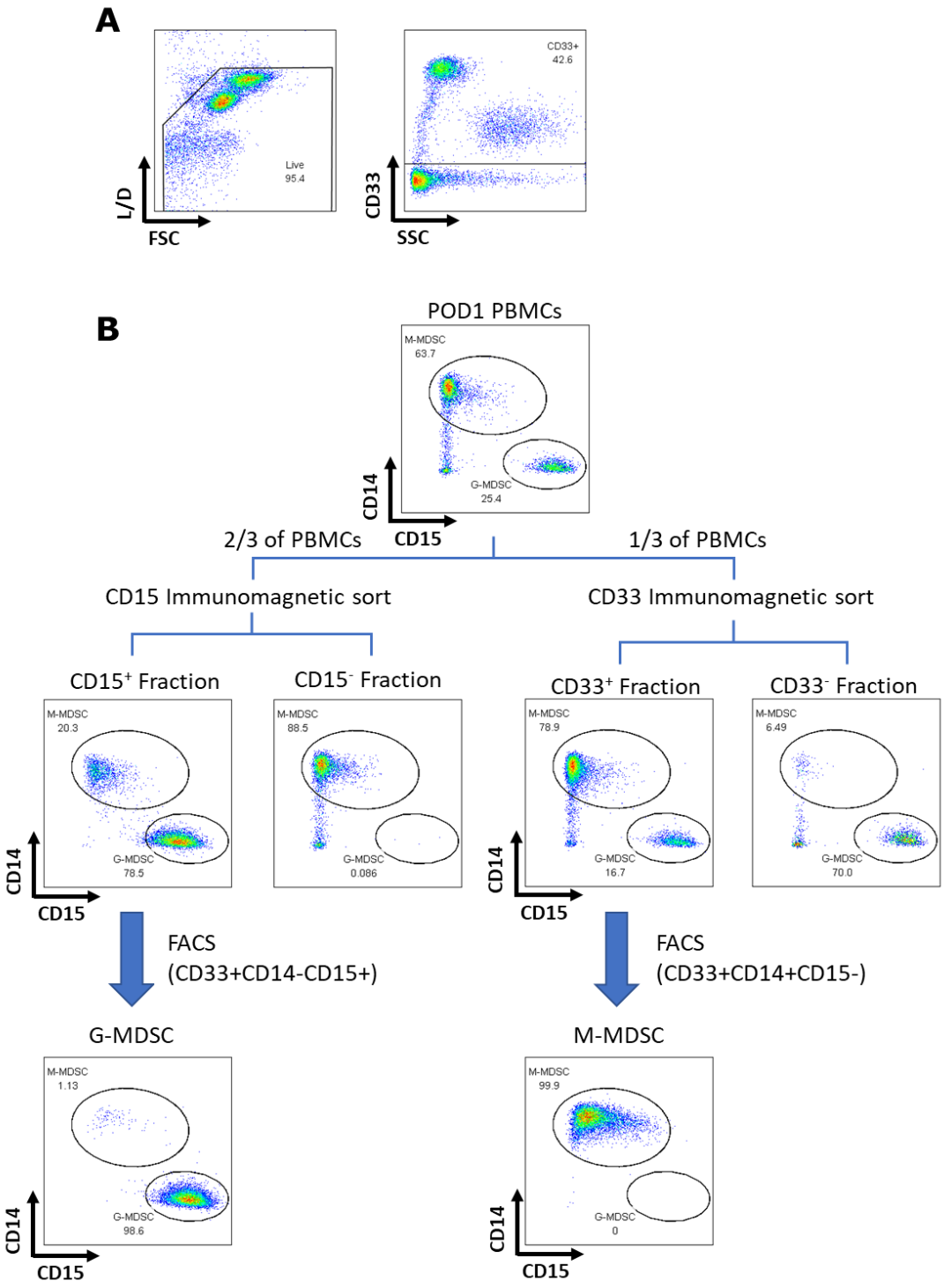

Supplemental Figure 4: M- and G-MDSC isolation strategy. A) Gating strategy for FACS of MDSC subpopulations. Cell debris, doublets, dead, and CD33- cells were gated out. $CD14^{+}CD15$-

(M-MDSC) and CD14-CD15^{+} (G-MDSCS) were gated within the CD33^{+} cell gate. B) CD14 vs CD15 flow plot from M- and G-MDSC FACS strategy.

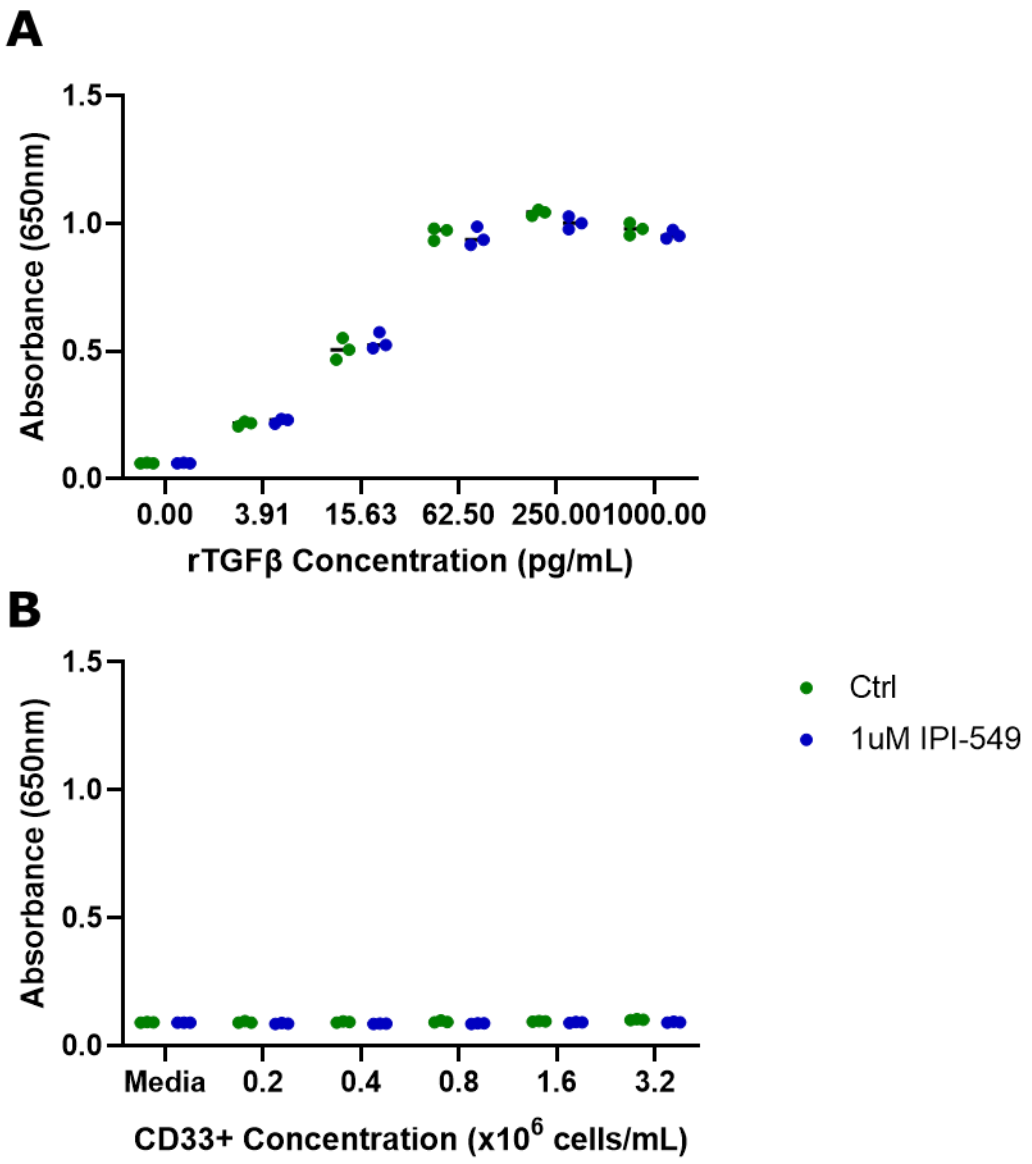

Supplemental Figure 5: Titration curve of TGF-β cell reporter assay with rTGF-β or CD33^{+} cells. HEK-Blue^{TM} TGF-β cells were plated and increasing concentrations of A) rTGF-β or B) CD33^{+} (MDSC) cell supernatant was added. After 24 hour incubation, QUANTI-Blue^{TM} assay was used to measure SEAP production, proportional to quantity of bioactive TGF-β (n=3).

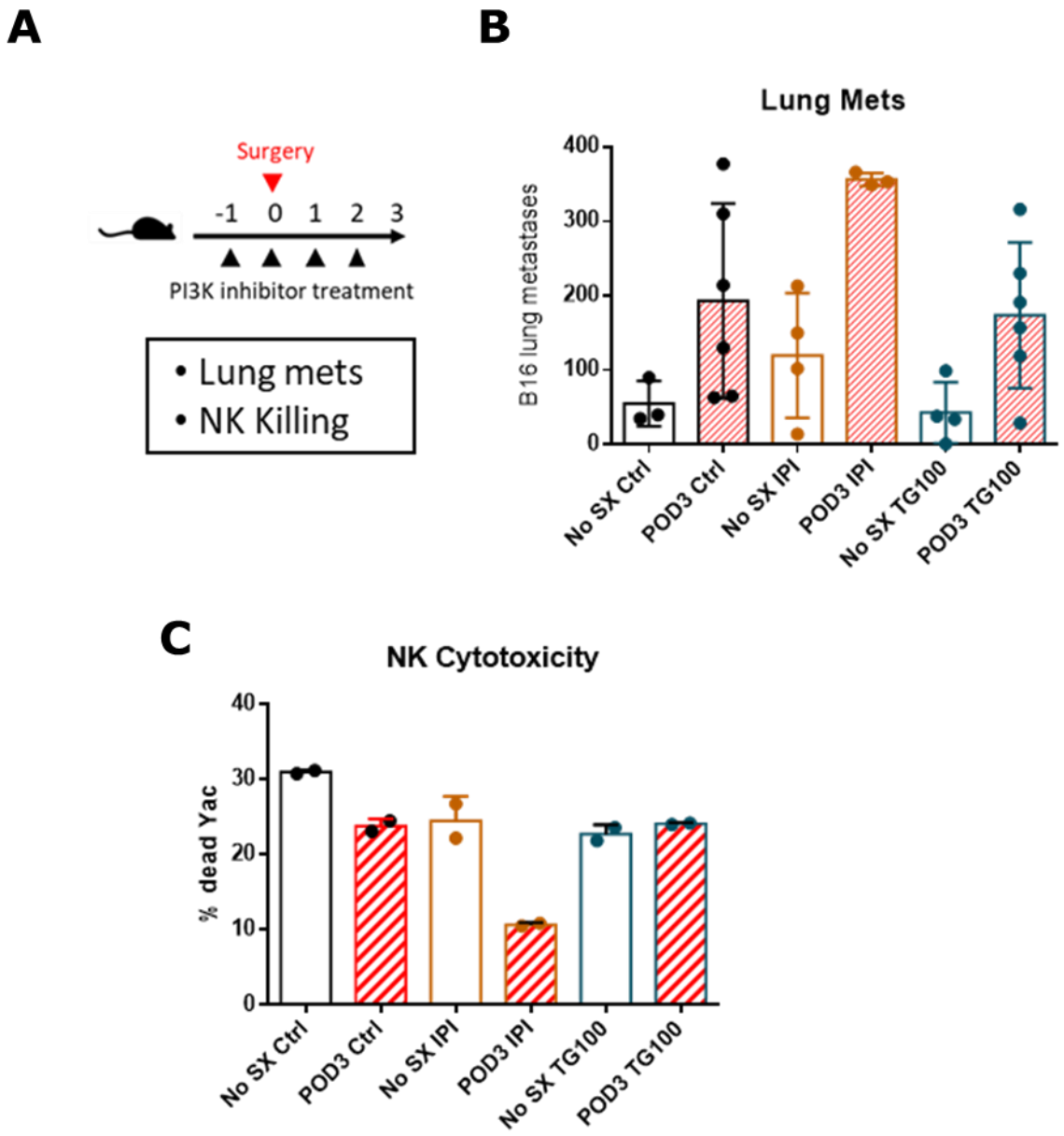

Supplemental Figure 6: Systemic administration of PI3Kγ inhibitors leads to deleterious reduction in NKC and increased postoperative metastasis in the B16F10LacZ murine model of surgical stress. A) Experimental outline and endpoints. Mice were administrated TG100-115 (3mg/kg) intrapertinonarly or IPI-549 (15mg/Kg) by oral gavage. TG100-115 was administrated twice a day, while IPI-549 was given once a day. Drug administration began one day before surgery (POD-1) and continued daily until POD3, at which point experiment reached endpoint. Immediately prior to surgery, mice underwent tumour challenge with lung metastases forming B16F10LacZ cells. B) On POD3 endpoint, lung metastases were counted following X-Gal staining (n=6). C) NK cells were isolated on POD3 endpoint, and cytotoxicity against NK-sensitive Yac-1 targets was determined in *ex vivo* killing assay (n=2). This experiment was conducted and analyzed by Dr. Leonard Angka.

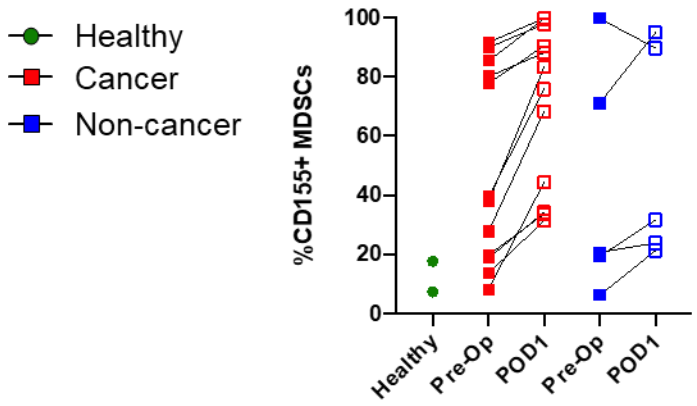

Supplemental Figure 7: CD155^{+} MDSCs expand following surgery. PBMCs were collected from healthy donors as well as cancer/non-cancer patients before (pre-op) and after (POD1) surgery. A) Proportion of MDSCs that are CD155^{+}. This experiment was conducted and analyzed by Dr. Andre Martel.

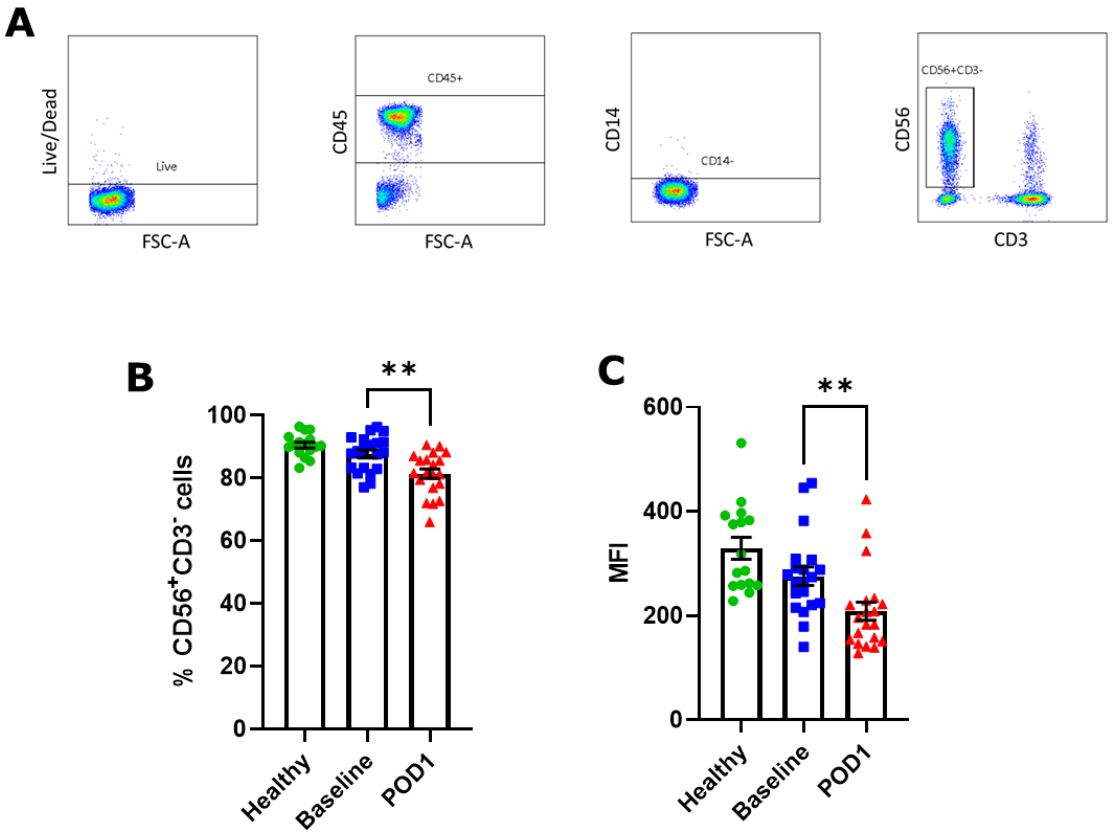

Supplemental Figure 8: Postoperative NK cells exhibit reduced DNAM-1 expression. A) Representative flow plot used as gating strategy to immunophenotype NK cells (CD56^{+}CD3^{-} CD14^{-}). Cell debris and non-singlets were excluded. B) Proportion of NK cells that are DNAM-1^{+} in healthy (green), baseline (blue) and POD1(red) PBMCs (n=20). C) MFI of DNAM-1 expression in NK cells (n= 20). I had conducted this experiment for my honours thesis.

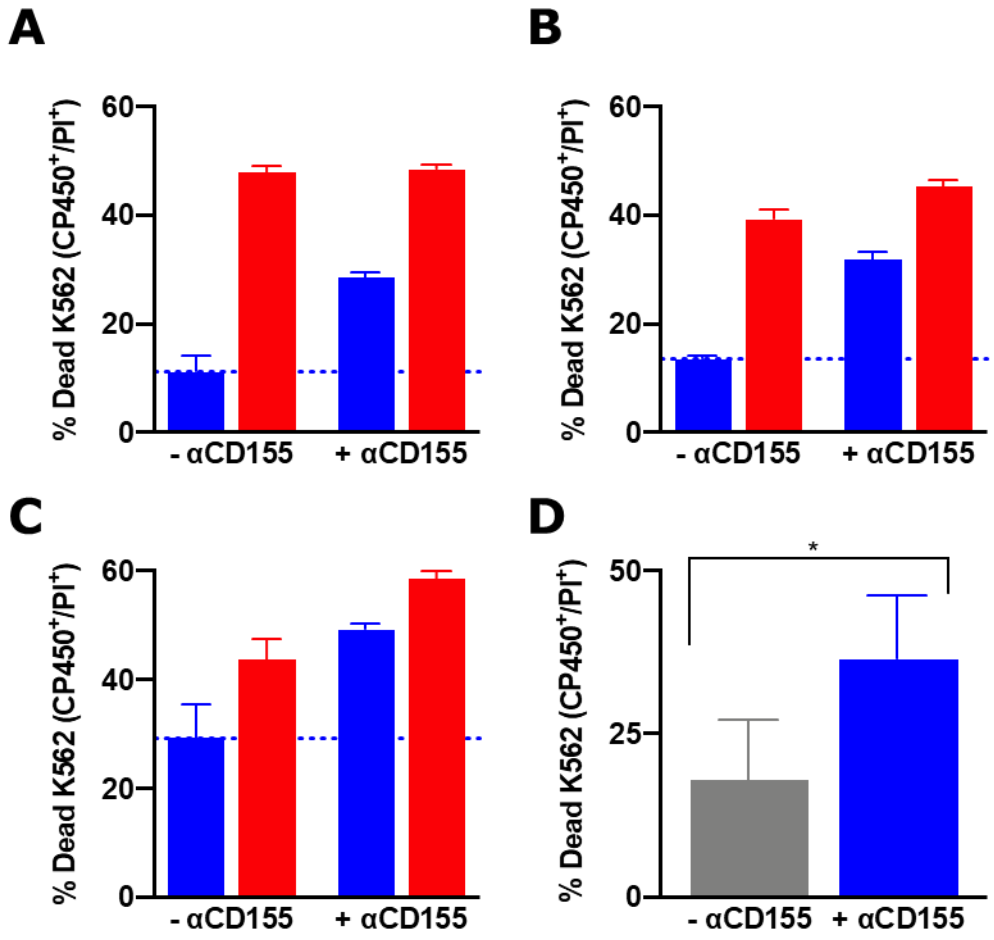

Supplemental Figure 9: Ex vivo CD155 Blockade Decreases the Suppressive Effect of Sx-MDSCs. A-C) Suppression assays with POD1 Sx-MDSCs of 3 cancer patients (A – lung cancer lobectomy, B – retroperitoneal sarcoma resection, C – lung cancer lobectomy). % killing of K562s with Sx-MDSCs (blue, MDSC:NK:K562) or without Sx-MDSCs (red, NK:562). The suppression control without α-CD155 is represented as the blue dotted line. Increase in killing with α-CD155 (0.5 µg/mL) is the proportion above this blue line. D) Mean % killing with Sx-MDSCs of all triplicates (n=9), comparing no α-CD155 (grey) to $^{+}$ α-CD155 (blue). All samples shown are Mean of triplicates ± SD. *$p<0.05$. This experiment was conducted and analyzed by Dr. Andre Martel.

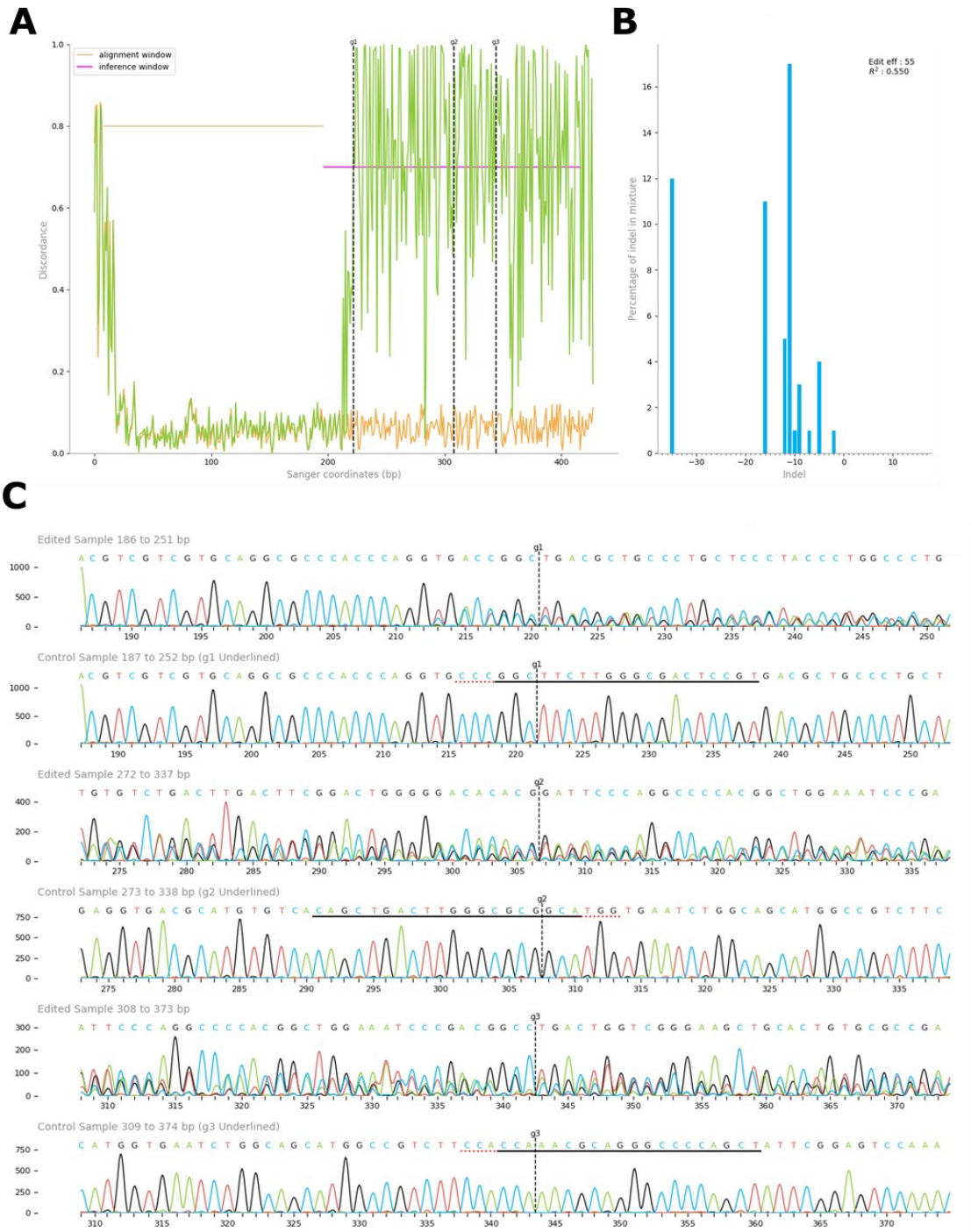

Supplemental Figure 10: ICE analysis of multi-guide Knockout of CD155 in K562 Clone 6. A) The discordance plot shows the level of disagreement between the non-edited wild type (control) and the edited sample in the region around the cut site. It shows, base-by-base, the average amount of signal that disagrees with the reference sequence derived from the control trace file. On the plot, the green (edited sample) and orange (control sample) lines should be close

together before the cut site. The vertical dotted lines mark the cut site for each guide (g1, g2 and g3). The alignment window indicates the region of the traces with high agreement between the two sequences that is used to align the edited and control traces. The inference window marks the region of the traces around the cut site, which will be used to infer the change in sequence between the edited and control traces. High discordance between the control and editing sequence in the inference window represents a high level of sequence difference. B) Insertion or deletion (indel) sizes along with their relative prevalence in the entire edited population of genomes. C) Edited and control, non-edited Sanger traces in the region around the guide binding sites for each guide RNA. The horizontal black underlined region represents the guide sequence, along with the red underlined PAM. The vertical black dotted line represents the cut site. Cutting and error-prone repair typically result in mixed sequencing bases downstream of the cut.